AN ABSTRACT OF THE THESIS OF

JAMES RICHARD BUDAHN for the degree of MASTER OF SCIENCE
(Name of student) (Degree)

in CHEMISTRY presented on July 26, 1979
(Major) (Date)

Title: GEOCHEMICAL STUDY OF HAWAIIAN BASALTS

Abstract approved: Redacted for privacy
Roman A. Schmitt

The abundances of 29 elements in 55 tholeiitic, transitional, and alkali olivine basalts from six major volcanoes of the Hawaiian Islands have been determined by instrumental neutron activation analysis. The abundances of the major rock-forming elements Ti, Al, Fe, Mg, Ca, Na, K, and Mn; the minor elements Cr, Co, Ni, V, Ba, Sr, and Zr; and the trace elements, including nine rare earth elements (REE) (La, Ce, Nd, Sm, Eu, Tb, Dy, Yb and Lu), and Sc, Hf, Ta, Th, and U were obtained. These data were used to determine and/or examine possible geochemical processes involved in the evolution of Hawaiian magmas.

Comparison of basalt compositions having similar MgO contents reveals that although basalts from an individual volcano are very uniform, systematic differences are observed among magmas from each of the studied volcanoes. These differences cannot be explained by variations in crystal fractionation from a common parental magma; instead they suggest that distinct mantle or source compositions have been melted in producing the basalts.

Partial melting calculations using REE and Sc abundances of average basalt compositions confirm this observation and indicate possible unique

source materials for the magmas observed on 1) Mauna Kea, Kohala, and Kilauea; 2) Mauna Loa and Lanai; and 3) Koolau. These calculations, which incorporated a model for light REE depletion for each magma batch, indicate that the best model of Mauna Kea-Kohala-Kilauea magma generation is given by 3-5% partial melting of a garnet pendotite composed of 84% olivine and orthopyroxene (ol+opx), 12% clinopyroxene (cpx), and 4% garnet (gar). Similarly, the Lanai and Mauna Loa magmas could be the result of 3-5% partial melting of a source composed of 75% ol+opx, 20% cpx, and 5% gar; and the melts of Koolau may be generated by 3-6% partial melting of 90% ol+opx, 6% cpx, and 4% gar.

Determination of absolute REE abundances in each source was based on various estimates on the amount of olivine crystal fractionation occurring from a most probable primary melt(s). These estimates are consistent with the interpretation that at least 45% olivine (Fo_{93-80}) has been removed prior to the eruption of the low MgO (7%) basalts resulting in a twofold increase of the REE, Sr, Ba, and many of the major elements (e.g., TiO_2, Al_2O_3, and CaO). The REE abundances calculated for the Mauna Kea-Kohala-Kilauea source region were 1.1x (times chondrite) for La and 1.5x for Lu. For the Lanai-Mauna Loa mantle, La = 0.84x and Lu = 1.8x and for the Koolau source La = 0.64x and Lu = 1.24x. Although these absolute abundances may be questionable because of uncertainties about the amount of olivine fractionation, such abundances agree very closely with REE data on alpine peridotites (Loubet et al., 1975).

Evidence from basalt mineralogies suggests that a significant amount of heterogeneity existed among primary melt compositions. Differences in normative plagioclase and in pyroxene/plagioclase ratios among the magma groups have been attributed to distinct pressures associated with melting. Modal variations of clinopyroxene and garnet in liquids have been shown to cause shifts in the normative character of melts (Yoder, 1976) and can be associated with pressure.

The occurrence of garnet pyroxenite in Hawaiian volcanism can be explained by using the Koolau mantle composition in a partial melting model. Major, minor, and REE abundances observed in garnet pyroxenites (Reid and Frey, 1971) can be obtained in liquids produced by 10% partial

melting of the Koolau source material, followed by 24% olivine plus garnet (1:1) crystal fractionation. The low REE abundances which are required for this relationship and which were determined in the development of tholeiitic basalt generation enhance the models of Hawaiian basalt generation.

Geochemical Study of Hawaiian Basalts

by

James Richard Budahn

A THESIS

submitted to

Oregon State University

in partial fulfillment of
the requirements for the
degree of

Master of Science

Completed July 26, 1979

Commencement June 1980

APPROVED:

Redacted for privacy

Professor of Chemistry
in charge of major

Redacted for privacy

Head of Department of Chemistry

Redacted for privacy

Dean of Graduate School

Date thesis is presented July 26, 1979
(Date of examination)

Typed by Lina Romero for James Richard Budahn

ACKNOWLEDGMENTS AND DEDICATION

It is impossible for me to completely express my gratitude to Dr. Roman A. Schmitt for the professional guidance and financial support he provided me during my study at Oregon State University. Dr. Schmitt's professional guidance continues to this day, and it has been instrumental in my obtaining the success I now enjoy. The financial support he provided was through a grant from the National Aeronautics and Space Administration.

This project would not have been undertaken had it not been for the enormous effort of Dr. William P. Leeman. I would like to greatly acknowledge him for developing the framework for this study and for supplying the samples for analysis. The numerous discussions we had appreciably enhanced the quality of this work. However, I take full responsibility for any differing opinions expressed.

Drs. Maw-Suen Ma and T. Fukuoka provided invaluable assistance in the analysis of the samples, and their discussions and comments concerning this study are appreciated. Dr. Ma also provided much needed support during the processing of the gamma-ray spectra via computer.

Drs. Douglas P. Blanchard, Klaus J. Schulz, and Michael Dungan provided pertinent comments during the preparation of the manuscript.

I would like to thank T. V. Anderson, W. T. Carpenter, and S. L. Bennett at the Oregon State University reactor for their assistance in the neutron activations.

Finally, I would like to thank my wife, Amy, for the moral support she provided me during the completion of this study.

This paper is dedicated to the memories of Dale Jackson and Gordon Macdonald, both of whom made immeasurable contributions to the understanding of the world we live in; these will be long remembered.

TABLE OF CONTENTS

LIST OF ILLUSTRATIONS

LIST OF TABLES

GEOCHEMICAL STUDY OF HAWAIIAN BASALTS

I. INTRODUCTION

Previous Studies on Hawaiian Basalt Generation

The processes that control the generation of basaltic magma — by far the most common magma type on earth — have been the topics for numerous investigations over the past 15 years. From those investigations, a considerable amount of data has been obtained relating the production of these magmas to a number of variables such as the melting depth, the source materials, the degree of melting, etc., as well as the melting phenomenon itself (Yoder, 1976). As a result, many models have been postulated to encompass the total evolutionary process of basalt generation. Although the more recent studies have focused on characterizing the early mantle system (e.g., Sun and Nesbitt, 1978; Arth and Hanson, 1975; and Hart and Brooks, 1974), the processes responsible for the formation of the Hawaiian Archipelago basalts have not gone unnoticed in these modeling attempts. This is probably due to its current volcanic activity, making the Hawaiian Islands one of the more ideal localities for first-hand studies concerning basaltic generative processes.

Earliest data collected from the Hawaiian Island volcanic chain, which extends 3,500 km across the Pacific Ocean seafloor, have provided a basis for qualitative and quantitative descriptions of the geophysical processes associated with the formation of these basaltic shield-volcanoes. Dana (1849a, 1849b), for example, was the first to present evidence of an age progression among the islands by noting erosional changes on successive islands. When McDougall (1964) substantiated this observation by obtaining potassium-argon ages on the major islands of Hawaii, several hypotheses concerning possible geophysical descriptions of a spatially fixed melting spot phenomenon were introduced. In brief, there are four plausible models. 1) The "hot spot" hypothesis: Proposed by Wilson (1963), this model suggests that the Pacific oceanic plate is being transported over an anomalously hot mantle area causing melting of the overlying lithospheric material. The resultant magma would then rise through the crust and form the island basalts [Fig. 1A].

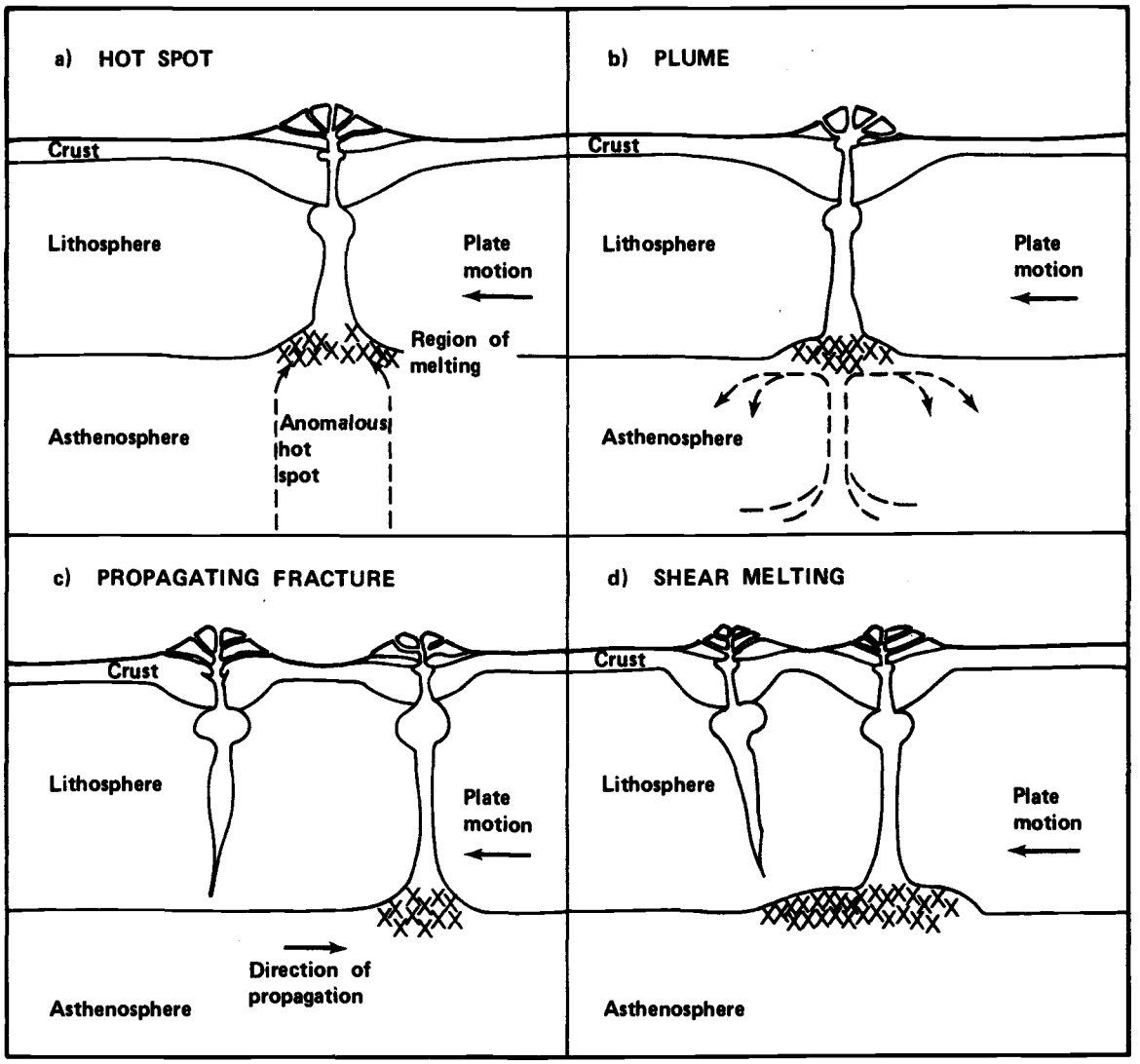

Fig. 1. Proposed models for the origin of the melting spot beneath Hawaii. a) Hot spot – Anomalous hot spot in mantle melt's lithospheric material. b) Plume – Stream of hot mantle material melt's base of lithosphere. c) Propagating fracture – Radiogenic mantle material propagates fracture in opposite direction as crust. d) Shear melting – Lithosphere sheared over asthenosphere. Cross-hatching refers to region where partial melting occurs. The figures are not drawn to scale.

2) The plume generation hypothesis: W. J. Morgan (1971) has advanced the hot spot model and suggests a plume generation model. Convection within the mantle would produce a narrow, relatively high-velocity stream of hot material. Magmas are formed by the upwelling of the mantle material through the crust as a result of its gravitational instability [Fig. 1B]. 3) The propagating fracture hypothesis: McDougall (1971) proposes that radiogenic mantle material propagates a tensional fracture in the lithosphere. The upwelling of mantle material into the lithosphere and the associated pressure release would cause partial melting and consequently the formation of tholeiitic lavas [Fig. 1C]. 4) The shear-melting hypothesis: Advanced by H. R. Shaw (1973), this model is based on the observation that a viscous medium will heat up when sheared. He has noted that in an event of this type, the shearing rate would increase as the temperature rises and viscosity decreases; thus additional temperature increases would result. A potential melting event such as this is postulated to occur as the lithosphere is sheared over the less rigid asthenosphere [Fig. 1D].

Although, in part, these models have been used to adequately explain some aspects of the generation of Hawaiian basaltic magma, none have provided for the complete geophysical or geochemical description. For example, the plume, the hot spot, and the propagating fracture models fulfill the requirement that new material is being resupplied in the magmatic process. On the other hand, none of the hypotheses account for the sigmoidal loci of volcanic centers or the consistent chemical cycle of magma generation. The shear melting model, although capable of explaining many of the distance-age-volume relations, does not provide evidence that would account for its confinement to melting in a single spot.

Because of these failures, it might be concluded that much about the melting process involved in Hawaiian basalt formation remains rather ill defined. Nevertheless, the depth at which melting occurs has been fairly accurately determined. Earthquake and seismic tremor data suggest that magma has been transported from at least 60 km (Eaton and Murata, 1960), inferring that the zone of melting is in the mantle region at or below this depth. Additionally, many xenoliths and garnet peridotite modules, believed to be derived from the mantle, have mineralogies and textures indicating solidification at a depth in excess of 60 km (Wright, 1971;

Boyd and Nixon, 1975). Consequently, from these and other data, it has been widely proposed that the source is probably some form of garnet peridotite; such an assemblage would be stable under these deep-seated conditions. Moreover, it has been shown that basaltic compositions can be produced upon partial melting of a garnet peridotite at high pressure. Other more or less direct evidence for considering garnet peridotite to be representative of the source material is 1) the close compositional relationship of garnet peridotite to the meteoritic model of mantle evolution and 2) the similarity of garnet peridotite's density and seismic velocity properties to those recorded in the upper mantle.

Finally, geophysical and geodetic studies (Eaton, 1962, 1967; Fiske and Kinoshita, 1969) have provided a general description of the magma transport system beneath the volcanoes. Following formation in the zone of melting, the magma ascends to an intermediate storage reservoir located at 20-30 km in depth. This, in turn, is connected to a shallow (2-4 km) magma reservoir that periodically feeds lava to the rift and summit vents.

Various models have also been proposed concerning the series of geochemical events that produce the two predominant types of Hawaiian magma compositions observed on the islands. Although most of these models consider the source to be a garnet peridotite, many different mechanisms have been suggested to form the tholeiitic and alkali olivine basalts from such a source by 1) varying the pressure and/or temperature of the partial melting event, 2) varying the pressure of the fractional crystallization event(s) that follow, or 3) varying the amount of partial melting. Some of the more advanced origins for basaltic magma are as follows: 1) Tholeiitic melts are the products of high-temperature or low-pressure partial melting, and alkali olivine basalts result from low-temperature or high-pressure partial melting (e.g., Green and Ringwood, 1967). 2) Fractionation of a basaltic liquid at high pressures produces alkali olivine basalts, and fractionation of this same liquid at low pressures gives tholeiitic basalts (e.g., Yoder and Tilley, 1962; McBirney and Williams, 1969). 3) Tholeiitic basalts are the first liquids produced from partial melting, whereas the alkali olivine basalts are produced upon further melting (e.g., O'Hara and Yoder, 1967). 4) A small degree of melting would give rise to the

alkali olivine magmas, and higher degrees of melting would give tholeiitic magma (Gast, 1968; Philpotts and Schnetzler, 1970). Despite the apparent contradictions in production mechanisms, each of these models has its basis in fact. Experimental studies on the phase relationships of source rocks and basaltic liquids have been used in obtaining some of these models. Other approaches are based on trace element partitioning between the solid and the liquid during partial melting and crystal fractionation.

In any event, a comprehensive model must be able to explain the role of olivine fractional crystallization in the generative process. It has been clearly demonstrated (Powers, 1955; Tilley, 1960; Murata and Richter, 1966; Arakami and Moore, 1969; Wright, 1971; Wright and Fiske, 1971; and Bonhommet et al., 1977) that olivine fractional crystallization is an important process in controlling compositional variations among tholeiitic summit lavas. Variation diagrams of major element oxide abundances versus MgO indicate that the simple addition of olivine to a low (7%) MgO basalt can produce compositions equivalent to other observed magma compositions within the same volcano. The extent of olivine fractionation, however, is not well understood. The high (20-25%) MgO basalt compositions are suggested by some (e.g., Wright, 1971) to represent unevolved primary liquids, whereas others (Hart and Davis, 1978) consider these basalts to be olivine cumulates.

In view of these uncertainties on Hawaiian basalt generation, additional studies are needed to define the processes involved more fully. It must be mentioned that these uncertainties are not unique to the formation of Hawaiian magmas. Basalt compositions such as those observed in Hawaii are found throughout the world, suggesting that similar generative processes have evolved these basalts. In particular, the Hawaiian basalts are excellent examples for describing analogous basaltic magma generation for the following reasons: 1) Detailed working models on the final generative processes have been developed. These include the aforementioned olivine fractionation models and hybridization mixing models, such as those involving the Mauna Ulu variants (Wright and Fiske, 1971). Selection of appropriate samples for additional study is dependent on these models. 2) Petrological data, available on most of the magmas, provide constraints on proposed magmatic models. 3) The Hawaiian

basalts show no evidence of crustal contamination; therefore, the basaltic compositions will reflect basaltic generative process only.

The purpose of this study will be to present a quantitative geochemical model(s) of Hawaiian basalt generation. The modeling approach taken involves applying reliable rare earth element (REE) and trace element data from the tholeiitic olivine-controlled basalts to the theoretical equations that describe trace element behavior during partial melting and olivine fractional crystallization. It is widely accepted that the tholeiitic basalts can be related to the source region by these mechanisms. These postulated models will be complemented by major and minor element evaluations and may provide possible explanations as to how such variables as the melting depth, source composition, melt composition, the degree of melting, and olivine fractionation are involved in the production of the tholeiitic magma compositions observed on the Hawaiian Islands. Although a detailed model for alkali olivine basalt generation will not be pursued, a brief discussion concerning its origin will be presented. The models will be primarily limited to the chemical description of basalt formation; however, these may prove amenable to a partial geophysical description of the melting process.

Geographical and Geological Setting of the Hawaiian Islands

The basalts of this study erupted from seven major volcanoes comprising three islands of the Hawaiian group. The Mauna Kea, Kohala, and Kilauea-Mauna Ulu volcanic summit vents lie along a recently recognized sigmoidal fracture, the depth of which is believed to be a controlling factor in the chemical evolution of these volcanoes. The summit vents of Koolau, Lanai, Hualalai, and Mauna Loa are situated along a parallel sigmoidal ridge to the south [Fig. 2]. The cause of these fractures is thought to be the result of regional strain similar to that producing the parallel rift orientation on the isolated volcanoes (Fiske and Jackson, 1972).

The magmas from these volcanoes represent material derived from the mantle during the last 2.5 million years (m.y.). Koolau is the oldest of the studied volcanoes (2.5 m.y.) and constitutes the western part of

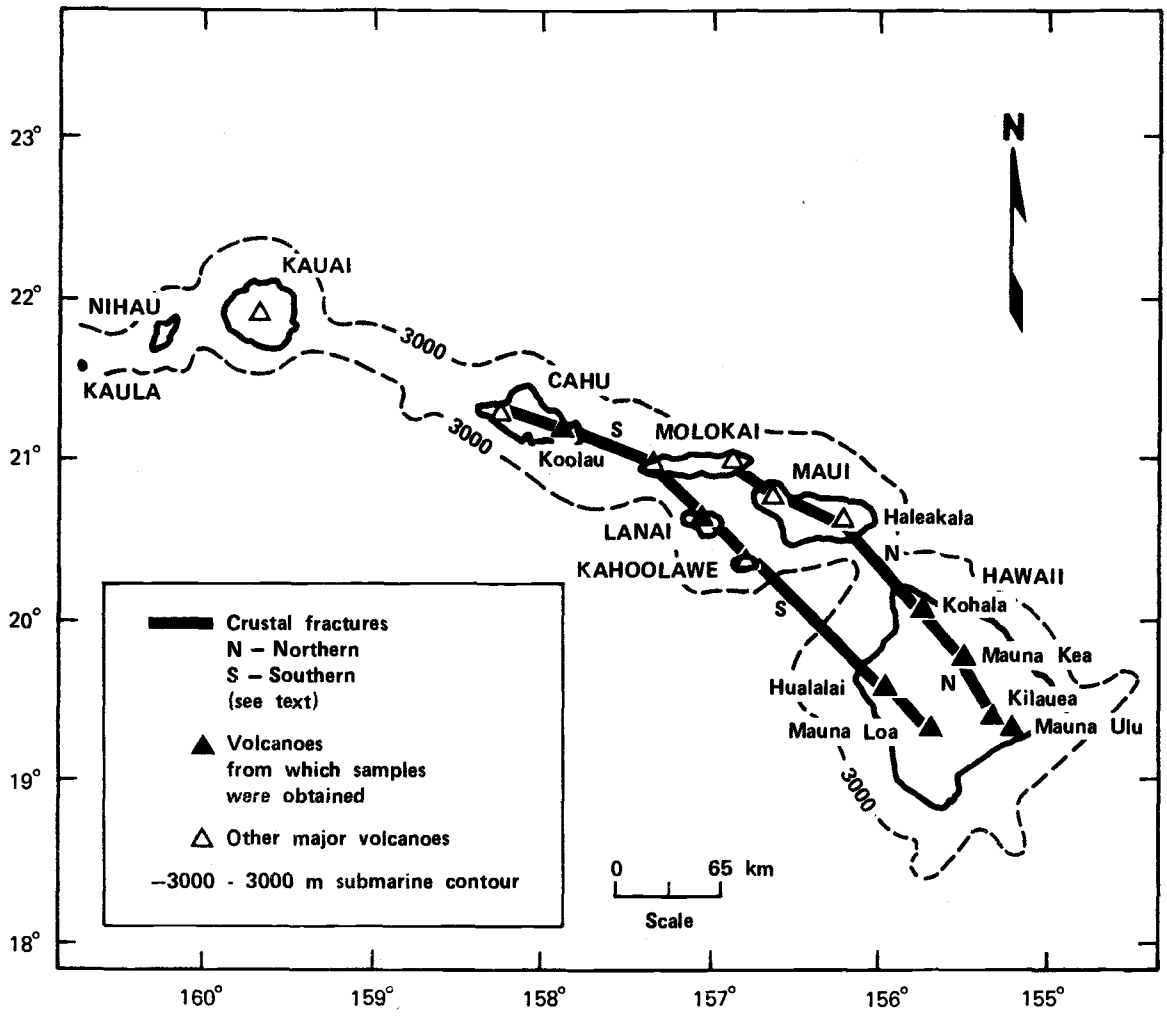

Fig. 2. Map of the Hawaiian Islands

the island of Oahu. Lanai was formed 1.3 m.y. ago following Maui I and Maui II. The remaining volcanoes comprise the island of Hawaii. Kohala, the oldest of these, has been dated at 0.45 m.y. The Hualalai and Mauna Kea volcanoes have approximate ages of 0.3 m.y. and 0.2 m.y., respectively. Mauna Loa and Kilauea-Mauna Ulu are currently active, although Mauna Loa is the older of the two. Kilauea's last eruption occurred in 1977. An eruption had been predicted for Mauna Loa in late 1978 or early 1979. The basalts from Mauna Ulu situated on Kilauea's east flank are from eruptive events that began in 1968 and ended abruptly in 1972.

The sequence of lava production in time is very similar from volcano to volcano within Hawaii. The primary mountain building episode occurs over ~0.5 m.y. and is dominated by the eruption of tholeiitic magmas that comprise over 99% of the volume of these volcanoes. In the latter part of this episode, less voluminous lavas (<1%), chiefly alkali olivine basalts, erupt and form a thin cap atop the volcano. These tholeiitic and alkalic basalts can be distinguished on the basis of alkali (Na_2O + K_2O) and silica (SiO_2) contents [Fig. 3]. In addition, as can be seen from Figure 3, there are also slight differences in tholeiitic magma compositions among the volcanoes.

Following a 1-2 m.y. period of dormancy and erosion, very small volumes of more undersaturated (low SiO_2) high alkaline basalts are erupted from scattered vents across the shield. These final magmas, which include basanite and nephenilite, are found only among the older volcanoes and frequently contain the garnet peridotite and pyroxenite xenoliths important in the description of basaltic generative processes.

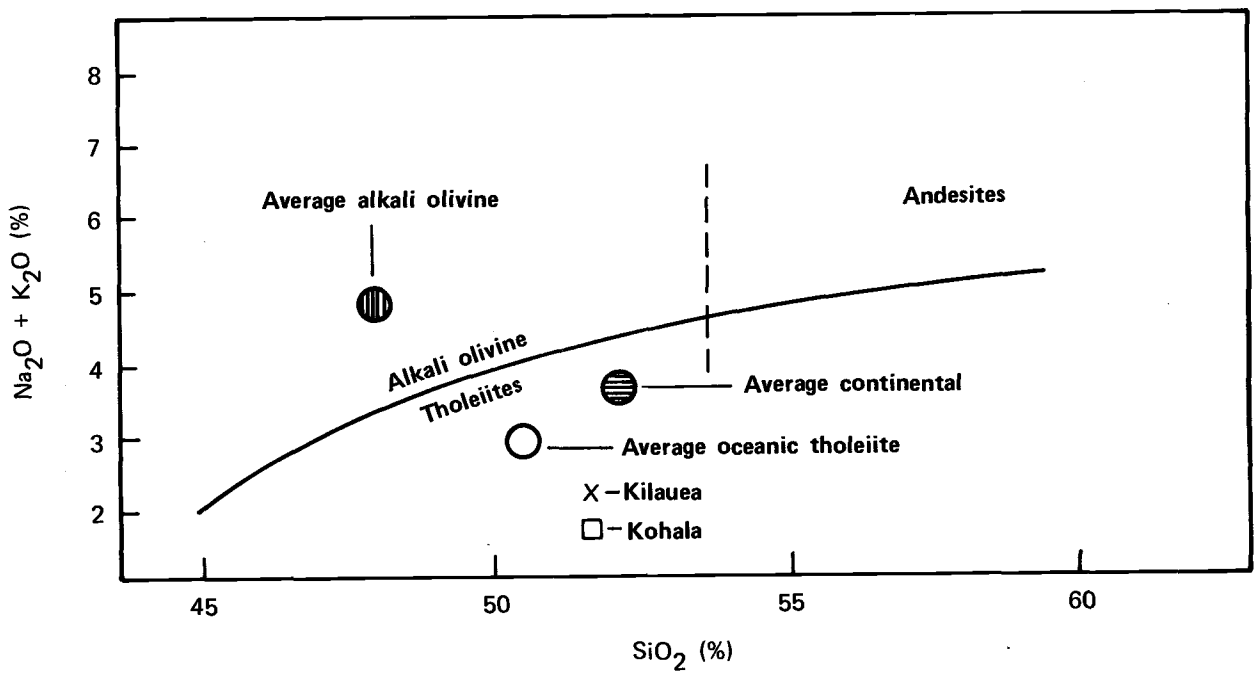

Fig. 3. Classification of tholeiitic and alkalic basalts based on alkali ($Na_2O + K_2O$) versus silica variation.

II. EXPERIMENTAL: SAMPLE PREPARATION AND ANALYSIS

The basalt samples received for analysis (see Appendix A) were fine- to medium-grained powders. About 500 mg of each powder were weighed into 2.5 dram polyethylene vials and heat-sealed following the sample preparation procedure given by Laul and Schmitt (1973). All activations were performed at the Radiation Center at Oregon State University (OSU) using a TRIGA Mark II nuclear reactor (Mark III core). Individual liquid and solid element standards were used as primary reference material in each activation. A duplicate set of CRB-1 (CRB-1 is an in-house standard obtained from the same quarry as was the U.S.G.S. BCR-1 standard) and USGS BHVO-1 were also analyzed in each activation set as secondary standards. Whenever CRB-1 values differed from values obtained from repeated analysis, sample abundances were recalculated using the CRB-1 values given in Table 5E.

Twenty-nine elements were determined in each of the basalts from Hawaii by instrumental neutron activation analysis (INAA). Briefly, the procedure of INAA involves activating the sample nuclides with thermal neutrons to produce radioactive gamma ray emitting radionuclides. Since each of the radionuclides being detected has a characteristic gamma ray energy and decay scheme, these can be distinguished by sequential counting using a Ge(Li) detector coupled to a multichannel analyzer system. The abundances of an element in a sample can be calculated by comparing the number of gamma rays emitted per unit time for an element to that emitted from the same element of known abundance. The direct correlation of count rates can only be made by 1) obtaining the same sample position relative to the crystal face of the detector and 2) assuming identical nuclear parameters between samples (i.e., neutron flux, isotopic abundance, etc.). For a more detailed discussion of the principles involved in neutron activation analysis, the reader is referred to the many excellent texts on the subject.

Table 1 is a compilation of the nuclides and their nuclear parameters used in the analysis. Two facilities of the OSU reactor were used in these determinations. The abundances of Al, Ti, Ca, Mg, V, Dy, Mn, and Na were obtained by activating the samples sequentially and reproducibly for a short period of time (3-5 min) in the pneumatic terminal facility

TABLE 1. COMPILATION OF NUCLIDES USED IN THE INAA OF HAWAIIAN SAMPLES.

Short-lived Radionuclides				
Target Isotope	Product Isotope	Half-life	Best Gamma-ray for Measurement (keV)	Associated Gamma Rays (keV)
164-Dy	165-Dy	2.32 hr	95	362
50-Ti	51-Ti	5.79 min	320	608, 928
26-Mg	27-Mg	9.46 min	1014	844
23-Na	24-Na	15.0 hr	1369	2754
51-V	52-V	3.75 min	1434	None
27-Al	28-Al	2.24 min	1779	None
55-Mn	56-Mn	2.579 hr	847	1810, 2113
48-Ca	49-Ca	8.73 min	3084	4072
Long-lived Radionuclides				
Target Isotope	Product Isotope	Half-life	Best Gamma-ray for Measurement (keV)	Associated Gamma Rays (keV)
146-Nd	147-Nd	11.06 days	91	531
152-Sm	153-Sm	46.8 hr	103	No major
151-Eu	152-Eu	12.7 yr	122	1408
140-Ce	141-Ce	32.5 days	145	None
176-Lu	177-Lu	6.71 days	208	113
238-U	239-Np[a]	72.1 days	298	879, 962
232-Th	233-Pa[b]	27.0 days	312	No major
50-Cr	51-Cr	27.7 days	320	None
74-Yb	175-Yb	4.19 days	398	283
180-Hf	181-Hf	42.4 days	483	133, 136, 346
130-Ba	131-Ba	11.8 days	496	124, 216, 373
84-Sr	85-Sr	64.85 days	514	No major
94-Zr	95-Zr	65.5 days	724	757
58-Ni	58-Co[c]	70.8 days	811	511
45-Sc	46-Sc	83.8 days	889	1121
58-Fe	59-Fe	44.6 days	1099	142, 192, 1292
59-Co	60-Co	5.27 yr	1173	1332
181-Ta	182-Ta	115.1 days	1221	100, 1121, 1189
23-Na	24-Na	15.0 hr	1369	2754
41-K	42-K	12.36 hr	1524	313
139-La	140-La	40.2 hr	1596	328, 487, 816

[a]Uranium is measured by counting 239-Np daughter of 239-U.

[b]Thorium is measured by counting 233-Pa daughter of 233-Th.

[c]Nickel is measured by counting 58-Co (n,p) reaction product of 58-Ni.

at OSU. The neutron flux selected was ~2×10^{11} neutrons cm^{-2} sec^{-1}. Following a decay period of 8-10 min, the gamma ray emissions of the short-lived radionuclides (Table 1, Part A) were counted (Table 2). The cooling times and the counting length (400 sec) used for these determinations were chosen to give optimum count rates with consideration given to counting short-lived radionuclides in the presence of long-lived nuclides. Following these counts, the samples are again counted for 1000-2000 sec for Dy, Mn, and Na (Table 2).

A major problem encountered in the determination of one of the short-lived nuclides, Mg, arises because of the additional production of ^{27}Mg by an (n,p) reaction involving ^{27}Al. The amount of ^{27}Mg produced by this reaction is dependent upon the fast neutron flux of the reactor and was determined in each activation set by activating a pure Al_2O_3 standard. During the course of the investigation, the reactor fuel elements were replaced and also relocated giving three contribution effects:

1. before replacement: 100% Al_2O_3 → 11.8% MgO
2. after replacement: 100% Al_2O_3 → 35.8% MgO
3. after relocation: 100% Al_2O_3 → 20.3% MgO

Other (n,p) reactions producing additional nuclides to those produced by (n,γ) reactions are $^{24}Mg(n,p)^{24}Na$ and $^{28}Si(n,p)^{28}Al$. These were neglected because of the small contribution of each to the relatively large abundances of the primary element.

The remaining elements, Fe, Na, K, Cr, Co, Ni, Ba, Sr; the REE's (La, Ce, Nd, Sm, Eu, Tb, Yb, Lu); and Sc, Hf, Ta, Th, U, and Zr were determined by activating the samples simultaneously in the rotating rack facility with a neutron flux of ~3×10^{12} neutrons $cm^{-2}sec^{-1}$ for 3 hours. The half-lives and gamma ray energies of these nuclides are given in Table 1 (Part B) with the counting schedule presented in Table 3.

The count shortly after activation (24-36 hrs) is primarily for determining K. The background and associated Compton due to Na is too large to give accurate results for the other elements. La and Sm, and occasionally K, can be determined in the first count of 2000 sec, and this count provides an additional check for these elements. The second count is delayed for about a week following irradiation to allow for the

TABLE 2. HYPOTHETICAL INAA PROCEDURE IN THE ANALYSIS OF FIVE 500 mg HAWAIIAN ROCK SAMPLES FOR Dy, Ti, Mg, Na, V, Al, Mn, AND Na USING TWO SAMPLES.

Sample no.	Time (min)[a]			
	T_1	T_2	T_3	T_4 (b)
Part 1[c]				
Sample #1	0.00	3.00	12.00	19.67
Sample #2	9.00	12.00	21.00	28.67
Standard #1	18.00	21.00	30.00	37.67
Sample #3	27.00	30.00	39.00	46.67
Sample #4	36.00	39.00	48.00	55.67
Standard #2	45.00	48.00	57.00	64.67
Part 2A[d]				
Sample #1	. . .	. . .	180.00	218.33
Sample #2	. . .	. . .	220.00	258.33
Sample #3	. . .	. . .	260.00	298.33
Sample #4	. . .	. . .	300.00	338.33
Standard #1	. . .	. . .	340.00	378.33
Part 2B[e]				
	. . .	. . .	0.00	38.33
	. . .	. . .	40.00	78.33
	. . .	. . .	80.00	118.33
	. . .	. . .	120.00	158.33
	. . .	. . .	160.00	198.33

NOTES: Flux = 2×10^{11} neutrons $cm^{-2}sec^{-1}$. Activation period is 3 minutes.

[a] T_1 – irradiation begins; T_2 – irradiation ends; T_3 – counting begins; T_4 – counting ends.

[b] Assumes 15% mean dead time.

[c] Radionuclides measured: 51-Ti, 27-Mg, 52-V, 28-Al, and 49-Ca. Analyzer calibrated at ~2 keV/channel. Delay period = 9 min. Count period = 400 sec.

[d] Radionuclides measured: 164-Dy and 55-Mn. Analyzer calibrated at 0.5 keV/channel. Delay period = 3 hr. Count period = 2000 sec.

[e] Nuclide measured: 24-Na. Analyzer calibrated at 2 keV/channel. Delay period = 1 day. Count period is the next day.

TABLE 3. COUNTING SCHEDULE FOR THE DETERMINATION OF THE LONG-LIVED NUCLIDES IN HAWAIIAN ROCKS.

Count Designation	Decay Period	Counting Period (sec)	Radionuclides Measured (a)
A	24-36 hrs	1000	42-K (24-Na)
First	3-4 days	2000	153-Sm, 24-Na, 141-La (42-K)
Second	7 days	10,000	147-Nd, 153-Sm, 177-Lu, 239-Np, 233-Pa, 175-Yb, 131-Ba, 24-Na, 141-La (42-K, 151-Eu, 141-Ce, 160-Tb, 181-Hf, 95-Zr, 58-Co, 59-Fe, 60-Co, 182-Ta)
Third	Immediately following Second	20,000	Same as First count, except 42-K
Fourth	40-50 days	40,000	151-Eu, 141-Ce, 160-Tb, 181-Hf, 95-Zr, 58-Co, 59-Fe, 60-Co, 182-Ta (147-Nd, 131-Ba)

NOTES: Flux = $\sim 3 \times 10^{12}$ neutrons $cm^{-2}sec^{-1}$. Activation period is 3 hr.

[a]The radionuclides within the parentheses indicate marginal measurement. Marginal measurement refers to a determination that either (a) has a large uncertainty due to a large background or (b) is not as precise as in another count because of interferences, background variation, etc.

decay of 24-Na. The third count set begins immediately after the first to provide at least two determinations for each element. The fourth and final count is made approximately one month after irradiation and gives the best results for the long-lived elements due to the reduced Compton continuum background.

Although the use of Ge(Li) detectors is able to resolve most of the peaks in question, some interfering peaks remain which either cannot be separated or would require a change in analyzer parameters. In most cases, the interferences can be approximated quite accurately by activating a pure sample and obtaining a peak-to-peak ratio. The interferences taken into consideration are given in Table 4.

The two primary interferences observed in these samples are the 142 keV ^{59}Fe in the 145 keV ^{141}Ce and the 300 kev ^{233}Pa (daughter of ^{232}Th) in the 298 keV ^{160}Tb. In most cases, the Ce and Fe peaks were partially resolved. Two methods were employed to determine Ce; both methods used gave nearly identical results, well within the counting statistic uncertainty (1σ). The first method involved integrating a partial (half-peak) Ce peak on the high energy side, and the second involved integrating the doublet peak and subtracting the Fe contribution. The contribution due to Fe was obtained by activating a pure Fe sample and applying the ratio determined for the 142 peak between the peaks at 192 keV, 1099 keV, and 1292 keV.

The Pa(Th) interference in the Tb peak was obtained in a manner similar to the second method for the Ce-Fe pair. A pure Th standard was activated, and the ratio between the 300 and 312 keV peak was applied to each Pa(Th) peak in the sample. It will be noted that these ratios are dependent upon the efficiency spectra of the detector and hence were determined for each count set.

Other peak interferences which were less important but which were accounted for are the following: 1) the 124 keV Ba^{B1} peak in the 122 keV ^{152m}Eu (the use of the 1408 keV Eu peak, which is interference-free, gave the best value for Eu determinations); 2) the 811 keV ^{152}Eu peak in the 811 keV ^{58}Co(Ni); and 3) the 758 keV ^{152}Eu peak in the 757 keV ^{95}Zr.

The main interference due to the radioactive decay of a parent nuclide that contributes a daughter radionuclide in addition to that used in these analyses is ^{177}Yb producing ^{177}Lu. To correct for this

TABLE 4. PHOTOPEAK INTERFERENCES CONSIDERED IN THE ANALYSIS OF HAWAIIAN SAMPLES.

Radionuclide	Gamma Ray (keV)	Interference		Comment: Correction Applied
		Radionuclide	Energy (keV)	
27-Mg	1014	27-Mg	1014	Additional production via 27-Al (n,p) 27-Mg; see text for correction
147-Nd	91	153-Sm others	90 85-90	Primary interference due to variable background; one-channel background taken and abundance normalized to standard (std) with similar Sm-Nd abundances
153-Sm	103	239-Np	104 106	Not significant in low U (<1 ppm) samples; ratio of 104 + 106 to 228 peak in U std applied to sample
152-Eu	122	131-Bu	124	Ratio of 124 to 496 peak in Bu std applied to sample; otherwise 1408 keV Eu peak can be used
141-Ce	145	59-Fe 175-Yb	142 145	Two corrections applied for Fe; see text. Yb interference not significant in final count.
177-Lu	208	177-Lu	208	Additional production from daughter of 177-Yb; see text for correction
160-Tb	298	233-Pa	300	Ratio of 300 to 312 peak in Th std applied to sample[a]
233-Pa	312	160-Tb	310	Ratio of 310 to 298 peak in Tb std applied to sample[a]
95-Zr	724 757	154-Eu	724 757	Ratios of 724 and 757 to 873 peak in Eu std applied to sample
58-Co	811	152-Eu	811	Ratio of 811 to 1408 peak in Eu std applied to sample

[a]As a first-order approximation, the smaller correction factor between these two peaks was applied first (i.e., the Tb contribution in the Pa peak was subtracted; then the 300/312 Pa ratio was applied to the resultant peak and the net Tb peak calculated).

contribution, the amount of Lu produced in the Yb standard was determined, and the Lu ppm/Yb ppm ratio obtained was applied to each sample.

Data reduction of the gamma ray spectrum was performed by computer. The program was written by Borchardt et al. (1970) and edited by Dave Cawfield, Dr. M.-S. Ma, and J. R. Budahn at OSU. All of the photopeaks in each sample spectrum that fit the statistical criteria were calculated using the program, but abundance calculations were carried out only on selected peaks. Problematic peaks (those with interferences, low intensities, etc.) were hand-integrated.

Errors given for each element in the analysis represent propagated 1σ counting uncertainties due to photopeak statistical errors and were calculated by the following equation:

$$1\sigma = \sqrt{T + \frac{N^2}{4}\left(\frac{c_1}{n_1^2} + \frac{c_2}{n_2^2}\right)}.$$

where T = total counts in peak and background channels
N = number of channels in peak
c_1 = number of counts in left background channels
n_1 = number of left background channels (3)
c_2 = number of counts in right background channels
n_2 = number of right background channels (3)

III. RESULTS AND DISCUSSION

The major, minor and trace element data obtained for the basalts are given in Table 5A-E. A brief sample description for each is presented in Appendix A. Most of the samples chosen for analysis are tholeiitic in nature and contain 7-10% MgO. These basalts lie on the low MgO end of the olivine-control lines that characterize a majority of the Hawaiian summit lavas (Powers, 1955; Tilley, 1960; Murata and Richter, 1966; Arakami and Moore, 1969; Wright and Fiske, 1971; and Bonhommet et al., 1977). Tholeiitic olivine-controlled basalts such as these have been suggested to retain compositions that can easily be related to magmas that have been derived directly from melting the mantle. However, because of the uncertainty regarding the high MgO basalts (whether they are of cumulate origin or are primary liquids), none were chosen for analysis. The low MgO tholeiitic basalts are more ideal for modeling since these basalts are the most olivine fractionated magmas and are least likely to contain cumulate olivine. Other basalt types analyzed included some "differentiated" and highly fractionated lavas. These basalts are the result of highly complicated fractionation patterns and hence would be difficult to model. For these reasons, the following discussion will be directed toward identifying the tholeiitic basalts.

Individual Volcanoes

In discussing the chemistry of the samples obtained from each volcano, evidence will be presented to identify the basalts that 1) are tholeiitic and may be related to other tholeiitic basalts within the same volcano by olivine fractionation; 2) are tholeiitic but are derived by more complex fractionation of plagioclase, pyroxene, etc.; and 3) are derived by "secondary" partial melting events (i.e., alkali basalts). Evidence will rely on major element abundances and REE abundances and ratios. In this manner, the basalt compositions that are of interest in this study, that is, representative mantle-derived material (those of Group 1), will be obtained for use in modeling.

TABLE 5A. ELEMENTAL ABUNDANCES IN HAWAIIAN SAMPLES.

Element	Sample Number											
	P71-5 (1)	P71-13 (2)	C66 (3)	C53 (4)	C62 (5)	P71-4 (6)	C70 (7)	P71-3 (8)	72M-36 (9)	H71-3 (10)	72M-42 (11)	H71-10 (12)
TiO_2 (%). . .	2.14	2.63	2.21	2.10	2.29	2.32	3.01	2.81	2.08	2.35	1.81	1.52
Al_2O_3 (%) . .	13.4	14.1	13.7	14.5	14.8	14.0	15.9	13.5	17.5	16.5	17.2	18.3
FeO (%)[a]. . .	11.3	11.9	11.1	10.6	11.0	10.5	11.3	12.3	9.1	10.6	8.3	8.3
MgO (%) . . .	9.3	9.3	8.2	8.1	7.3	6.2	5.9	5.3	3.7	3.2	2.6	2.5
CaO (%) . . .	10.8	10.2	10.3	11.6	11.3	10.8	11.6	10.1	5.1	6.3	4.5	4.1
Na_2O (%). . .	2.11	2.01	2.04	2.18	2.13	2.12	3.41	2.32	5.66	5.47	6.25	5.87
K_2O (%) . . .	0.09	0.08	0.24	0.13	0.23	0.04	1.20	0.20	1.4	1.8	1.8	1.8
MnO (%) . . .	0.16	0.17	0.19	0.19	0.19	0.17	0.21	0.16	0.23	0.21	0.23	0.23
Cr (ppm). . .	510	416	375	375	320	300	240	265	20	14	30	13
Co (ppm). . .	48	48	[60]	52	[57]	38	[52]	48	8	12	6	7
Ni (ppm). . .	200	200	140	100	40	85	110	200	30	27	40	20
V (ppm) . . .	286	324	295	290	320	326	270	360	39	60	22	15
Sr (ppm). . .	385	400	375	320	285	400	533	385	1600	1805	1930	1150
Ba (ppm). . .	105	60	125	115	105	125	400	95	765	705	890	960
La (ppm). . .	9.4	11.1	10.0	9.1	9.1	10.0	33.9	21.5	62.0	59.5	68.4	82.8
Ce (ppm). . .	24.5	29.3	26.3	26.0	25.7	26.0	71	39.4	140	138	155	175
Nd (ppm). . .	19	21	19	19	21	20	47	39	83	90	95	99
Sm (ppm). . .	5.39	5.66	5.34	5.06	5.20	5.21	10.1	9.35	17.0	18.4	17.0	17.0
Eu (ppm). . .	1.83	1.95	1.70	1.72	1.73	1.77	3.10	3.20	5.31	5.58	5.19	5.01
Tb (ppm). . .	0.85	0.90	0.96	0.90	0.93	0.90	1.3	1.6	1.9	2.1	1.9	2.3
Dy (ppm). . .	5.6	4.3	4.6	4.5	5.4	4.8	7.3	7.3	9.1	7.0	8.7	9.9
Yb (ppm). . .	2.18	2.16	2.12	1.98	2.29	2.17	3.01	3.97	4.02	3.92	3.88	4.40
Lu (ppm). . .	0.28	0.28	0.29	0.28	0.33	0.27	0.42	0.54	0.55	0.48	0.51	0.60
Sc (ppm). . .	31	32	32	31	32	30	24	31	5.7	7.3	4.9	4.8
Hf (ppm). . .	4.0	4.3	4.3	3.9	5.0	4.0	7.9	5.0	11.2	10.8	13.0	19.3
Ta (ppm). . .	0.5	0.7	[2.6]	[1.6]	[2.3]	0.7	[2.6]	0.7	4.0	3.5	4.6	5.3
Th (ppm). . .	0.3	0.4	0.5	0.4	0.4	0.4	0.5	0.5	3.9	3.6	4.2	6.7
U (ppm) . . .	0.14	0.14	0.2	0.1	0.1	0.14	0.2	0.4	1.5	2.1	2.2	3.3
Zr (ppm). . .	140	150	170	130	155	150	350	165	670	580	590	970
Volcano	Kohala	Kohala	Kohala	Kohala	Kohala	Kohala	Kohala	Kohala	Kohala	Kohala	Kohala	Kohala

NOTES: Values in brackets may be high because of contamination.

[a]Total Fe as FeO.

TABLE 5B. ELEMENTAL ABUNDANCES IN HAWAIIAN SAMPLES.

Element	Sample Number											
	72M-33 (13)	72M-35 (14)	C74 (1)	710826-1 (2)	741011-11 (3)	720803-9 (4)	720819-1 (5)	720817-1 (6)	720821-2 (7)	710818-1 (8)	720900-1 (9)	710805-2 (10)
TiO_2 (%). . .	2.01	0.76	2.97	2.80	2.76	4.04	2.72	2.81	3.33	3.56	4.17	2.48
Al_2O_3 (%) . .	17.0	18.2	14.9	13.4	14.1	15.0	13.1	14.3	14.3	13.6	13.6	17.0
FeO (%)[a]. . .	9.0	6.3	13.0	11.6	12.2	12.2	12.3	12.2	12.2	13.4	13.3	10.2
MgO (%) . . .	1.7	0.4	6.7	7.7	5.4	5.2	6.6	6.3	5.1	4.9	4.0	3.8
CaO (%) . . .	5.8	2.3	10.8	12.3	11.5	10.5	10.8	11.2	10.7	10.6	9.2	6.1
Na_2O (%). . .	5.59	7.20	2.30	2.36	2.40	2.81	2.56	2.66	2.76	2.80	3.19	4.85
K_2O (%) . . .	1.6	2.3	0.17	0.46	0.78	0.59	0.93	0.71	0.45	0.86	1.0	1.9
MnO (%) . . .	0.20	0.22	0.22	0.18	0.17	0.18	0.17	0.18	0.18	0.19	0.19	0.21
Cr (ppm). . .	26	15	65	400	105	110	310	150	65	35	28	20
Co (ppm). . .	12	3	[69]	50	48	44	52	47	44	48	40	15
Ni (ppm). . .	30	25	90	190	90	95	190	105	90	75	45	20
V (ppm) . . .	15	4	350	314	325	444	318	336	367	386	437	91
Sr (ppm). . .	1430	1485	430	550	500	665	615	610	680	530	495	1120
Ba (ppm). . .	675	895	155	155	200	200	220	190	290	260	300	615
La (ppm). . .	60.3	60.8	14.6	14.2	16.2	15.0	20.3	19.9	23.0	21.6	29.3	48.5
Ce (ppm). . .	134	128	37.0	36.0	40.5	36.8	48.3	46.1	55.3	53.7	68.5	97
Nd (ppm). . .	84	60	26	27	30	27	33	34	40	36	44	73
Sm (ppm). . .	15.2	12.5	7.30	6.10	6.40	6.23	6.96	6.97	7.91	8.03	9.95	13.6
Eu (ppm). . .	4.61	4.20	2.44	2.21	2.14	2.46	2.30	2.49	2.59	2.73	3.08	4.37
Tb (ppm). . .	1.7	1.9	1.1	0.95	0.92	0.93	0.94	0.95	0.98	1.1	1.4	1.65
Dy (ppm). . .	9.8	9.4	6.5	4.8	5.3	4.4	4.2	5.7	5.4	4.9	6.7	7.8
Yb (ppm). . .	3.59	3.83	2.33	2.03	2.05	2.04	2.02	2.16	2.14	2.24	2.88	3.31
Lu (ppm). . .	0.47	0.52	0.35	0.26	0.28	0.27	0.25	0.29	0.33	0.30	0.41	0.50
Sc (ppm). . .	6.5	2.4	32	30	30	30	30	31	25	29	25	8.9
Hf (ppm). . .	12.2	17.0	5.1	4.9	5.1	5.0	5.2	5.1	6.1	6.4	7.6	10.7
Ta (ppm). . .	4.2	5.4	[3.4]	1.0	1.4	1.3	1.4	1.3	1.8	1.8	2.2	3.5
Th (ppm). . .	4.9	6.1	1.0	1.0	1.1	1.1	1.2	1.2	1.6	1.7	2.0	3.6
U (ppm) . . .	2.5	1.3	0.4	0.4	0.4	0.7	0.5	0.2	0.6	0.4	1.0	2.8
Zr (ppm). . .	550	770	255	190	230	240	375	225	265	286	301	515
Volcano	Kohala	Kohala	Mauna Kea	Mauna Kea	Mauna Kea	Mauna Kea	Mauna Kea	Mauna Kea	Mauna Kea	Mauna Kea	Mauna Kea	Mauna Kea

NOTES: Values in brackets may be high because of contamination.

[a]Total Fe as FeO.

TABLE 5C. ELEMENTAL ABUNDANCES IN HAWAIIAN SAMPLES.

Element	Sample Number											
	710810-5 (11)	710827-1 (12)	720803-5 (13)	710826-2 (14)	D101471 (1)	D101473 (2)	D101474 (3)	D101472 (4)	0X069 (1)	0X068 (2)	0X067 (3)	0X078 (4)
TiO_2 (%). . .	2.32	2.73	2.72	2.38	1.84	2.38	2.20	2.23	1.76	2.22	2.38	2.28
Al_2O_3 (%) . .	16.8	16.6	16.6	16.6	14.9	14.8	13.9	15.2	14.6	14.5	14.3	15.0
FeO (%)[a]. . .	9.5	10.1	10.5	10.0	9.8	10.2	10.0	10.5	10.3	10.8	10.7	10.7
MgO (%) . . .	3.6	3.3	2.8	2.5	9.2	6.7	6.4	5.7	8.5	7.6	6.9	5.4
CaO (%) . . .	5.9	6.8	6.6	6.2	8.4	8.4	8.4	9.6	9.0	9.5	9.9	9.7
Na_2O (%). . .	5.17	4.52	4.76	4.80	2.56	3.01	2.42	2.39	2.36	2.25	2.42	2.47
K_2O (%) . . .	1.9	2.1	1.7	2.0	0.40	0.33	0.65	0.40	0.32	0.34	0.47	0.45
MnO (%) . . .	0.21	0.20	0.20	0.20	0.17	0.16	0.16	0.17	0.18	0.19	0.19	0.17
Cr (ppm). . .	20	15	25	15	525	200	225	285	375	305	225	200
Co (ppm). . .	12	16	17	14	44	37	39	40	45	43	41	39
Ni (ppm). . .	20	30	20	15	305	110	120	115	235	125	140	100
V (ppm) . . .	57	110	116	90	225	275	270	267	260	297	313	278
Sr (ppm). . .	1130	1170	1260	1210	420	510	380	420	335	350	350	365
Ba (ppm). . .	600	590	600	600	95	165	145	125	85	110	115	140
La (ppm). . .	58.3	45.8	44.7	48.7	8.11	13.3	11.5	10.8	7.45	9.40	12.1	12.8
Ce (ppm). . .	125	96	95	108	22.5	33.7	29.6	30.3	23.4	27.7	32.4	29.5
Nd (ppm). . .	81	69	68	67	18	25	23	23	18.5	24	27	25.5
Sm (ppm). . .	15.3	13.9	14.0	14.9	4.58	6.67	5.63	5.69	4.49	5.36	5.82	6.51
Eu (ppm). . .	5.19	4.49	4.49	4.64	1.66	2.15	1.86	1.93	1.51	1.79	1.90	2.27
Tb (ppm). . .	1.9	1.7	1.8	1.8	0.73	0.94	0.80	0.87	0.71	0.85	0.88	1.0
Dy (ppm). . .	10.6	8.7	9.1	6.7	3.8	4.7	4.4	4.7	3.9	4.2	5.0	4.7
Yb (ppm). . .	3.76	3.31	3.36	3.24	1.67	1.80	1.70	1.79	1.84	1.97	2.11	2.33
Lu (ppm). . .	0.50	0.43	0.48	0.40	0.22	0.25	0.25	0.27	0.28	0.29	0.31	0.33
Sc (ppm). . .	7.5	9.7	10.5	8.5	23	23	23	28	26	29	28	27
Hf (ppm). . .	12.9	10.2	10.2	11.3	2.6	4.1	3.5	3.6	2.7	3.3	3.8	3.6
Ta (ppm). . .	3.9	3.3	3.2	3.6	0.4	0.6	0.5	0.6	0.5	0.4	0.6	0.65
Th (ppm). . .	4.4	3.5	3.3	3.8	0.2	0.6	0.5	0.5	0.25	0.4	0.5	0.5
U (ppm) . . .	1.6	1.9	2.5	1.9	[0.6]	0.5	0.3	0.3	0.25	0.2	0.8	0.4
Zr (ppm). . .	590	420	450	500	180	220	185	270	170	135	100	250
Volcano	Mauna Kea	Mauna Kea	Mauna Kea	Mauna Kea	Koolau	Koolau	Koolau	Koolau	Lanai	Lanai	Lanai	Lanai

TABLE 5D. ELEMENTAL ABUNDANCES IN HAWAIIAN SAMPLES.

Element	Sample Number											
	TLW67-56 (1907)	TLW67-62 (1942)	TLW67-65 (1899)	TLW67-67 (1935)	TLW67-68 (1942)	TLW67-73 (1950)	TLW67-77 (1919)	ML775-26 (1975)	TLW67-29 (PH)	TLW67-70B (PH)	TLW67-119 (PH)	TLW67-123 (PH)
TiO_2 (%). . .	2.29	2.03	1.97	2.01	2.10	2.29	2.31	1.84	2.10	2.09	2.18	2.02
Al_2O_3 (%) . .	14.0	13.9	14.1	14.0	13.9	14.2	13.8	14.7	14.0	14.1	14.0	13.9
FeO (%)[a]. . .	11.1	11.1	11.1	11.0	11.1	11.2	10.7	11.1	10.5	10.8	10.8	10.9
MgO (%) . . .	7.3	8.8	7.5	7.1	7.1	7.0	7.3	7.1	6.3	7.4	6.6	6.4
CaO (%) . . .	10.2	10.2	10.3	10.1	10.4	10.9	9.9	10.7	11.0	9.5	10.5	9.8
Na_2O (%). . .	2.27	2.40	2.36	2.36	2.40	2.42	2.23	2.33	2.33	2.36	2.29	2.31
K_2O (%) . . .	0.37	0.38	0.35	0.37	0.32	0.41	0.36	0.36	0.40	0.43	0.43	0.40
MnO (%) . . .	0.15	0.17	0.16	0.16	0.17	0.16	0.15	0.20	0.16	0.15	0.16	0.15
Cr (ppm). . .	260	300	235	250	260	220	240	245	222	237	185	263
Co (ppm). . .	43	43	43	42	43	43	42	42	40	40	40	42
Ni (ppm). . .	125	75	75	90	85	105	100	65	105	85	100	80
V (ppm) . . .	282	278	282	283	282	282	280	297	279	290	291	285
Sr (ppm). . .	250	330	280	260	350	285	305	290	349	361	383	338
Ba (ppm). . .	50	60	60	70	70	100	80	95	85	91	120	112
La (ppm). . .	8.6	8.8	8.6	8.8	8.8	8.9	8.8	9.0	9.8	10.9	10.6	9.5
Ce (ppm). . .	23.5	24.6	23.6	24.5	23.2	23.8	23.4	24.6	26.1	28.7	26.8	25.5
Nd (ppm). . .	20.0	20.1	20.4	18.4	20.4	19.8	21.4	20.2	21	22	21	19
Sm (ppm). . .	4.85	4.86	4.87	4.85	4.88	5.00	4.79	4.97	4.88	5.41	5.20	4.89
Eu (ppm). . .	1.75	1.73	1.75	1.71	1.68	1.75	1.70	1.70	1.78	1.85	1.79	1.74
Tb (ppm). . .	0.79	0.74	0.74	0.71	0.75	0.75	0.76	0.84	0.77	0.80	0.79	0.78
Dy (ppm). . .	4.4	5.4	4.0	4.3	4.4	4.6	4.6	5.3	4.8	5.0	4.7	4.8
Yb (ppm). . .	2.03	1.96	1.99	1.83	1.97	2.08	2.00	1.92	1.99	1.99	2.00	1.92
Lu (ppm). . .	0.28	0.27	0.25	0.27	0.28	0.31	0.25	0.30	0.23	0.25	0.27	0.25
Sc (ppm). . .	30	30	29	29	29	29	29	29	28	29	29	28
Hf (ppm). . .	3.3	3.6	3.6	3.3	3.3	3.3	3.6	3.1	3.6	3.6	3.4	3.2
Ta (ppm). . .	0.5	0.6	0.6	0.6	0.6	0.5	0.5	0.6	0.6	0.7	0.7	0.6
Th (ppm). . .	0.4	0.3	0.3	0.4	0.4	0.4	0.6	0.4	0.4	0.4	0.45	0.4
U (ppm) . . .	0.2	0.2	0.1	0.1	0.2	0.2	0.2	0.2	0.1	0.1	0.1	0.2
Zr (ppm). . .	150	200	160	120	[55]	150	120	150	95	95	115	110
Volcano	Mauna Loa	Mauna Loa	Mauna Loa	Mauna Loa	Mauna Loa	Mauna Loa	Mauna Loa	Mauna Loa	Mauna Loa	Mauna Loa	Mauna Loa	Mauna Loa

NOTES: Values in brackets may be high because of contamination.

[a]Total Fe as FeO.

TABLE 5E. ELEMENTAL ABUNDANCES IN HAWAIIAN SAMPLES.

Element	Sample Number										Estimated Errors Due to Counting Statistics (%)[b]
	TLW67-59 (1887)	DAS69 1-3 Variant #1	DAS69 78-9 Variant #2	DAS69 8-1 Variant #3	DAS70 1213-25 Variant #4	DAS71 1213-134 Variant #5	DAS71 1213-134 Variant #5 (a)	Kan FL 1801	CRB-1	BHVO-1	
TiO_2 (%)	1.98	2.52	2.33	2.51	2.58	2.47	2.31	2.24	2.20	2.75	5
Al_2O_3 (%)	13.8	12.7	12.8	13.3	13.3	13.6	13.63	15.0	13.7	13.9	2
FeO (%)[c]	10.9	11.1	11.2	11.4	11.2	11.5	11.20	12.7	12.3	11.0	2
MgO (%)	7.1	9.7	10.0	9.4	8.3	7.3	8.14	8.3	3.3	7.3	8
CaO (%)	9.9	10.2	10.4	10.7	10.8	10.4	11.05	9.3	6.9	11.6	10
Na_2O (%)	2.34	2.23	2.22	2.27	2.26	2.34	2.22	2.92	3.30	2.29	2
K_2O (%)	0.30	0.47	0.50	0.46	0.42	0.40	0.41	1.2	1.7	0.46	10
MnO (%)	0.17	0.16	0.16	0.16	0.16	0.17	0.17	0.21	0.176	0.17	5
Cr (ppm)	285	413	451	409	391	393	. . .	390	12	266	5-30
Co (ppm)	44	50	53	49	48	48	. . .	55	36	44	2
Ni (ppm)	75	220	235	235	150	135	. . .	160	<10	110	10-30
V (ppm)	261	294	306	321	322	304	. . .	325	410	328	10
Sr (ppm)	294	322	381	379	339	368	. . .	515	330	445	15
Ba (ppm)	65	113	129	118	108	127	. . .	365	720	150	15
La (ppm)	8.0	13.9	13.8	13.9	13.0	12.1	. . .	19.0	25.1	15.0	2
Ce (ppm)	22.1	33.8	34.7	34.4	32.6	30.5	. . .	34.9	53.5	39.0	7
Nd (ppm)	18.4	23	24	25	23	23	. . .	20	29	25.5	5-10
Sm (ppm)	4.60	5.79	5.88	5.91	5.51	5.48	. . .	5.02	6.75	6.37	2
Eu (ppm)	1.64	1.95	1.95	1.95	2.00	1.90	. . .	1.65	1.97	2.05	5
Tb (ppm)	0.74	0.88	0.78	0.80	0.85	0.82	. . .	0.86	0.93	0.91	10
Dy (ppm)	4.6	4.4	4.6	4.3	4.9	4.6	. . .	5.5	5.9	5.2	15
Yb (ppm)	1.92	1.75	1.93	1.88	1.90	1.92	. . .	1.92	3.45	1.97	5
Lu (ppm)	0.25	0.26	0.26	0.26	0.26	0.28	. . .	0.28	0.51	0.28	5
Sc (ppm)	28	29	29	29	29	30	. . .	25	32	30	2
Hf (ppm)	2.9	3.8	4.0	4.1	4.0	4.0	. . .	3.4	4.9	4.5	5
Ta (ppm)	0.55	1.0	1.0	1.0	1.0	0.9	. . .	1.5	0.78	1.3	10
Th (ppm)	0.35	0.7	0.8	0.8	0.7	0.7	. . .	1.3	5.6	1.0	10
U (ppm)	<0.1	0.3	0.2	0.3	0.2	0.2	. . .	0.9	1.8	0.3	25
Zr (ppm)	120	170	170	170	125	120	. . .	250	178	200	30
Volcano	Mauna Loa	Mauna Ulu	Mauna Ulu	Mauna Ulu	Mauna Ulu	Mauna Ulu	Mauna Ulu	Hualalai	CRB-1	BHVO-1	

[a] From Wright et al. (1975).

[b] These estimated errors refer to all analyses given in tables 5A through E except data for DAS-71-1213-134 from Wright et al. (1975).

[c] Total Fe as FeO.

Northern Fracture

Kohala - Fourteen samples from this volcano were analyzed (Table 5A-B). Six of these can be classified as tholeiitic olivine-controlled basalts on the basis of their MgO (6.2-9.3% MgO) and major element abundances. Chromium abundances range from 300 ppm in the low MgO basalt to 510 ppm in the high MgO basalt. Although the basalts represent flows erupted over 0.2 m.y., only slight differences are observed in REE abundances (27X-33X La and 9.1-10.5X Yb; Fig. 4C where X ≡ times the respective chondrite meteorite abundance). Compositional similarities are also exhibited in Sc, Hf, Ta,[1] and Th abundances. For these reasons, it will be suggested that these basalts are olivine-derived products of very similar or the same generative event(s) involving mantle melting.

Two samples have slightly lower MgO contents (~5.5%) and much higher REE abundances than the previous basalts (63-100X La; Fig. 4C) and cannot be related by olivine control. This implies that they are differentiated tholeiites having compositions controlled by pyroxene and/or plagioclase fractionation. The negative Ce anomaly observed in sample 8 may be due to experimental error. To explain this anomaly by seawater leaching would require excessive amounts of seawater.

The six remaining basalts have been extremely fractionated, as suggested by their major element and REE compositions. Five of these basalts can be classified as mugearites (Table 6C, cols. 1, 2, and 5). The BaO/SrO ratio in one of these samples, however, is significantly higher (0.7) than in the other basalts (0.4), perhaps indicating a different generative process. The major element chemistry of the final basalt resembles that of a trachyte (Table 6C, cols. 3 and 6).

[1]The anomalously high Co and Ta abundances observed in three of these samples are probably the result of contamination due to grinding in tungsten mortars.

Mauna Kea - Nine olivine-controlled tholeiitic basalts[2] have been identified from the suite of Mauna Kea samples. These exhibit significant variations in bulk and trace element chemistry; there is an indication that two or more distinct melts have been sampled. Evidence relies on differences in La/Yb ratios among these samples. Five basalt samples (Table 5B, 5-9) have La/Yb ratios of ~10.0, three samples (Table 5B, 2-4) have La/Yb ratios of ~7.5, and one sample (Table 5B, 1) has an La/Yb ratio of 6.3 (Fig. 4D). REE, Cr, Ni, and Co abundances suggest that the samples in the first two groups may be related to the high MgO basalts by opx fractionation. With Na_2O as a measure of the degree of fractionation, the average D values for MgO, Cr, Co, and Ni partitioning among the samples in these groups are 2.6, 8.8, 1.7, and 4.5, respectively. At 1200°C, experimentally determined values for opx are very similar; namely, D_{MgO} = 2.6 (Grove and Bence, 1977), D_{Cr} ~10, D_{Co} ~1.5, and D_{Ni} ~5 (Irving, 1978). Because D_{REE} values are similar between opx and olivine (in addition to the identification of opx control), little error is introduced in using some of these basalts and their REE data in subsequent partial melting model applications (see Table 7B).

Five basalts analyzed from this volcano are clearly differentiated tholeiites (Table 5B, 10; 5C, 11-14) and are very similar to each other in composition. The average MgO content in the basalts is 3.2%, and the average La abundance is 144X. They have highly fractionated REE patterns, the mean La/Yb ratio being 14.4. Sc is depleted by a factor of ~3.5 relative to the olivine-controlled basalts.

Kilauea - The Kilauea basalts used in modeling were analyzed by Murali et al. (1977). Two distinct tholeiitic basalt compositions related to time of eruption are observed from this volcano, historic and prehistoric. The historic basalts have higher light REE abundances (46X vs. 35X) but lower heavy REE abundances (9X vs. 9.7X Yb) relative to the prehistoric basalts (Fig. 4B). This would suggest that at least two olivine-derived melts have been sampled among Kilauea basalts. Both data sets will be used in the modeling calculations.

---

[2]It will be shown that only three of these can be termed olivine-controlled basalts; the rest exhibit an almost perfect opx control.

Mauna Ulu - The Mauna Ulu samples analyzed represent five variant flows that were erupted between 1968 and 1971 (Wright and Fiske, 1971). The chemical characteristics of these basalts will be discussed later in this paper.

Southern Fracture

Koolau - Four samples were obtained from Koolau (Fig. 4F, Table 5C). These basalts have been determined to follow the olivine control lines typical of Hawaiian tholeiites (Jackson and Wright, 1970). Three of the basalts cannot be distinguished from each other (allowing for minor olivine fractionation) on the basis of REE ratios or abundances. The fourth basalt sample has a smaller La/Yb ratio, indicating derivation from a different parental melt. This basalt is also less fractionated, as is evident by the higher MgO, Cr, Co, and Ni contents. These basalts provide for two data sets to be used in subsequent calculations.

Lanai - Four samples were analyzed from Lanai. As with Koolau, three of the basalts have very similar major and REE compositions and may be related by olivine fractionation to a single parental melt (Table 5C, Fig. 4G). The remaining basalt has distinctly higher MgO and transition element abundances with lower REE abundances. The lower La/Yb ratio of this basalt suggests that it was fractionated from a different parental melt. All four samples represent olivine-controlled lavas. Again, two basalt compositions will be used in modeling.

Mauna Loa - Thirteen samples from the Mauna Loa volcano have been analyzed (Table 5D-E, Fig. 4H) and previously identified as olivine-controlled tholeiitic basalts (Wright, 1971). These samples represent lavas erupted during prehistoric and historic time. Seven of the eight historic basalts show remarkable similarities in REE trace and major element compositions. The standard deviations of the mean concentrations in these flows are less than the analytical uncertainties for almost every REE and trace element. Since these basalts were erupted over a 75-year period and since it has been determined that magmas ascend from the source to the surface in a few months' period, it could

be suggested that the fractionation processes that control the Mauna Loa magma compositions must occur in the mantle reservoir prior to ascent and that any shallow, low-pressure fractionation events have very minor roles in altering these lava compositions. The average chondrite-normalized abundances of La and Yb in these basalts are 25.9X and 9.1X, respectively; Sc = 3.6X, Hf = 17X, and Ta = 27X.

The 1887 basalt flow has lower light REE abundances (23.9X La) but very similar major element (Table 5E) and heavy REE compositions (Yb = 8.7X) compared to the other historic basalts. This would suggest generation from a unique parental melt; however, this composition will not be used in modeling.

The five basalt samples that have erupted during prehistoric times have variable REE chemistries among themselves but similar major element compositions. The major element compositions of these basalts are also very much like those observed in the historic basalts. Each of the prehistoric basalts could be products of different melts; but for modeling purposes, they will be assumed to represent lavas derived from a single partial melt.

General Description — Tholeiitic Basalts

The Hawaiian tholeiitic basalts studied in this work have major element compositions very similar to the average composition of 200 tholeiites obtained by Macdonald (1969) and Macdonald and Katsura (1964). This can be seen upon examination of Table 6A. On closer inspection there are, however, systematic and important variations in some elemental abundances among the Hawaiian basalts that correlate with generation from vents situated either along the northern or the southern fractures. Transition element abundances, such as Cr, Co, Ni, and V, are statistically higher in basalts from the northern rift as are the major elements, TiO_2 and CaO; Al_2O_3 abundances, on the other hand, are lower in these basalts (Table 6B). Since the processes of tholeiitic magma generation are not considered to be vastly different among samples

TABLE 6A. AVERAGE MAJOR ELEMENT COMPOSITION OF THE HAWAIIAN THOLEIITE BASALTS ANALYZED IN THIS WORK.

Element	Composition (%)			
	This Work (a)	Northern (b)	Southern (c)	Average of 200
TiO_2	2.3	2.6	2.1	2.5
Al_2O_3	14.1	14.0	14.3	13.9
FeO[d]	11.1	11.3	10.9	11.2
MgO	7.1	7.4	6.7	8.4
CaO	10.4	11.1	9.6	10.3
Na_2O	2.4	2.3	2.4	2.2
K_2O	0.4	0.4	0.4	0.4

NOTES: For comparison, the average of 200 tholeiitic compositions obtained by Macdonald (1969) and Macdonald and Katsura (1964) are presented. Selected average abundances for the northern and southern rift basalts are also given to show a possible difference in basalt compositions.

[a]Average of 39 including 7 Kilauea (Murali et al., 1977).

[b]Average of 19 northern rift basalts.

[c]Average of 20 southern rift basalts.

[d]Total Fe as FeO.

TABLE 6B. COMPARISON OF AVERAGE TRANSITION ELEMENT ABUNDANCES IN NORTHERN AND SOUTHERN RIFT BASALTS.

Element	Northern Rift Volcanoes			Southern Rift Volcanoes		
	Kohala	Mauna Kea	Kilauea	Koolau	Lanai	Mauna Loa
Cr (ppm). . .	383	355	335	255	245	240
Co (ppm). . .	47	52	43	40	40	41
Ni (ppm). . .	200	160	160	120	120	104
V (ppm) . . .	310	327	320	270	295	285
Sc (ppm). . .	31.0	30.5	29.7	23.0	28.0	28.8
MgO (%) . . .	8.0	6.8	7.5	6.3	6.6	7.0

NOTES: Individual basalt compositions used for averaging are discussed in text and listed in Table 7.

TABLE 6C. SELECTED MAJOR AND TRACE ELEMENT ABUNDANCES OF SOME FRACTIONATED BASALTS FROM KOHALA.

Element	Group (a)					
	1	2	3	4	5	6
SiO_2 (%). . .	55.4[b]	57.1[b]	62.1[b]	45.4	53.2	62.0
TiO_2 (%). . .	2.1	1.5	0.8	3.0	1.8	0.3
Al_2O_3 (%) . .	17.1	18.3	18.2	14.7	17.7	16.3
FeO[c] (%). . .	9.3	8.3	6.3	12.9	8.5	4.0
MgO (%) . . .	2.8	2.5	0.4	7.8	2.8	0.4
CaO (%) . . .	5.4	4.1	2.3	10.5	5.4	0.9
Na_2O (%). . .	5.7	5.9	7.2	3.0	6.0	6.9
BaO/SrO . . .	0.4	0.7	0.4	. . .	. . .	. . .
La (ppm). . .	62	83	61	. . .	. . .	. . .
Lu (ppm). . .	0.50	0.60	0.52	. . .	. . .	. . .

[a]The groups are as follows: 1: Four Kohala basalts — 72M-33, -36, -42; H71-3. 2: One Kohala basalt — H71-10. 3: One Kohala basalt — 72M-35. 4: Average Alkali basalt, Hawaii (Macdonald, 1969). 5: Mugearite, Molakai, Hawaii (Macdonald, 1969). 6: Trachyte, Hualalai, Hawaii (Macdonald, 1949).

[b]SiO_2 estimated by subtraction.

[c]Total Fe as FeO.

containing the same amount of MgO (that is, having been involved by equivalent amounts of olivine fractionation), these trace element abundance variations would provide the first indication that some type of chemical heterogeneity exists between these fractures. In earlier works (e.g., Wright, 1971), compositional variations of source materials were postulated on the basis of K_2O, P_2O_5, and TiO_2 contents.

Chondrite-normalized REE abundance patterns for the tholeiitic basalts are characterized by slight to moderate depletion of La relative to Nd, light REE abundances of 30X-50X (times chondrite) and heavy REE abundances of about 8.2X-10X for Yb (Fig. 4A). Although these patterns appear to be indistinguishable (except in terms of LREE abundances), light REE abundance ratios provide additional evidence that compositional differences may exist between basalts generated from the northern and the southern fractures. The $(La/Nd)_{c.n.}$ (chondrite normalized) ratios of the northern rift (Kilauea group) basalts vary from 0.95 for Kohala to 1.08 for Mauna Kea. The southern rift (Mauna Loa group) basalts have significantly lower $(La/Nd)_{c.n.}$ ratios of 0.93, 0.86, and 0.83 for Koolau, Lanai, and Mauna Loa (historic) lavas, respectively. It can be shown that neither mineral fractionation nor partial melting can cause these observed variations between magma groups.

Chondrite-normalized Sr abundances are nearly identical to the $La_{c.n.}$ abundances. This is expected based on their similar solid/liquid partitioning behavior among the controlling minerals in terrestrial processes. Since Ba should also exhibit similar chondritic abundances for this same reason, the light to moderate depletions relative to Sr observed in some of these basalts would suggest that Ba is depleted to some extent on the mantle regions, although the presence of phologopite in the residual minerals cannot be discounted.

Sc abundances appear to be slightly higher (average of ~30 ppm) in the Kilauea group basalts compared to the Mauna group (28.5 ppm). Although this difference may be fortuitous because of counting statistic uncertainties, other elemental abundances (having similar ionic radii), such as Hf, Ta and Zr, are significantly higher in the Kilauea group basalts (Fig. 4A). For example, Hf abundances range from 3.7 ppm

to 5.1 ppm in the Kilauea and Mauna Kea basalts, respectively; whereas the abundances range from 2.6 ppm in Koolau to 3.4 ppm in the Mauna Loa basalts. These variations cannot be explained by simple fractionation processes.

Hence, a partial melting model that accounts for the observed systematic differences in trace element abundances, especially the REE, may reveal the extent of heterogeneity between the source regions, if any exists. Such a model is described in the next section.

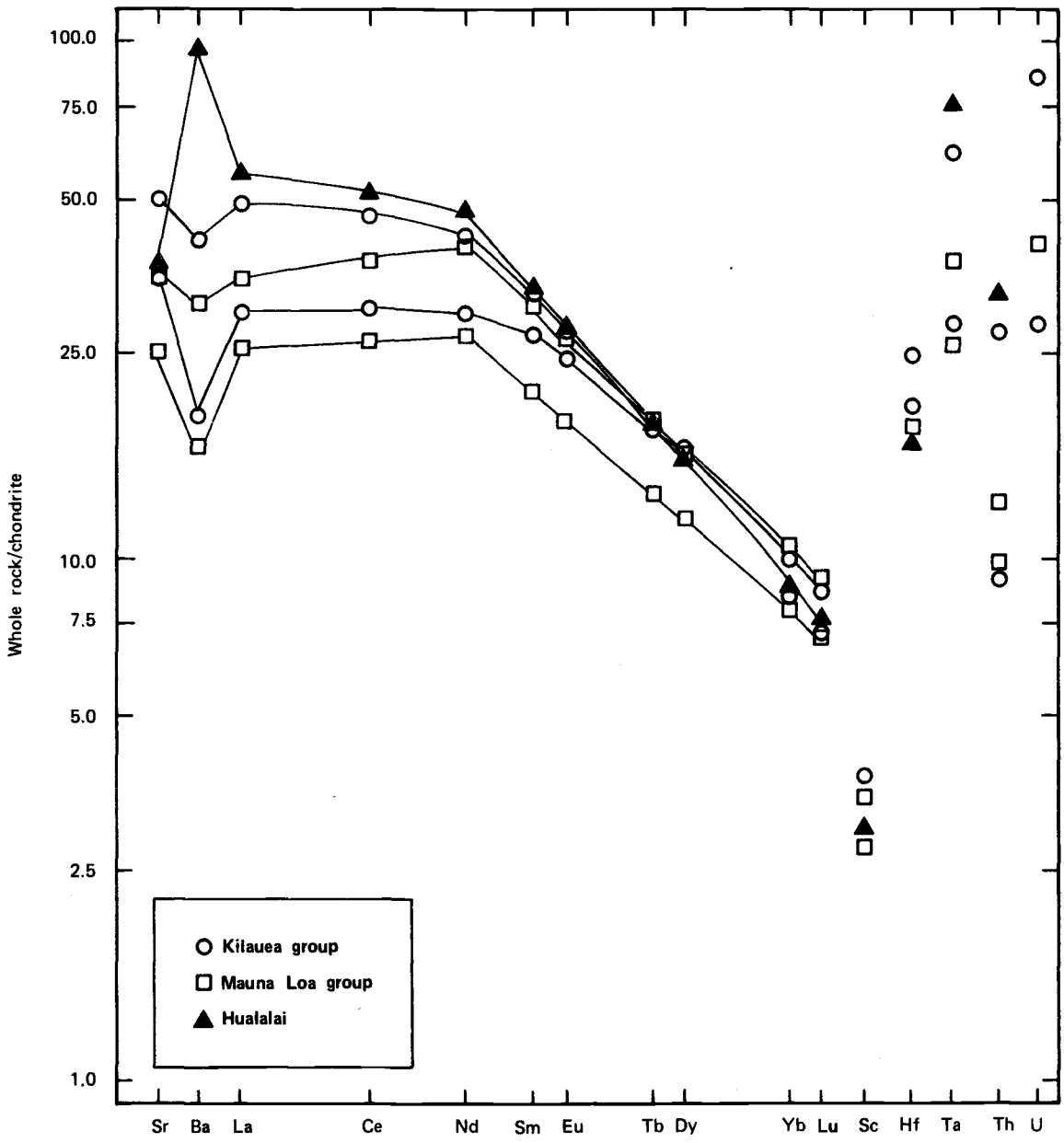

Fig. 4A. Range of chondrite-normalized trace element abundance patterns of the Kilauea group, Mauna Loa group, and Hualalai basalts versus ionic radius (Whittaker and Muntus, 1970). Chondrite normalization factors used in this study: Sr = 11, Ba = 3.8, La = 0.34, Ce = 0.85, Nd = 0.64, Sm = 0.195, Eu = 0.073 , Tb = 0.047, Dy = 0.31, Yb = 0.22, Lu = 0.034, Sc = 8, Hf = 0.2, Ta = 0.02, Th = 0.04, U = 0.005.

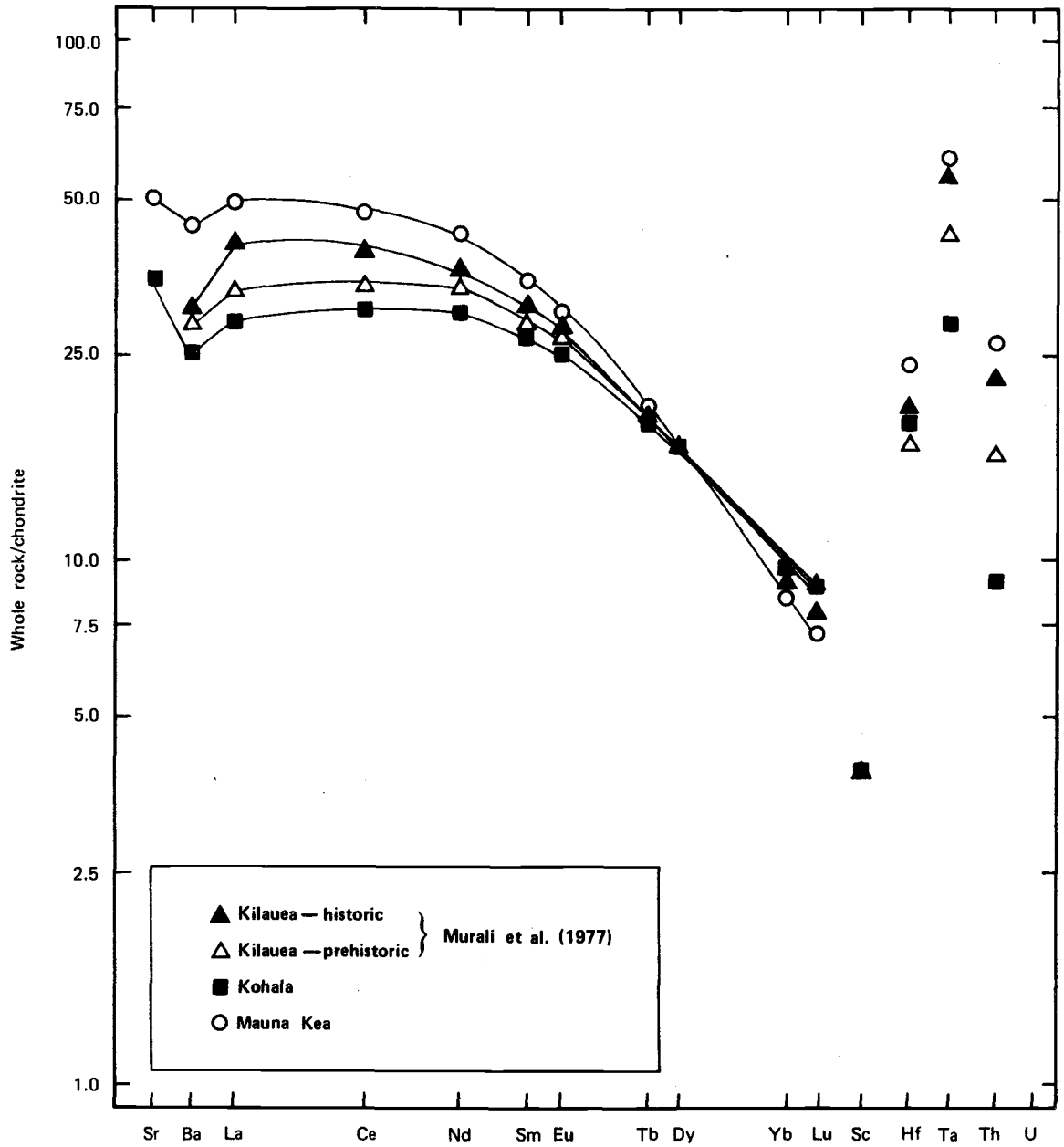

Fig. 4B. Average chondrite-normalized trace element abundance patterns of the northern rift generated tholeiitic basalts analyzed in this work and those from Murali et al. (1977).

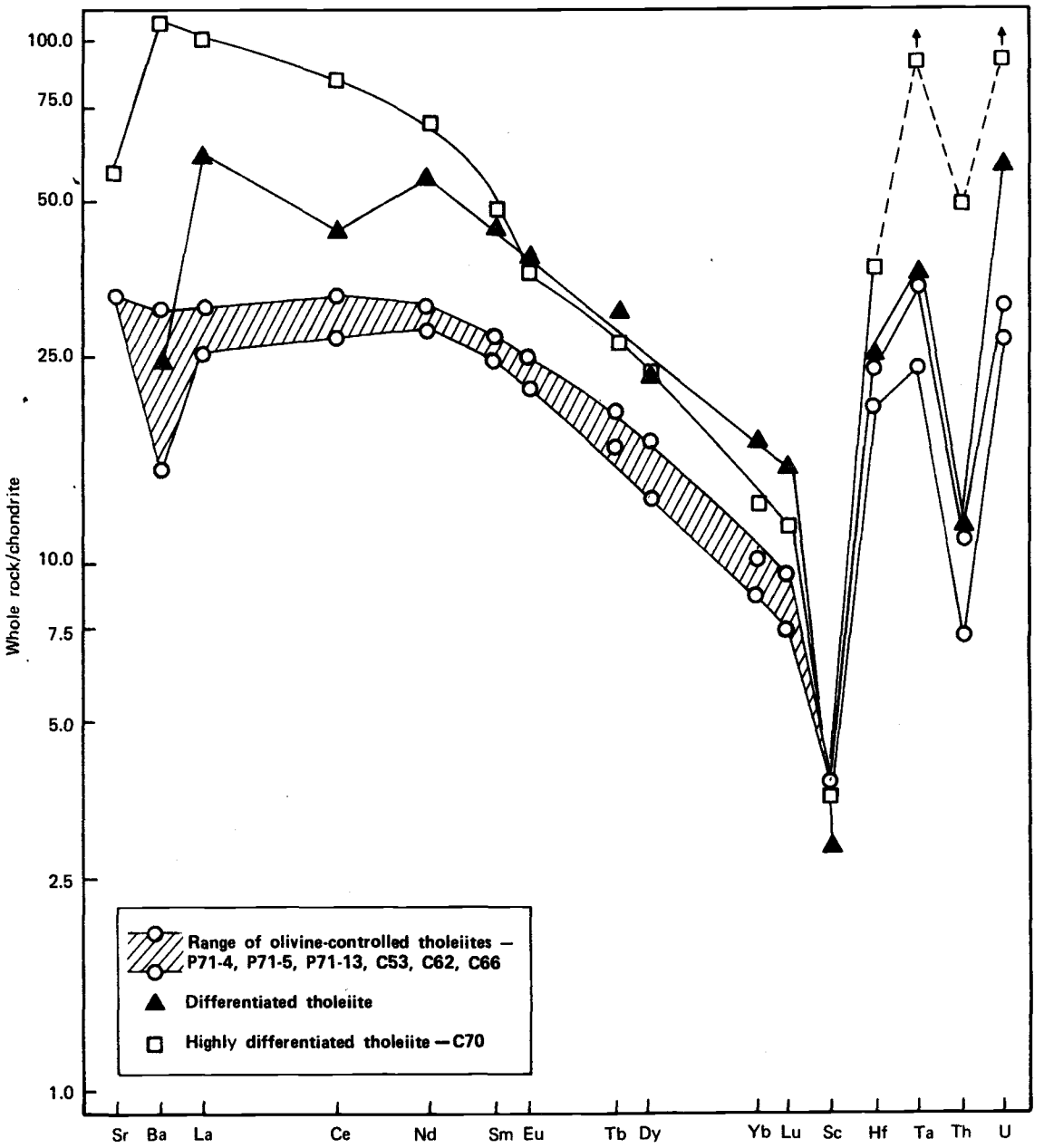

Fig. 4C. Chondrite-normalized trace element abundance patterns of the Kohala basalts analyzed in this work.

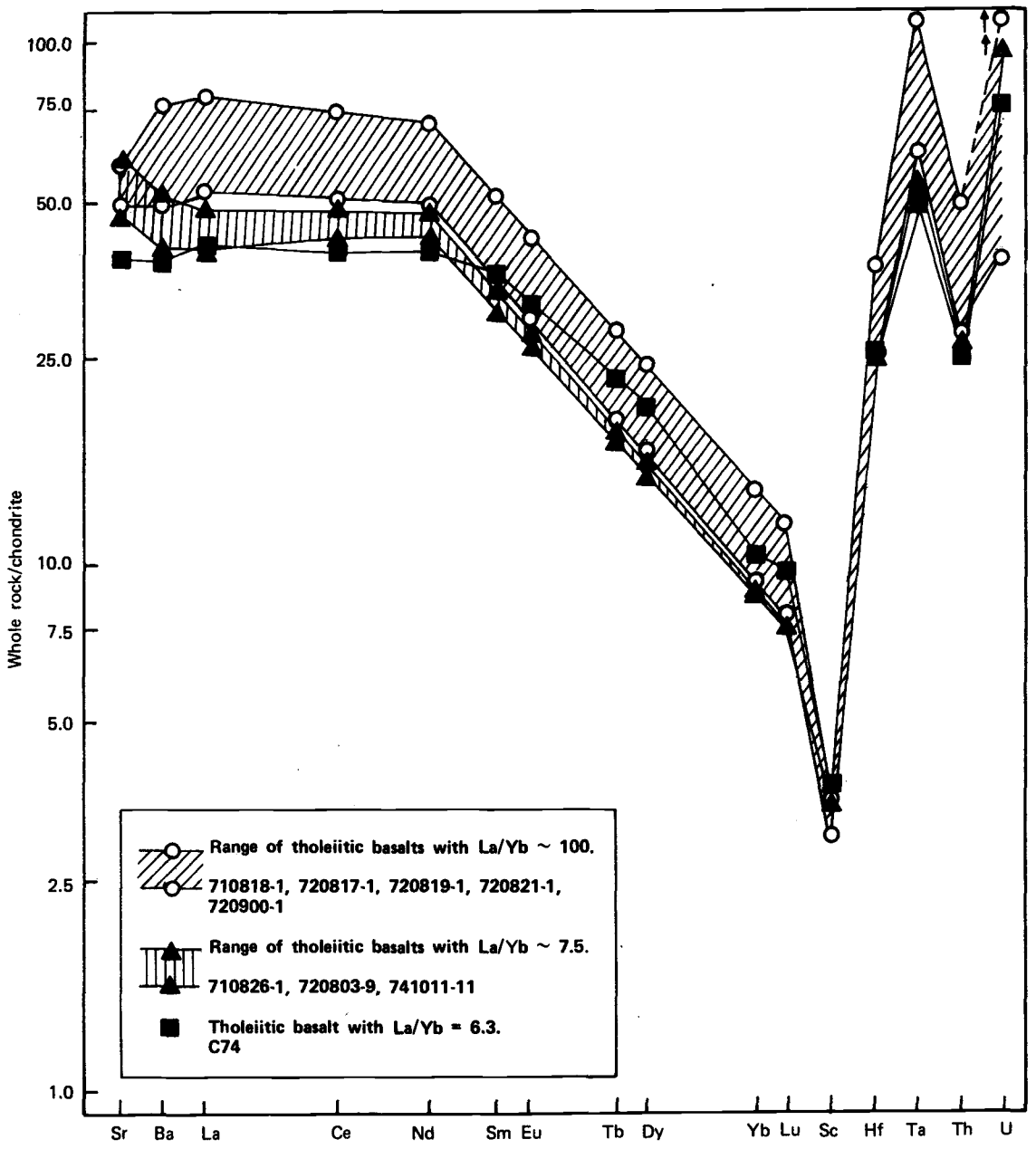

Fig. 4D. Chondrite-normalized trace element abundance patterns of the Mauna Kea basalts analyzed in this work.

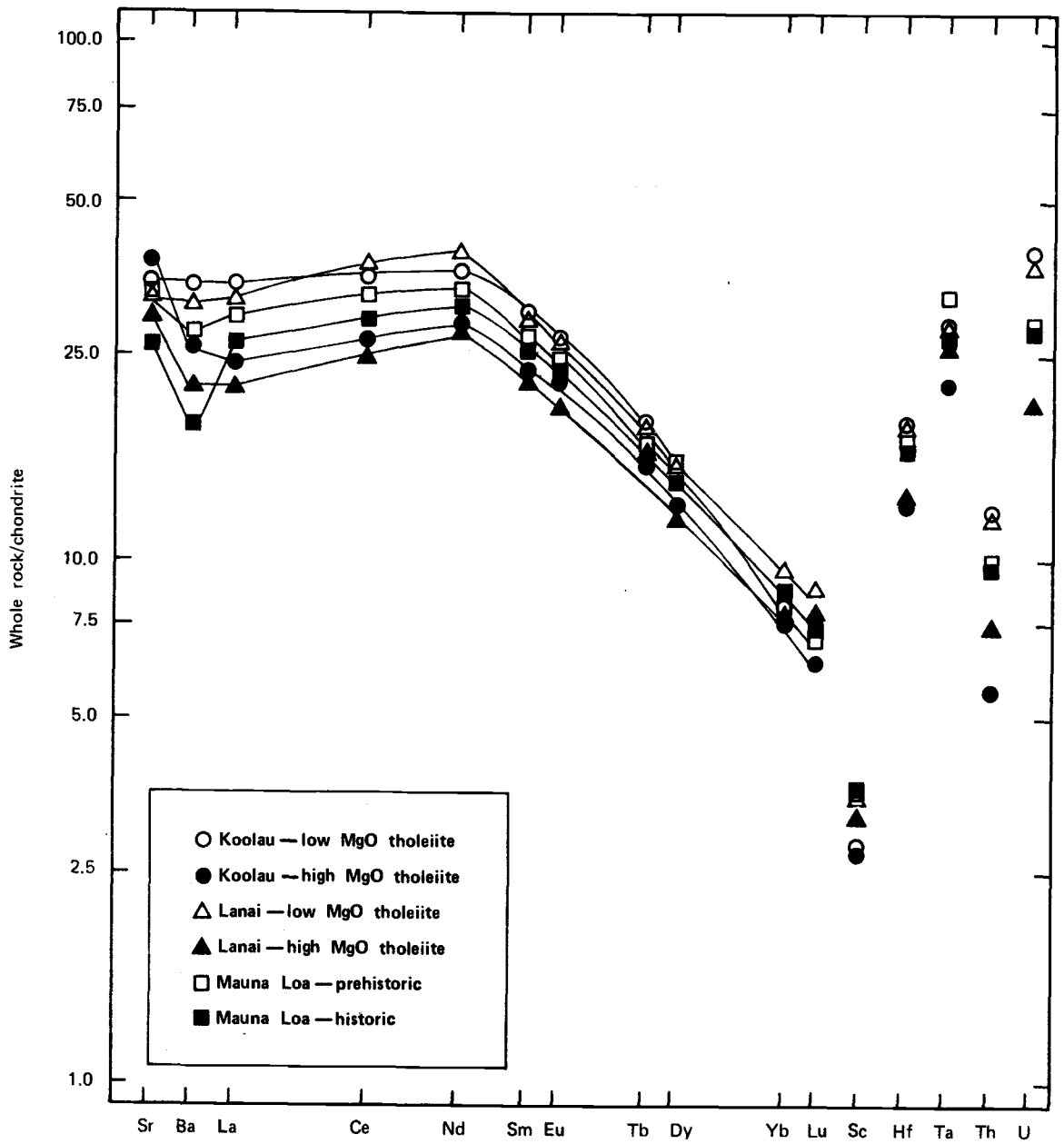

Fig. 4E. Average chondrite-normalized trace element abundance patterns of the southern rift generated tholeiitic basalts analyzed in this work.

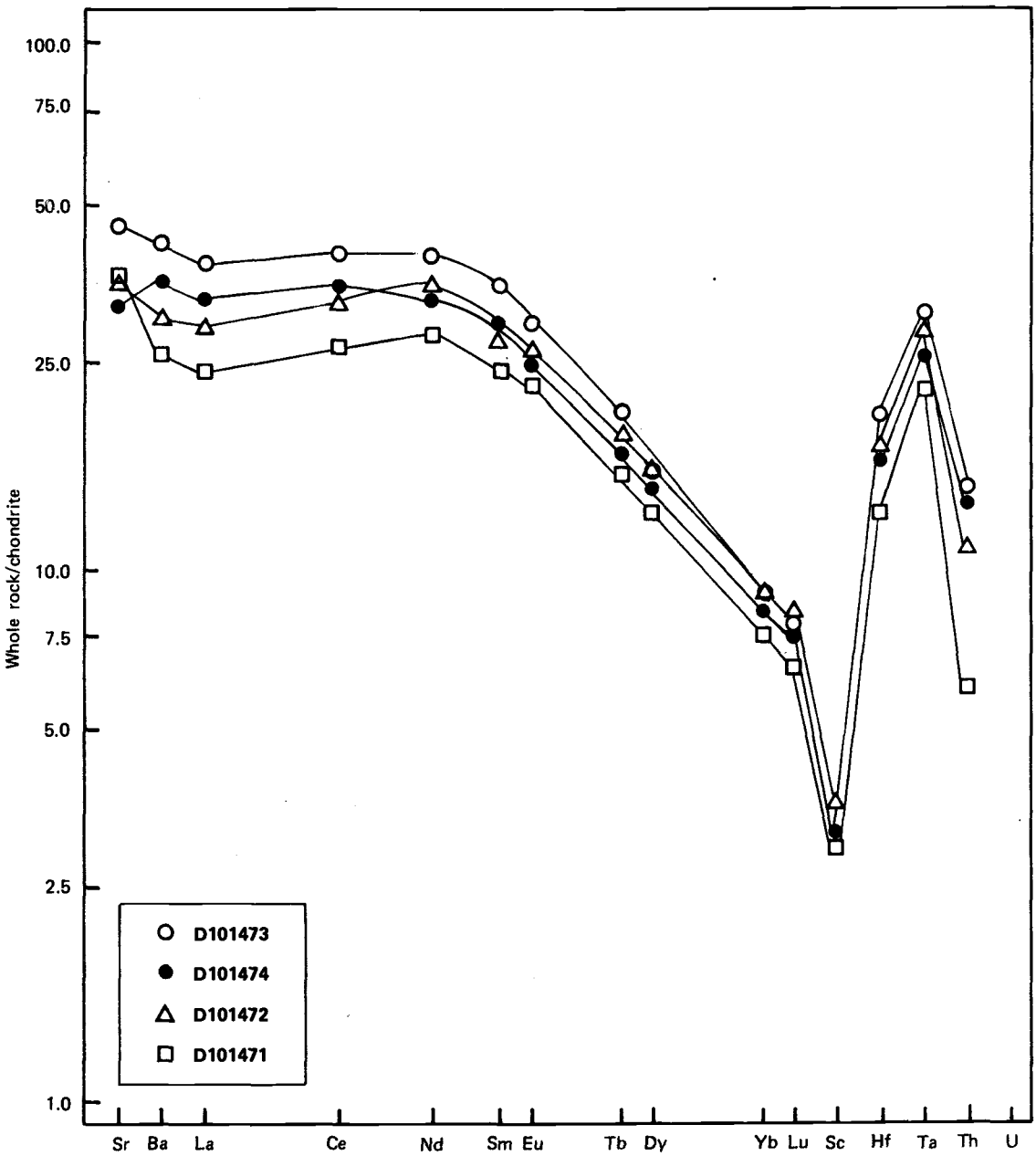

Fig. 4F. Chondrite-normalized trace element abundance patterns of the Koolau basalts analyzed in this work.

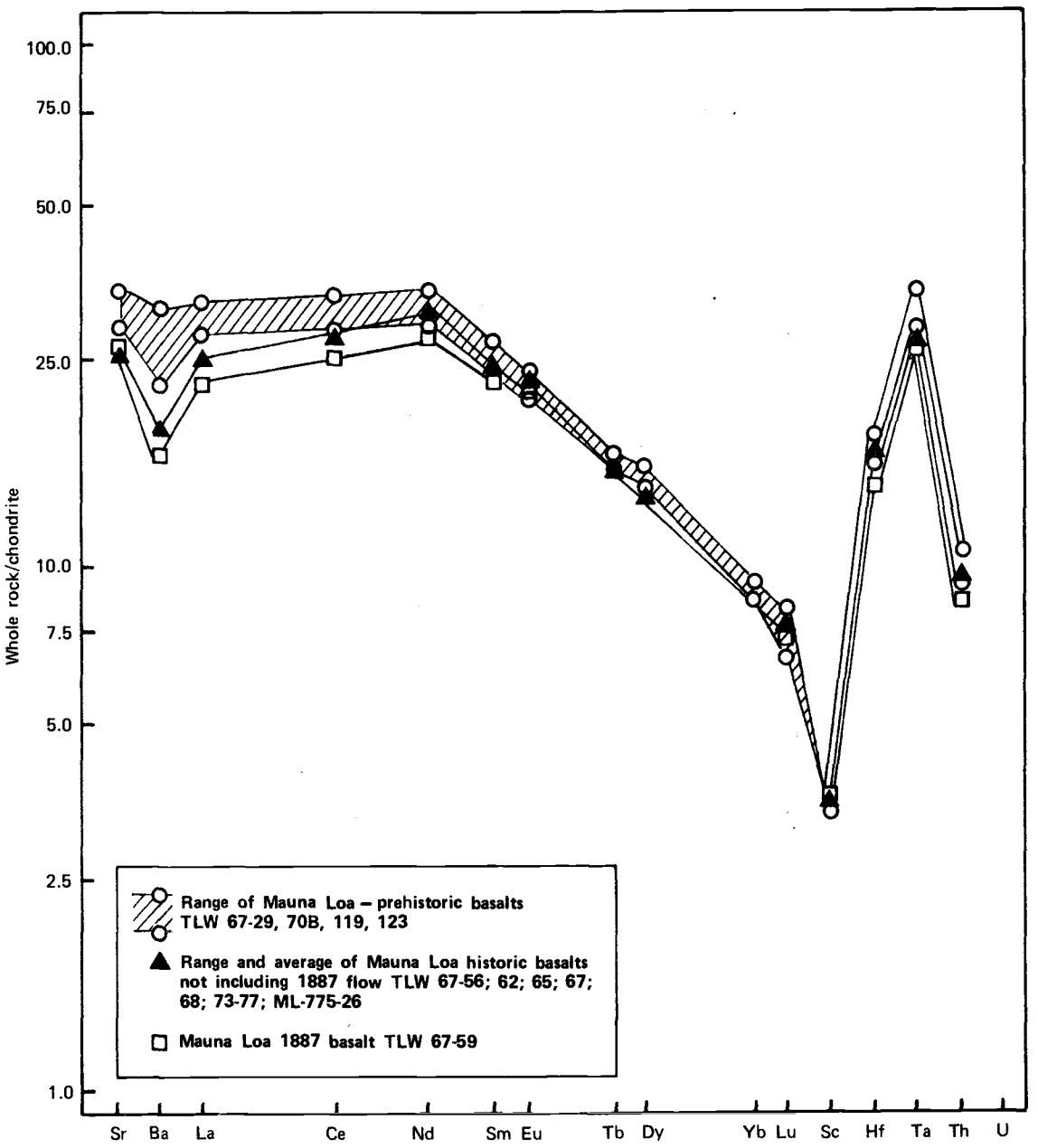

Fig. 4H. Chondrite-normalized trace element abundance patterns of the Mauna Loa basalts analyzed in this work.

IV. DETERMINATION OF SOURCE MATERIALS

Partial Melting Model

The following sections describe in detail the method used in obtaining estimates of possible parental materials from which the Hawaiian tholeiitic basalts were derived. The procedure involved relating selected basalt abundances (REE, Sr, Ba, Sc) to the source via a partial melting process. Discussion will include assumptions made in obtaining the equations and the related parameters required for this type of modeling.

A partial melting model relating magma batches to a source composition(s) is preferred over a crystal fractionation model relating the magmas to a common parental liquid for the following reasons: 1) The samples chosen for modeling lie along olivine-control lines; and although differences in the rate and extent of olivine fractionation could be postulated in producing the observed variations in MgO, Co, and Ni abundances, for example, REE abundance profiles cannot be related by this mechanism. The very low and similar $D^{Ol/l}$ values for La, Ce, and Nd will not produce the observed LREE depletion variations between the magma groups. 2) The aforementioned observation, together with REE and Sc data, precludes the possibility of pyroxene and/or garnet fractionation to account for Al_2O_3 and CaO differences. Removal of either phase in an amount needed for these variations would produce trace element profiles severely depleted in the heavy REE and Sc; this is not observed. 3) It would be difficult to envisage a partial melting process that consistently produces an identical liquid composition throughout time. Thus, it will be reasonably suggested that differences in REE and major element contents are the result of variable source composition or melting conditions.

Modeling Elements - As just stated, the REE (La, Ce, Nd, Sm, Eu, Tb, Dy, Yb, and Lu), Sc, Sr, and Ba were used in obtaining estimates of possible source materials. In particular, the abundance patterns of the REE contain much information concerning the composition of the Hawaiian source regions. Because of the extensive use of the REE in

these types of geochemical applications, a considerable amount of reliable REE partitioning data has been obtained (Irving, 1978) that can be used. For these reasons, REE modeling will provide for the best description of mantle-source materials.

Sc was also considered an important element in modeling for the following reasons: 1) As with the REE, Sc occurs in trace amounts in the magma and thus behaves as a dispersed trace element; 2) there are significant differences in its partitioning behavior among the controlling minerals; and 3) Sc partitioning is relatively independent from the REE. The latter two distinctions place additional constraints on the modeling calculations.

Ba and Sr were used in some of the modeling calculations because of their similar partitioning behavior to the LREE. In the initial calculations, they helped to define the light REE trend.

Partial Melting - To mathematically describe the behavior of these trace elements in the partial melting process initially requires an understanding of the melting process itself and the products derived. In all of the hypotheses concerning the melting event (see Introduction), it had been suggested that melting occurs at or near the mantle-crust boundary. The liquids associated with production at this depth would probably remain in contact with the melting zone for some period prior to ascent to the surface. This would suggest an equilibrium-type melting process. Since basalts derived from these liquids have very similar major element compositions throughout time, it appears that a uniform melt in terms of mineral components is constantly being produced; that is, melting is eutectic-like.

Hence, nonmodal equilibrium partial melting[3] is considered to be the most realistic description of the melting event, and the equation

---

[3]Other types of melting processes involving trace element partitioning have been considered in deriving a melting model, but these have not proved amenable for various reasons. Difficulty arises when applying the equation for aggregate or fractional partial melting, for instance, to a straightforward least-squares computer approach due to its exponential dependency on P (see Shaw, 1970). Dynamic melting was proposed by Langmuir and Hanson (1977) to explain anomalous REE patterns

presented by Shaw (1970) for this type of melting has been adopted. The equation characterizes the partitioning of a dispersed trace element into a liquid that is in continuous contact with the solid:

$$\frac{C^{\ell}}{C_o} = \frac{1}{\bar{D} + F(1 - P)} \tag{1}$$

where C^{ℓ} ≡ concentration of a trace element in the liquid

C_o ≡ concentration of a trace element in the solid

$\bar{D}$ ≡ bulk partition coefficient of the solid

F ≡ degree of melting

P ≡ bulk partition coefficient of the liquid

The definitions for $\bar{D}$ and P can be clarified. The bulk partition coefficients for element y can be written as the sum of the weight fractions of the minerals in the solid (w) or as the sum of the melting proportions in liquid (x) times the mineral to liquid partition coefficient, D, for that mineral (i, j, k, etc.). That is,

$$\bar{D}_y = w_i D_{iy} + w_j D_{jy} + w_k D_{ky} + \ldots$$

and

$$P_y = x_i D_{iy} + x_j D_{jg} + x_k D_{ky} + \ldots$$

In a melting process involving garnet peridotite, four minerals must be represented in the equation: olivine (ol), orthopyroxene (opx), clinopyroxene (cpx), and garnet (gar). The bulk partition coefficient of the solid can then be written

$$\bar{D} = w_{ol} D_{ol} + w_{opx} D_{opx} + w_{cpx} D_{cpx} + w_{gar} D_{gar} \tag{2}$$

and for the liquid

$$P = x_{ol} D_{ol} + x_{opx} D_{opx} + x_{cpx} D_{cpx} + w_{gar} D_{gar} \tag{3}$$

Equation (1) can be rearranged to give a linear equation:

$$\frac{C_o}{C^{\ell}} - \bar{D} = F(1 - P), \tag{4}$$

one such equation for every constraining element used in modeling. This will allow for solutions to be obtained by multilinear regression

---

in basalts from the FAMOUS area. However, the Hawaiian basalts appear to be very systematic in composition, suggesting that this type of melting was not involved in generating these basalts.

analysis (MLRA) or by the use of an unconstrained mixing program. The solution involves the determination of optimal values of C_o (trace element abundances in the source) and w_{ol}, w_{opx}, w_{cpx}, and w_{gar} (source mineral contents) after substitution of equations (2) and (3) into equation (4) and insertion of values for F (the degree of melting), x_{gar}, x_{ol}, x_{opx}, and x_{cpx} (the eutectic composition), the partition coefficients, and c^{ℓ} (trace element abundances in the melt).

Input Parameters

The degree of partial melting, F, is not known. Shaw (1973), for example, has estimated that ~4% partial melting is required to produce the average Hawaiian shield based on source volume considerations. Jackson and Wright (1970), on the other hand, noted that 50% melting is necessary for "hot" spot generation of the volcanoes. Consequently, values of F were varied from 1-60%, resulting in numerous solutions to the partial melting equation, one unique solution for each postulated degree of melting.

The input parameters, x_{gar}, x_{ol}, etc., and the D values[4] are very dependent upon the pressure and temperature of the melting event; the latter, to some extent, is dependent on composition, f_{O_2}, etc. It has been demonstrated that the eutectic of a garnet-peridotite (that is, the system forsterite-diopside-pyrope) varies with depth (Yoder and Tilley, 1962). The available data on partition coefficients compiled by Irving (1978) show the strong dependence of these values on the

[4]It can be shown that even large variations (20%) in these parameters do not appreciably affect the solutions obtained in this type of melting model. The reader can verify this by multiplying the bulk partition coefficients given in the figure in Appendix B by 0.8 and calculating C^{ℓ} using the source compositions that will be proposed. The most important factor determining trace element partitioning between the melt and the mantle will be the composition of the source (providing that the degree of melting is relatively small). Nevertheless, the most accurate solution will be determined if the most appropriate parameters are selected.

pressure, temperature, etc., associated with melting. A regression on mantle condition is thus appropriate.

As mentioned earlier, the magmas of Hawaii ascend from a depth of at least 60 km, corresponding to a pressure of ~20 kb. Melting of an anhydrous garnet peridotite at this depth would produce a liquid corresponding to 40% ol+opx, 20% cpx, and 40% gar; and the melting temperature would be 1400-1500°C (Yoder, 1976, p. 140). There is considerable evidence (Spetzler and Anderson, 1968; Anderson and Spetzler, 1970), however, that suggests that melting occurs in the low velocity zone (LVZ) of the mantle located from 100-150 km in depth. For this reason, the LVZ will be considered as the region of partial melting. In this region of the mantle, P = 40 kb, and the liquidus of an anhydrous garnet peridotite would have a composition corresponding to ~10% ol+opx, 45% cpx, and 45% gar (Davis and Shairer, 1965). This melting proportion will thus represent the invariant point of melting and will be assumed, for the moment, to remain constant for and during all melting events.

Very few mineral to liquid partition coefficients are available for minerals equilibrated under these conditions. Nevertheless, reasonable estimates can be made upon examination of existing data (Irving, 1978). The general trend in most minerals is that $D^{min/l}$ will decrease with an increase in equilibration temperature. REE partition coefficients were chosen (Appendix B) for ol-opx and cpx that represent complete sets of values obtained under the highest temperature and pressure conditions.

Garnet to liquid partition coefficients are an exception to the aforementioned trend; Harrison (1977) has determined that $D_{Sm}^{gar/l}$ increases with increasing temperature. These data were used as the criterion for selecting D_{REE} values limited to two sets of reasonable partition coefficient data (Philpotts et al., 1972; Arth and Hanson, 1975); these values are given in Appendix B.

The trace element concentrations in the liquid, C^{ℓ}, are the chondrite-normalized abundances for the REE, Sr, Ba, and Sc obtained experimentally. The insertion of chondrite-normalized abundances in equation (4) will implicitly assume that the source is characterized by

chondritic abundances. The concentrations represent average basalt compositions from each identifiable magma suite in each of the volcanoes [Table 7]. As described earlier, the basalts within a group include only those magmas that have similar major and trace element compositions and that can be interrelated by simple olivine fractionation. The data set included five Kilauea historic lavas and two Kilauea prehistoric basalts from Murali et al. (1977), six Kohala basalts, six Mauna Kea basalts, four Koolau basalts (three low MgO), four Lanai basalts (three low MgO), seven historic Mauna Loa lavas, and five prehistoric Mauna Loa basalts from this work.

Final Equation

At this point, every obtainable parameter has been estimated for solving the partial melting equations except F, the degree of melting. However, two modifications of input parameters to equation (4) will be made in order to reduce the number of unknown variables and to reduce the errors associated with some of the input parameters. The low and similar D_{REE} values (see Appendix B) for ol+opx will intrinsically introduce large uncertainties into the estimation of w_{ol} and w_{opx}, since the computer cannot distinguish ol from opx on the basis of REE partitioning. However, $w_{ol} + w_{opx}$ should have a relatively small uncertainty. Petrographic studies on garnet peridotites and lherzolites (Maaloe and Aoki, 1977; and Carswell and Dawson, 1970) indicate that ol and opx are found in a 3:1 ratio in these rocks. Therefore, a more realistic and accurate solution was obtained by treating these minerals as a single phase (ol+opx) in the calculations.

An additional modification to the equation involved constraining the sum of the weight fractions in the source and liquid to one, further reducing the number of unknown variables (as well as input parameters).[5] The expressions $w_{cpx} = 1 - w_{gar} - w_{ol+opx}$ and

[5]Actually, it is irrelevant to consider a reduction in the number of input parameters important since the value determined from these parameters will be the same constant with or without the constraint.

TABLE 7A. AVERAGE COMPOSITION OF SIX OLIVINE-CONTROLLED THOLEIITIC BASALTS FROM KOHALA.

Element	Composition	Element	Composition
TiO_2 (%). . .	2.28	Ce (ppm). . .	26.2
Al_2O_3 (%) . .	13.8	Nd (ppm). . .	20
FeO[a] (%). . .	11.1	Sm (ppm). . .	5.36
MgO (%) . . .	8.0	Eu (ppm). . .	1.83
CaO (%) . . .	10.8	Tb (ppm). . .	0.91
Na_2O (%). . .	2.10	Dy (ppm). . .	4.9
K_2O (%) . . .	0.15	Yb (ppm). . .	2.10
MnO (%) . . .	0.17	Lu (ppm). . .	0.29
Cr_2O_3 (%) . .	0.056	Sc (ppm). . .	31
Co (ppm). . .	47[b]	Hf (ppm). . .	4.3
Ni (ppm). . .	200[c]	Ta (ppm). . .	0.6[d]
V (ppm) . . .	300	Th (ppm). . .	0.4
Sr (ppm). . .	345	U (ppm) . . .	0.14
Ba (ppm). . .	100	Zr (ppm). . .	150
La (ppm). . .	9.8		

NOTES: Samples used in averaging: P71-5, P71-13, C66, C53, C62, P71-4.

Estimated degree of olivine fractionation from hypothetical 24% MgO melt = 44.8% (refer to section entitled "Olivine Fractionation."

[a]Total Fe as FeO.

[b]P71-5, P71-13, C53, P71-4; average of 4.

[c]P71-5, P71-13; average of 2.

[d]P71-5, P71-13, P71-4; average of 3.

TABLE 7B. AVERAGE COMPOSITION OF THE OLIVINE-CONTROLLED THOLEIITIC BASALTS FROM MAUNA KEA.

Element	Composition		Element	Composition	
	A	B		A	B
TiO_2 (%). . .	2.78	2.81[a]	Ce (ppm). . .	43.4	40.8
Al_2O_3 (%) . .	13.6	14.0[a]	Nd (ppm). . .	29	29
FeO[b] (%). . .	12.0	12.3	Sm (ppm). . .	6.68	6.66
MgO (%) . . .	6.9	6.8[c]	Eu (ppm). . .	2.33	2.39
CaO (%) . . .	11.4	11.2	Tb (ppm). . .	0.95	0.96
Na_2O (%). . .	2.51	2.51	Dy (ppm). . .	4.9	5.2
K_2O (%) . . .	0.52	0.61	Yb (ppm). . .	2.07	2.11
MnO (%) . . .	0.17	0.18	Lu (ppm). . .	0.28	0.29
Cr_2O_3 (%) . .	0.052[d]	0.052[d]	Sc (ppm). . .	30.5	30.5
Co (ppm). . .	51[e]	52[e]	Hf (ppm). . .	5.1	5.1
Ni (ppm). . .	160	145[c]	Ta (ppm). . .	1.2	1.3
V (ppm) . . .	327	330[a]	Th (ppm). . .	1.1	1.1
Sr (ppm). . .	590	565	U (ppm) . . .	0.45	0.4
Ba (ppm). . .	185	184	Zr (ppm). . .	265	228
La (ppm). . .	18.1	16.7			

NOTES: Samples used in averaging: A – C74, 710826-1, 720819-1; B – C74, 710826-1, 720819-1, 741011-11, 720803-9, 720817-1.

Estimated degree of olivine fractionation from 24% MgO melt: Group A – 48.8%; B – 49.0%.

[a]Excluding 720803-9.

[b]Total Fe as FeO.

[c]Excluding 741011-11 and 720803-9.

[d]Average of 2, C74 and 710826-1.

[e]Excluding C74.

TABLE 7C. AVERAGE COMPOSITION OF THE OLIVINE-CONTROLLED THOLEIITIC BASALTS FROM KILAUEA — PREHISTORIC AND HISTORIC (MURALI ET AL., 1977).

Element	Composition		Element	Composition	
	Prehistoric	Historic		Prehistoric	Historic
TiO_2 (%). . .	2.41	2.70	Ce (ppm). . .	29.4	38.8
Al_2O_3 (%) . .	14.0	13.7	Nd (ppm). . .	[22][b]	[25][b]
FeO[a] (%). . .	10.9	11.0	Sm (ppm). . .	5.5	6.0
MgO (%) . . .	7.3	7.5	Eu (ppm). . .	1.83	2.06
CaO (%) . . .	10.7	11.4	Tb (ppm). . .	0.88	0.96
Na_2O (%). . .	2.34	2.28	Dy (ppm). . .	5.4	5.0
K_2O (%) . . .	0.43	0.54	Yb (ppm). . .	2.14	1.98
MnO (%) . . .	0.17	0.17	Lu (ppm). . .	0.31	0.28
Cr_2O_3 (%) . .	0.045	0.053	Sc (ppm). . .	29	30
Co (ppm). . .	42	43	Hf (ppm). . .	3.7	4.3
Ni (ppm). . .	185	150	Ta (ppm). . .	0.9	1.2
V (ppm) . . .	300	330	Th (ppm). . .	0.7	0.95
Sr (ppm). . .	. . .	. . .	U (ppm) . . .	. . .	. . .
Ba (ppm). . .	100	110	Zr (ppm). . .	200	245
La (ppm). . .	11.8	15.6			

SOURCE: Murali et al., 1977.

NOTES: Samples used in averaging (from Murali et al., 1977): prehistoric: 8X002 and CCSW; historic: 64D-126 (1924), 53-2377CD (1952), TLW67-42 (1954), K61-1 (1961), 1967 HM (1967).

Estimated degree of olivine fractionation from 24% MgO melt: prehistoric, 48.0%; and historic, 46.8%.

[a]Total Fe as FeO.

[b]Nd values extrapolated.

TABLE 7D. AVERAGE COMPOSITION OF THE OLIVINE-CONTROLLED THOLEIITIC BASALTS FROM KOOLAU — HIGH AND LOW MgO BASALTS.

Element	Composition		Element	Composition	
	Avg. low MgO	D101471		Avg. low MgO	D101471
TiO_2 (%). . .	2.27	1.84	Ce (ppm). . .	31.2	22.5
Al_2O_3 (%) . .	14.6	14.9	Nd (ppm). . .	24	18
FeO[a] (%). . .	10.2	9.8	Sm (ppm). . .	6.00	4.58
MgO (%) . . .	6.3	9.2	Eu (ppm). . .	1.98	1.66
CaO (%) . . .	8.8	8.4	Tb (ppm). . .	0.87	0.73
Na_2O (%). . .	2.60	2.56	Dy (ppm). . .	4.6	3.8
K_2O (%) . . .	0.45	0.40	Yb (ppm). . .	1.76	1.67
MnO (%) . . .	0.16	0.17	Lu (ppm). . .	0.26	0.21
Cr_2O_3 (%) . .	0.037	0.077	Sc (ppm). . .	24.7	23
Co (ppm). . .	40	46	Hf (ppm). . .	3.7	2.6
Ni (ppm). . .	120	305	Ta (ppm). . .	0.6	0.4
V (ppm) . . .	270	225	Th (ppm). . .	0.5	0.2
Sr (ppm). . .	385	420	U (ppm) . . .	0.2	. . .
Ba (ppm). . .	135	95	Zr (ppm). . .	210	180
La (ppm). . .	11.9	8.1			

NOTES: Samples used in averaging low MgO basalt composition: D101473, D101474, D101472.

Estimated degree of olivine fractionation from 24% MgO melt: low MgO basalt — 51.5%; D101471 — 40.5%.

[a]Total Fe as FeO.

TABLE 7E. AVERAGE COMPOSITION OF THE OLIVINE-CONTROLLED THOLEIITIC BASALTS FROM LANAI — HIGH AND LOW MgO BASALTS.

Element	Composition		Element	Composition	
	Avg. low MgO	OX069		Avg. low MgO	OX069
TiO_2 (%). . .	2.29	1.76	Ce (ppm). . .	31.5	23.4
Al_2O_3 (%) . .	14.6	14.6	Nd (ppm). . .	25	18.5
FeO[a] (%). . .	10.8	10.3	Sm (ppm). . .	5.91	4.49
MgO (%) . . .	6.6	8.5	Eu (ppm). . .	1.99	1.51
CaO (%)	9.7	9.0	Tb (ppm). . .	1.0	0.71
Na_2O (%). . .	2.38	2.36	Dy (ppm). . .	4.6	3.9
K_2O (%) . . .	0.42	0.32	Yb (ppm). . .	2.13	1.84
MnO (%) . . .	0.18	0.18	Lu (ppm). . .	0.31	0.26
Cr_2O_3 (%) . .	0.036	0.055	Sc (ppm). . .	28	26
Co (ppm). . .	40	44	Hf (ppm). . .	3.6	2.7
Ni (ppm). . .	120	235	Ta (ppm). . .	0.6	0.5
V (ppm) . . .	295	260	Th (ppm). . .	0.5	0.3
Sr (ppm). . .	355	335	U (ppm) . . .	0.2	0.3
Ba (ppm). . .	120	85	Zr (ppm). . .	160	170
La (ppm). . .	11.4	7.5			

NOTES: Samples used in averaging low MgO basalt composition: OX068, OX067, OX078.

Estimated degree of olivine fractionation from 24% MgO melt: low MgO — 50.8%; high MgO — 43.3%.

[a]Total Fe as FeO.

TABLE 7F. AVERAGE COMPOSITION OF THE OLIVINE-CONTROLLED THOLEIITIC BASALTS FROM MAUNA LOA — HISTORIC AND PREHISTORIC.

Element	Composition		Element	Composition	
	Historic	Prehistoric		Historic	Prehistoric
TiO_2 (%). . .	2.14	2.10	Ce (ppm). . .	23.8	26.8
Al_2O_3 (%) . .	14.0	14.0	Nd (ppm). . .	20	21
FeO[a] (%). . .	11.0	10.8	Sm (ppm). . .	4.88	5.10
MgO (%) . . .	7.2	6.7	Eu (ppm). . .	1.72	1.79
CaO (%) . . .	10.3	10.2	Tb (ppm). . .	0.74	0.78
Na_2O (%). . .	2.35	2.32	Dy (ppm). . .	4.4	4.8
K_2O (%) . . .	0.37	0.42	Yb (ppm). . .	2.00	1.97
MnO (%) . . .	0.16	0.15	Lu (ppm). . .	0.27	0.25
Cr_2O_3 (%) . .	0.0365	0.033	Sc (ppm). . .	29	28.5
Co (ppm). . .	42	40	Hf (ppm). . .	3.4	3.5
Ni (ppm). . .	100	110	Ta (ppm). . .	0.6	0.7
V (ppm) . . .	280	290	Th (ppm). . .	0.4	0.4
Sr (ppm). . .	290	360	U (ppm) . . .	0.15	0.13
Ba (ppm). . .	70	100	Zr (ppm). . .	120	105
La (ppm). . .	8.8	10.2			

NOTES: Samples used in averaging: historic — TLW67-56, 62, 65, 67, 68; TLW67-73, 77; and ML775-26. Prehistoric — TLW67-29, 70B, 119; and TLW67-123.

Estimated degree of olivine fractionation from 24% MgO melt: historic — 50.4%; prehistoric — 48.4%.

[a]Total Fe as FeO.

$x_{cpx} = 1 - x_{gar} - x_{ol+opx}$ were arbitrarily inserted to give the final equation used in the calculations:

$$C_o\left[\frac{1}{C^{\ell}}\right] + W_{gar}\left[D_{cpx} - D_{gar}\right] + w_{ol+opx}\left[D_{cpx} - D_{ol+opx}\right] = F + (1 - F)D_{cpx} + 0.1_{ol+opx}(F)\left(D_{cpx} - D_{ol+opx}\right) + 0.45_{gar}(F)\left(D_{cpx} - D_{gar}\right)$$

Note that in this equation, everything in brackets on the left-hand side is known; and after selection of F, the entire expression on the right-hand side becomes a constant. The solution to a matrix of such equations involves selection of C_o, w_{gar}, and w_{ol+opx} that will best satisfy every equation for each element.

Preliminary Model Source

The first estimations of possible source materials did not include the effects that olivine fractionation or light REE depletion in the source would have on the magmatic trace element abundance patterns. The preliminary source models thus reflect parental materials required to directly evolve the Hawaiian magmas from a chondritic mantle; i.e., a flat REE, Sc, Sr, and Ba pattern. It was noted earlier that all of the Hawaiian basalts have undergone some degree of olivine fractionation. It is also evident upon inspection of the trace element abundance patterns [Fig. 4A-H] and D_{REE} values [Appendix B] that no equilibrium partial melting event can generate the depletion of La and Ce relative to Nd and the depletion of Ba relative to Sr unless the source itself is depleted in these elements. Nevertheless, some features of this first model will be discussed.

Figure 5A shows the results obtained by MLRA for three basalt suites. The solutions represent possible source compositions required for the generation of Kohala, Mauna Kea, and Kilauea historic basalts. Unrealistic solutions (e.g., negative components, <1% partial melting) were obtained for the Koolau, Lanai, and Mauna Loa basalt generation models and are not included in the discussion. The figure depicts the compositional dependence of the source and its chondrite-normalized REE, Sr, Ba, and Sc abundances required to generate the observed trace

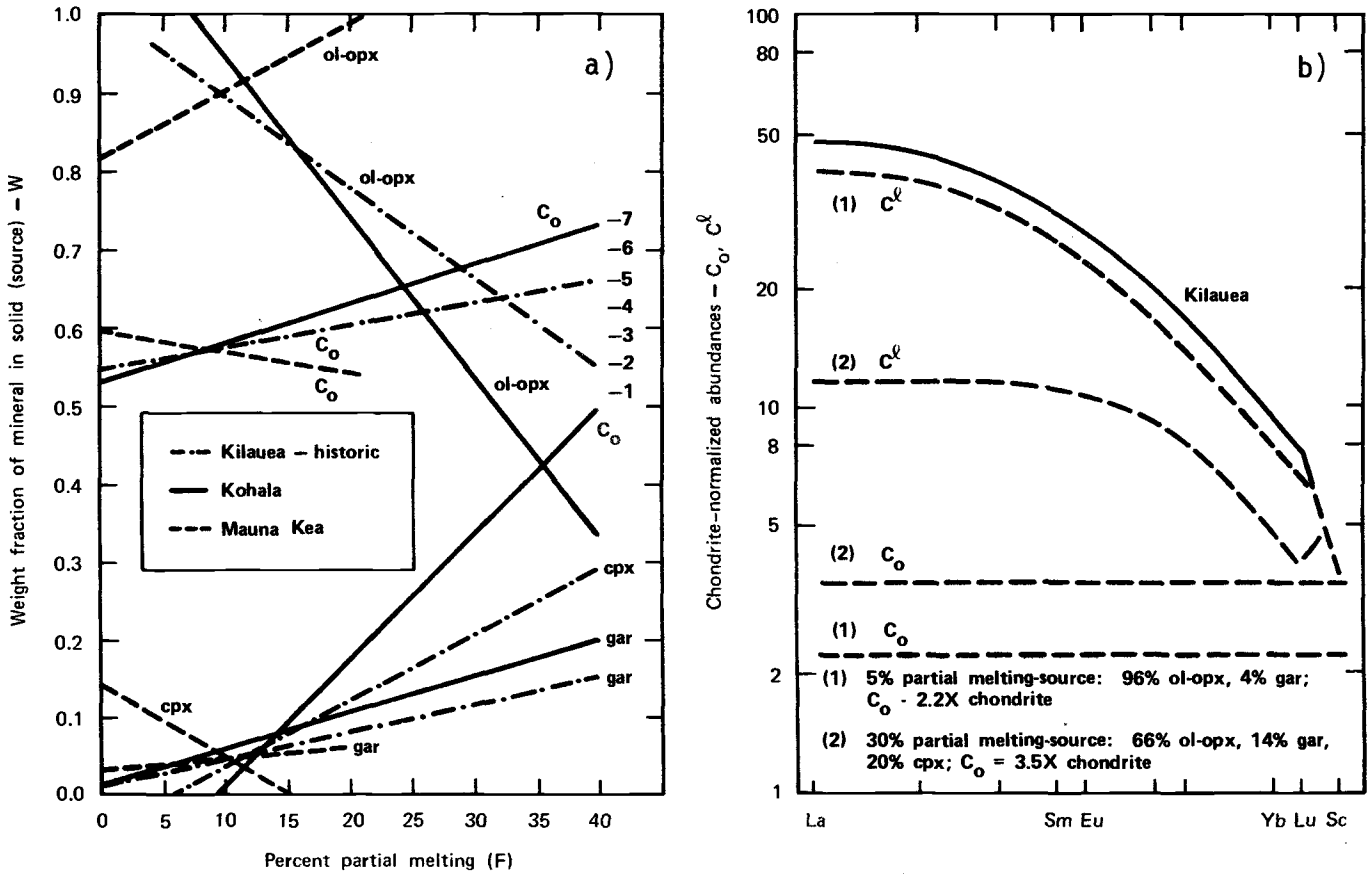

Fig. 5. Preliminary model. a) Results of multilinear regression analysis indicating the weight fraction modes and C_o values for source material that will yield optimal REE abundance patterns over a range of partial melting. b) Selected application of MLRA results for Kilauea to show the agreement obtained between calculated and observed REE and Sc abundance patterns at various degrees of melting.

element pattern in each representative basalts if 5%, 10%, 20%, etc., partial melting was responsible for the generation of the magmas. Inspection of this plot indicates that a source material composed of 85-90% ol + opx, 5-10% cpx, and 3-5% gar having a flat trace element abundance pattern of ~2-2.5 times chondrite could be parental to all of the northern rift tholeiitic basalts. The degrees of partial melting for the various magmas range from 5-15% in this model. Despite the obtaining of a possible model, more accurate primary basalt compositions can be estimated, and further discussion will be restricted to obtaining these estimates and thus a more exact model.

Although the first model gave source compositions needed for 0% partial melting processes ranging from 0-60%, the abundance patterns that are calculated using source compositions and that are required at greater than 25% melting do not resemble the observed abundance patterns (Fig. 5B). Futhermore, Yoder (1976, p. 114, Fig. 6-3) has deduced that only 30% partial melting of garnet peridotite can occur without a change in the eutectic composition. Based on these observations, further solutions for source materials can be limited to those required for 0-~25% partial melting.

The next two sections introduce the modifications made on the magmatic REE, Sr, Ba, and Sc abundances that approximate the effects of olivine fractionation[6] and light REE depletion in the source on magmatic compositions.

---

[6]The discussion concerning olivine fractionation is intended to provide for a total description of Hawaiian basalt generation, and subsequent trace element modeling will be based on the results obtained. It must be noted, however, that any disagreement among authors with the proposed amount of fractionation will not affect the REE modeling results, except in defining the REE abundances in the source. Nevertheless, evidence will be presented suggesting that the fractionation estimate is reasonable as applied to Hawaiian basalt formation.

V. OLIVINE FRACTIONATION

A more accurate representation of REE, Sr, Ba, and Sc abundances in the primary melt of the Hawaiian tholeiites requires that an estimation be made to the degree of olivine fractional crystallization that has evolved these magmas prior to eruption. Wright (1971) has used major element compositions of high and low MgO basalts in a least-squares computer model to arrive at an estimate. His results indicate that the low MgO Hawaiian magmas can be derived from 22-24% MgO magmas via 40% olivine fractionation. To conclude that this amount of fractionation occurs rests heavily on the assumption that the picritic basalts in his calculations represent noncumulate magmas, a fact that has not been demonstrated.

Two unique approaches concerning olivine fractionation will be undertaken in this study that will 1) define a hypothetical partial melt bulk composition and 2) independently define a minimum amount of olivine fractionation. The combined results will give a quantitative means for calculating the amount of olivine fractionation that has occurred in each magma batch. The first approach characterizes the composition of the melt as the sum of the weight fractions of the mineral melt components. The second relates the fractionated magma to two of the melt components (cpx and gar) by the addition of two compositionally distinct olivines. Additional data will then be presented to verify the conclusions reached by these combined observations.

As a first approximation of the melt composition, the compositions of the mineral components ol + opx, cpx, and gar were added together in their assumed eutectic modal ratio of 0.1:0.45:0.45, respectively. Mineral compositions were selected to reflect the high temperature and pressures (40 kb) associated with the melting event. These compositions are assumed to represent a solid solution relationship among the melt components.

The garnet component ($Py_{70}Gr_{15}Alm_5$) used was a low (2.2%) Cr_2O_3 variety equilibrated at 1300°C at 200 km (80 kb) (Danchin and Boyd, 1975). Garnet data obtained under different conditions (e.g., Kushiro et al., 1972) show little deviation from this composition. The cpx

component data are from Kushiro et al. (1972) and Mori and Green (1975), with compositions reflecting crystallization at ~1500°C and 30 kb. These data were modified somewhat by converting all Cr_2O_3 to FeO to account for the low concentrations of Cr_2O_3 and high contents of FeO observed in the magmas. The two cpx components were chosen to represent possible differences in melting conditions; the low Al_2O_3 variety coexisting with garnet at very high temperatures and pressures and the high Al_2O_3 cpx coexisting at slightly lower temperatures and pressures (Finnerty, 1976). The CaO-MgO abundances of the cpx-gar pair can also be shown to represent variations in the melting conditions.

Melts (1) and (2) in Table 8 were calculated in an attempt to reproduce the high FeO melts suggested by Wright (1971) to represent primary melts. Note that these melts require the olivine component to be almost pure fayalite, an improbable occurrence. A melt composition with a more realistic olivine component (Fo_{93}) is presented in Table 9 [Melt (3)].[7] Although none of these estimates will be used, at present, to represent the hypothetical composition of the melt, one point can be considered: All of these estimates indicate that the melt is MgO-rich; the fayalite melt contains 20% MgO, and the most realistic melt (containing a "real" olivine) contains 25% MgO. For the purpose of later discussion, it will be assumed that melts (1) and (3) represent extreme compositions and that the actual melt has a composition closer to the average of these two (Table 9). This MgO abundance, coincidentally, is very similar to that proposed by Wright (1971, Table 10, p. 26) to be present in the primitive Hawaiian melt. Nevertheless, as stated earlier, caution must be taken before applying his melt to quantitative description of olivine fractionation for the following reasons: 1) The FeO content is not fully defined. A high FeO-melt can only be attained by assuming a fayalitic olivine component. 2) The fractionated olivine (Fo_{86-88}) Wright has calculated is too forsteritic to be in equilibrium with the

[7] This melt was calculated using the cpx component given by Kushiro et al. due to Al_2O_3-Ca_2O requirements; the Al_2O_3/CaO ratio in the melt should be ~1.3 since olivine crystal fractionation will not alter this ratio in residual liquids.

TABLE 8. MINERAL COMPONENT ESTIMATE OF MELT COMPOSITION.

Element	ol (Fa_{100})	cpx (a)	cpx (b)	gar (c)	Melt (1)	Melt (2)
SiO_2	29.5	52.0	51.0	44.7	46.5	46.0
TiO_2	. . .	0.0	0.0	0.5	0.2	0.2
Al_2O_3	. . .	5.3	0.0	19.7	11.3	9.1
FeO[d]	70.5	5.4[d]	5.4[a,e]	6.5	12.4	12.4
MgO	. . .	22.5	27.0	21.5	19.8	21.8
CaO	. . .	13.8	14.8	5.2	8.6	9.0
Na_2O	. . .	0.7	0.7[a]	0.8	0.7	0.7
Cr_2O_3	. . .	0.0[d]	0.0	2.2	1.0	1.0

NOTES: Weight fractions used were 0.10 ol – 0.45 cpx + 0.45 gar.

[a]From Kushiro et al., (1972) used in melt (1).

[b]From Mori and Green (1975) used in melt (2).

[c]From Danchin and Boyd, 1975.

[d]Total Fe as FeO.

[e]All Cr_2O_3 converted to Fe_2O_3.

TABLE 9. MINERAL COMPONENT ESTIMATE OF MELT COMPOSITION USING A REALISTIC OLIVINE COMPOSITION.

Element	ol (Fo_{93}) (a)	cpx (a)	gar (b)	Melt (3)	Avg. of (1) and (3)
SiO_2	40.1	52.0	44.7	47.5	47.0
TiO_2	0.0	0.0	0.5	0.2	0.2
Al_2O_3	0.1	5.3	19.7	11.3	11.3
FeO[c]	6.5	5.4	6.5	6.0	9.2
MgO	51.3	22.5	21.5	24.9	22.4
CaO	0.3	13.8	5.2	8.6	8.6
Na_2O	0.0	0.7	0.8	0.7	0.7
Cr_2O_3	0.8	0.0	2.2	1.1	1.0

NOTES: Weight fractions used are given in table VIII.

[a]From Kushiro et al. (1972).

[b]From Danchin and Boyd (1975).

[c]Total Fe as FeO.

magma (Roeder and Emslie, 1970). Using a K_D = 0.3, the average magma (Table 6A, this work) can only have an equilibrium olivine of ~Fo_{80}.

These observations necessitate a second approach to be taken in determining the amount of olivine fractionation that has occurred. In this approach, it is assumed that the magma can be equated to the primary melt components, cpx and gar, by the addition of two compositionally distinct olivines on the basis of mg' values (molar MgO/MgO + FeO). The olivine added to the magma will represent the fractionated olivine, $Fo_{(R)}$, and the olivine added to the melt components will correspond to the olivine melt component $Fo_{(m)}$. A simple way of expressing this relationship can be written as

$$(1 - x)mg'_{cpx+gar} + x\ mg'_{Fo(m)} = (1 - y)mg'_{rock} + y\ mg'_{Fo(R)}$$

where x ≡ corresponding weight fraction of olivine in the primary melt $Fo_{(m)}$ and y ≡ weight fraction of fractionated olivine $Fo_{(R)}$. The actual equation used accounted for the changes in molar proportions of the resultant "melts." Note that this equation allows for multiple solutions for $Fo_{(R)}$ and $Fo_{(m)}$ to be obtained when both the amount of fractionation and the modal amount of olivine represented in the melt are varied.

Before these solutions can be calculated, mg'_{rock} and $mg'_{cpx+gar}$ must be determined. The mg'_{rock} value can be calculated directly from the experimental data. The average mg' value of a 7% MgO basalt is 0.55 (see Table 6A). (This value was used above in calculating the equilibrium olivine).

The mg' value for the cpx + gar component was estimated from "adjusted" mineral component data. For the purpose of an initial calculation, it will be assumed that the FeO and MgO abundances in the melt are those that are given by the average melt composition presented in Table 9. It was suggested previously that a primary melt containing ~12% FeO was not a realistic melt composition because of the high fayalitic olivine required. Since a 6% FeO melt was not considered to be representative of an actual melt, the average melt will be used. To attain a melt containing a ~9.2% FeO and ~10% Fo_{93}, the cpx + gar component must have ~9.5% FeO (this value will be arbitrarily taken to

be 10% FeO). Similarly, the MgO content in the cpx + gar component must be ~20%. The resultant $mg'_{cpx+gar}$ value is then 0.78. Although it may appear that this value is biased toward a high MgO melt, the effect that a more FeO-rich MgO-poor cpx + gar component will have on these calculations will be discussed shortly.

Solutions to the above equation involved assigning a forsterite content to the fractionating olivine (Fo_R was varied from 70 to 90) at a preselected degree of fractionation (x ranged from 30-50%) and calculating the mg' value of the initial olivine component. Two sets of solutions will be calculated for each degree of fractionation; the first corresponding to an equal amount of the initial olivine component (that is, y = x) and the second corresponding to substantially less (15-20%). The latter proportions represent a close approximation to the proposed modal ratio of melt components; namely, 10% ol-opx, 45% cpx, and 45% gar.

The results of these calculations are depicted in Figure 6. Plotted along the x-axis is the forsterite content of the fractionating olivine or phenocryst composition and along the y-axis the necessary forsterite content of the corresponding olivine melt component. As an example for determining the various solutions, assume that 50% fractional crystallization of Fo_{70} has occurred. The resultant mg' value by addition of 50% Fo_{70} to 50% whole rock would be 0.66. This value now represents the intial (primary) melt mg' value. To obtain this value in a melt corresponding to 50% of the cpx + gar component and 50% olivine, such an olivine would need an Fo_{60} content. This solution is represented by Point A in Figure 6. Point B represents the solution for 50% Fo_{90} fractionation from a primary melt (mg' = 0.81) corresponding to 50% cpx + gar and 50% Fo_{83}. The tie line joining these two points, labeled 1A, thus depicts the compositional dependence of the olivines when 50% olivine fractionation occurs from a melt containing 50% olivine. Tie line 1B represents 50% olivine fractionation and 20% melt olivine. Other solutions represented are 40% olivine fractionation and 40% melt olivine, tie line 2A; 40% olivine fractionation and 20% melt olivine, 2B; 30% olivine fractionation and 30% melt olivine, 3A; olivine fractionation and 15% melt olivine, 3B. These tie lines should

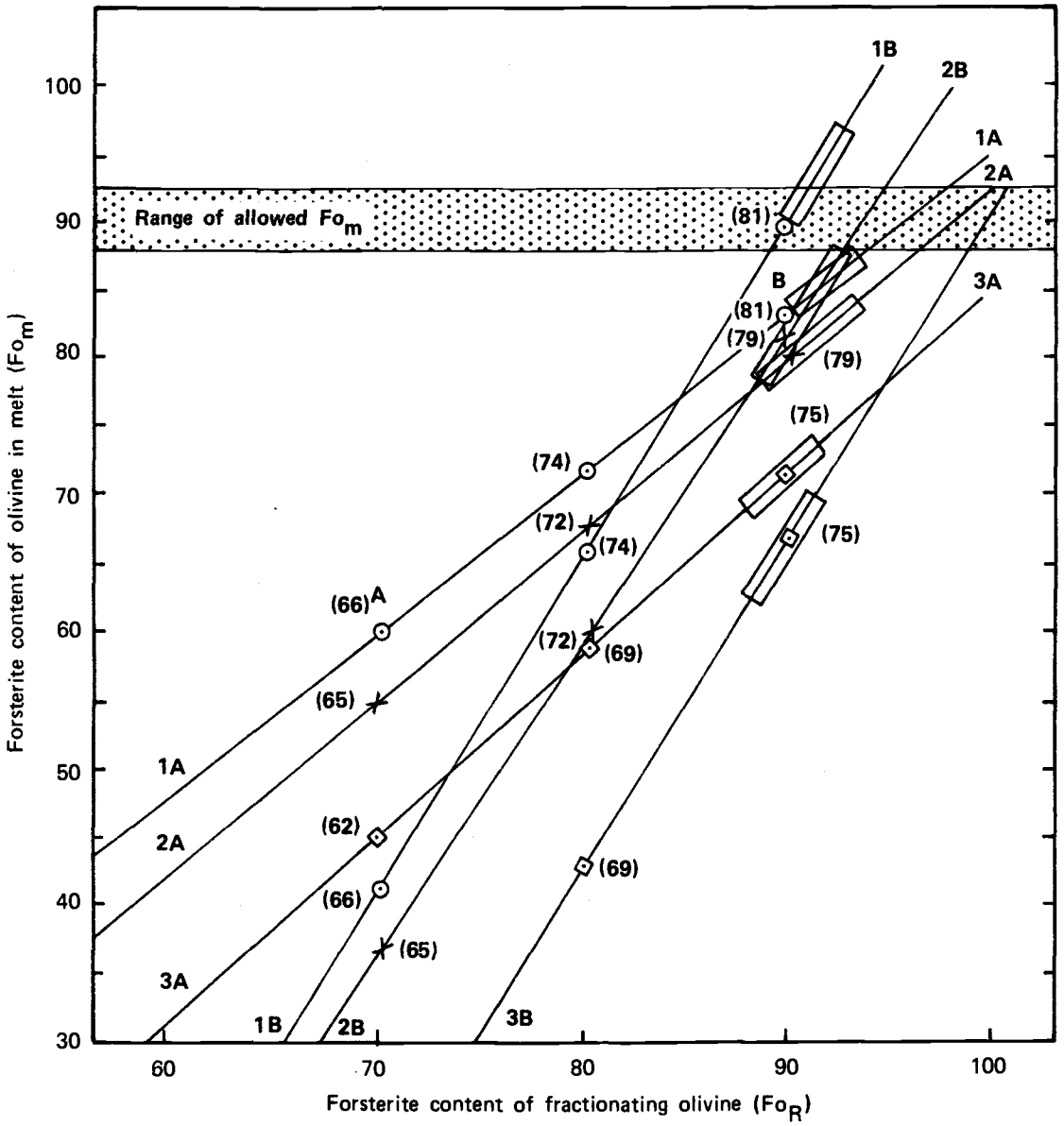

Fig. 6. Compositional dependence of $Fo_{(m)}$ vs. $Fo_{(R)}$ at various degrees of olivine fractionation for a typical low MgO Hawaiian basalt. See text for explanation. Numbers in parentheses are mg values of primary liquids. Wide portions of each tie line represent range of olivine (Fo_R) that can be in equilibrium with the melt (K_0 = 0.25 to 0.35).

actually show a slight curvature and be lower because of the compositional dependence of the fractionating olivine on the melt. Nevertheless, a qualitative description can be obtained from this approach.

Not all of these solutions represent probable melts nor are indicative of the fractionation event. Two constraints can be imposed to give a narrow range of realistic solutions. The first constraint imposed is that the fractionation olivine component must be such that the olivine can be in equilibrium with the melt (Roeder and Emslie, 1970). These compositions are dependent on the mg' value of the melt and were determined assuming a range of K_D values (0.25 = 0.35). Acceptable olivine compositions are represented in Figure 6 by the wide portions of each tie line. The second constraint imposed concerns the range of olivine compositions which are most representative of the corresponding melt component (Fo_m). Green (1971) has concluded that most olivines in equilibrium with parental melts must have compositions between Fo_{87}-Fo_{92}. This constraint is represented by the horizontal lines corresponding to these olivine compositions.

On the basis of these constraints, the following conclusions can be drawn as they apply to this particular example. 1) At least 40% olivine fractionation has evolved the average Hawaiian basalt; the solutions given by 50% fractional crystallization fulfill the constraints the best. 2) The amount of initial olivine component represented in the melt is about 20%; this is consistent with the assumed melting mode at 40 kb (Davis and Shairer, 1965). 3) The average primary melt parental to the Hawaiian basalts has an mg' value of approximately 0.80.

The solutions that are obtained when the mg' value of the cpx + gar component is lowered will now be examined. The effect that a higher FeO-lower MgO component would have on deriving these solutions can be visualized by simply raising the compositional tie lines of Figure 6 accordingly. Only a slight decrease in the $mg'_{cpx+gar}$ value to 0.71 would place the entire 40-20 tie line (2B) into the allowed field. However, to obtain the solution 40% Fo_{90} fractionation from a melt containing 40% olivine (Fo_{87}-Fo_{92}) would require that $mg'_{cpx+gar}$ be

about 0.64. Similarly, 30% Fo_{87}-Fo_{92} would require $mg'_{cpx+gar}$ to be ~0.60.

The latter two solutions are considered to be extreme lower limits to a realistic description. For example, the mean mg' value of an evolved cpx derived from magmatic processes occurring within oceanic plates is 0.72 (Nisbet and Pearce, 1977). A coexisting garnet would have an mg' value of 0.57,[8] and the mg' value of the combined component could be as low as 0.63. If the melting temperature is assumed to be ~1250°, slightly higher than the crystallization temperature of the surface lavas (Leeman and Scheidegger, 1977), the smallest mg' value of the combined components is 0.59 (mg'_{gar} = 0.50). Thus even if these solutions are considered to be representative of the olivine fractionation event, at least 30% olivine removal is still required for Hawaiian basalt generation.

On the basis of these observations together with the preceding arguments favoring an MgO-rich primary melt, a first-order approximation to the amount of olivine fractionation can be obtained. The final process of magma evolution will be defined as stated: that a 7% MgO basalt has been evolved from a ~24% MgO primary melt via 50% olivine fractionation. Quantitatively, fractional crystallization can be

---

[8]The mg' value of a garnet in equilibrium with cpx can be reasonably estimated from the equation presented by Raheim and Green (1974) for determining $K_d^{gar/cpx}$ and combining a mass balance constraint to the garnet component. Since $K_D = \frac{(FeOgar/MgOgar)}{(FeOcpx/MgOcpx)}$ can be calculated at the desired temperature and pressure and since FeOcpx and MgOcpx are known, the (FeO/MgO)gar ratio can be determined. The mass balance constraint imposed is based on the Al_2O_3 and CaO abundances required in the garnet component to produce a melt having reasonable abundances of these elements. That is, the combined cpx + gar component (assumed to be in a one-to-one proportion) must have an Al_2O_3/CaO ratio of ~1.3. This ratio is unchanged by olivine fractionation. The garnet composition given in Table 9 fulfills this constraint; therefore, the total abundance of FeO + MgO is dictated by this composition. The individual FeO and MgO abundances (and consequently the mg' value) can be calculated by solving the above two equations simultaneously.

expressed by the equation presented by Shaw (1970), also known as the Rayleigh equation:

$$\frac{C^{\ell}}{C_o} = (1 - F)^{D-1}$$

where C^{ℓ} ≡ concentration of an element in the final liquid

C_o ≡ concentration of an element in the initial liquid

F ≡ degree of fractionation

D ≡ mineral to liquid partition coefficient of the fractionating phase

If the above data are applied to this equation, a D value of ~2.8 is derived for MgO partitioning into olivine. This value was then used in determining the amount of olivine fractionation involved in generating each representative basalt from a 24% MgO melt. These estimates are given in Table 7.

Having obtained the $D_{MgO}^{ol/\ell}$ value, further information concerning the fractionating event can be sought. Leeman and Scheidegger (1977) have determined the temperature dependence of olivine MgO partitioning, and thus the average temperature of olivine fractionation can be obtained (~1400°C). Subsequent mineral to liquid partition coefficients for olivine can also be calculated using this temperature and their associated temperature-dependent equations. The olivine to liquid partition coefficient for FeO at 1400°C, for example, is ~0.93[9] (Leeman and Scheidegger, 1977). This permits a very rough estimate to the FeO contents in the initial liquid to be determined when the FeO data are applied to the Rayleigh equation (Table 6A). This abundance is calculated to be ~10.6%. And since the mg' value of the primary melt was determined to be ~0.80, a second estimate to the FeO concentration in the melt can be made. Assuming a 24% MgO melt, the FeO content in such a liquid would be ~10.0%, in good agreement with the first approximation.

---

[9]When possible, all partition coefficients will be calculated from experimentally determined temperature-dependent equations. Although it has been shown that olivine FeO/MgO partitioning is independent of temperature (i.e., K_D = constant), a range of acceptable K_D values has been reported (0.25-0.35).

There are other quantitative means for examining the validity of the proposed olivine fractionation process, as well as for obtaining the temperature and olivine composition that characterizes the initial fractionation event. Estimates of the FeO and MgO contents in a liquid derived by partial melting of a garnet peridotite have been made experimentally by numerous workers (e.g., Yoder, 1976), whereas Hanson and Langmuir (1977) have attempted to obtain such estimates theoretically. This latter approach will be investigated in detail in this study using more specific information; that is, appropriate mineralogies, melting modes, and D values will be applied to Hawaiian basalt generation. The mantle material melted will have the mineralogy given by the REE modeling attempt (85% 3:1 ol+opx, 10% cpx, and 5% gar) and a composition typical of a garnet peridotite (40% MgO and 7% FeO – see Table 13). The melting mode assumed is identical to that used throughout this work. Mineral to liquid partition coefficients were determined at temperatures ranging from 1200-1600°C at 100°C intervals.

Olivine and orthopyroxene FeO and MgO partition coefficients were calculated from the temperature-dependent equations given by Leeman and Scheidegger (1977) and Grove and Bence (1977), respectively. Less direct methods had to be used for obtaining the cpx and gar data. The relative partitioning of FeO and MgO between gar and cpx (Raheim and Green, 1974) and between ol and cpx (Duke, 1976) provided the basis for calculating some of these values. (It will be noted, however, that even a large error in the cpx and gar estimates will not greatly affect the results to be presented.) It appears from the data presented by Grove and Bence (1977) that FeO and MgO cpx partition coefficients are similar to these observed in opx but slightly lower. For this reason, and because the D_{FeO} values are less than 1, little error is introduced by assuming $D_{FeO}^{cpx/L} = 0.9\ D_{FeO}^{opx/L}$. MgO partition coefficients for cpx can then be calculated from ol-cpx data presented by Duke (1976). These values agree rather well with the limited data presented by Grove and Bence (1977) for cpx (Appendix C). The D_{MgO} value for gar was arbitrarily set equal to the D_{MgO} for cpx on the basis of similar MgO contents observed in these coexisting pairs under mantle conditions

(e.g., Wilkinson, 1976). The equation of Raheim and Green (1974) can then be used to calculate D_{FeO} for gar. Since their equation is also dependent on pressure, 40 kb was assumed. The D values for these elements at selected temperatures are presented in Appendix C along with the calculated bulk partition coefficients for the solid and the liquid.

The FeO and MgO contents in the melt as a function of temperature and degree of melting are depicted in Figure 7. Unlike the plot presented by Hanson and Langmuir (1977), several striking differences can be noted. The diagonal dashed line to the right of the melt field represents their melts at low (0-10%) melting. These melts are much more FeO-rich than this model indicates, even though a similar mantle composition was used as a parent. The horizontal dashed lines represent their geotherms in the melting process. These remain horizontal for large degrees of melting (60%). In this model, increased melting at constant temperature produces melts that become compositionally similar to the source. Such a feature is expected in a naturally occurring equilibrium-type melting process. The implications that this type of diagram would have on hypotheses concerning the generation of all types of basaltic magma are too numerous to discuss. However, the following observations can be made regarding Hawaiian basalt generation. 1) An average Hawaiian basalt (7% MgO, 11% FeO — see Fig. 7) can only be related by olivine fractionation to a high (20-30%) MgO melt. This observation assumes that the melt is generated from a typical garnet peridotite. Direct derivation of the magma by partial melting at 1300°C, for example, would require a source composition of ~30% MgO and 11% FeO. Although this composition is possible, it would not be considered to be a garnet peridotite. 2) The proposed primary melt (24% MgO and 10% FeO) has a composition that is within the theoretical field of derived liquids. Furthermore, this composition would be the result of partial melting near the amount (10%) suggested by the REE model. 3) The temperature of the proposed partial melting process (~1475°C) would coincide with the temperature indicated by the fractionating event. Roeder and Emslie (1970) have presented a plot (reproduced in Fig. 8) that can be used to obtain the temperature of olivine fractionation and

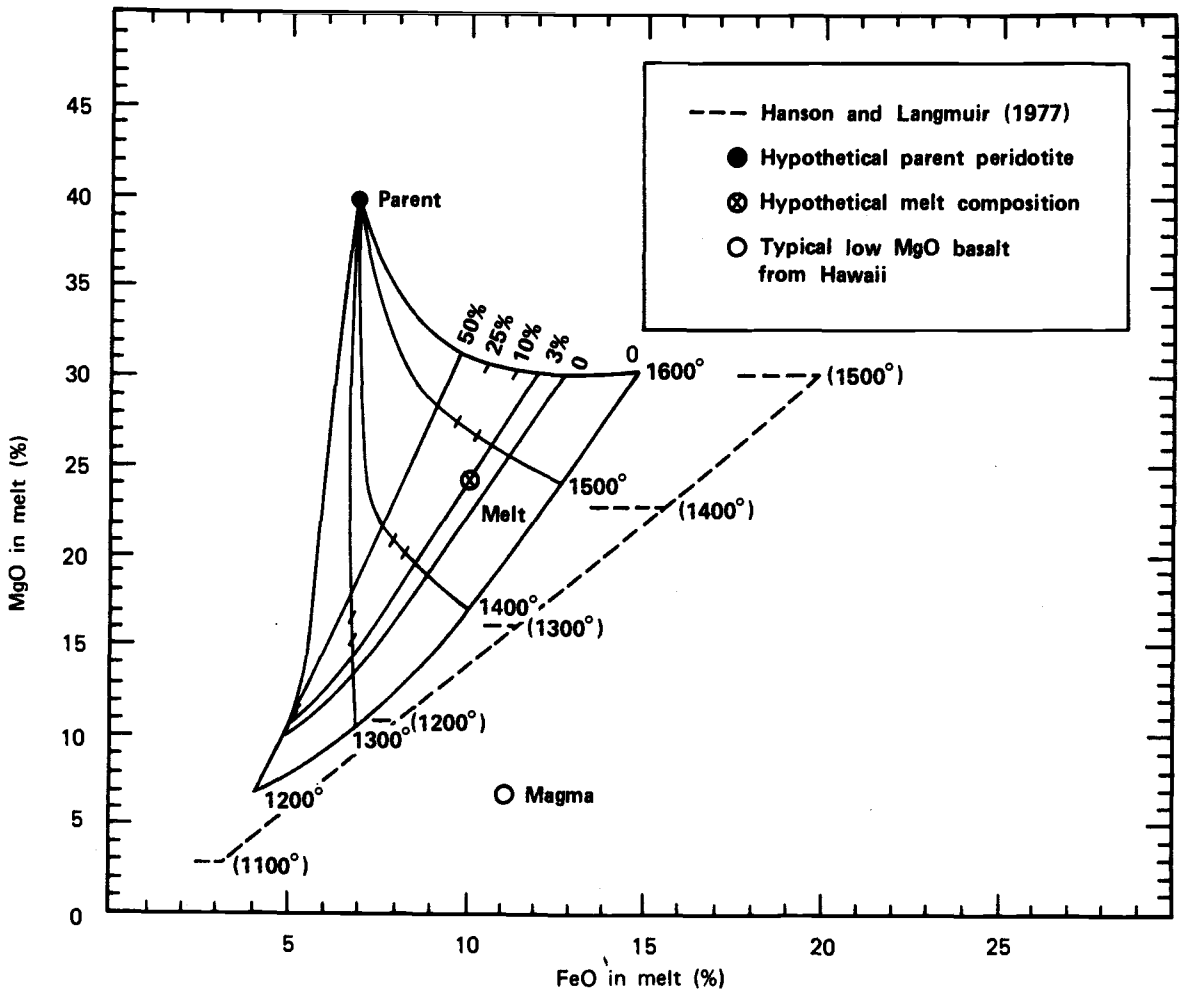

Fig. 7. Plot of MgO versus FeO melt compositions hypothetically produced at various temperatures and degrees of partial melting. Shown for comparison is a partial reproduction of a similar plot presented by Hanson and Langmuir at 1 percent melting. The contour connecting the squares represents 0 percent melting of a parent source material composed of 90 percent olivine. All temperatures are in degrees Centigrade.

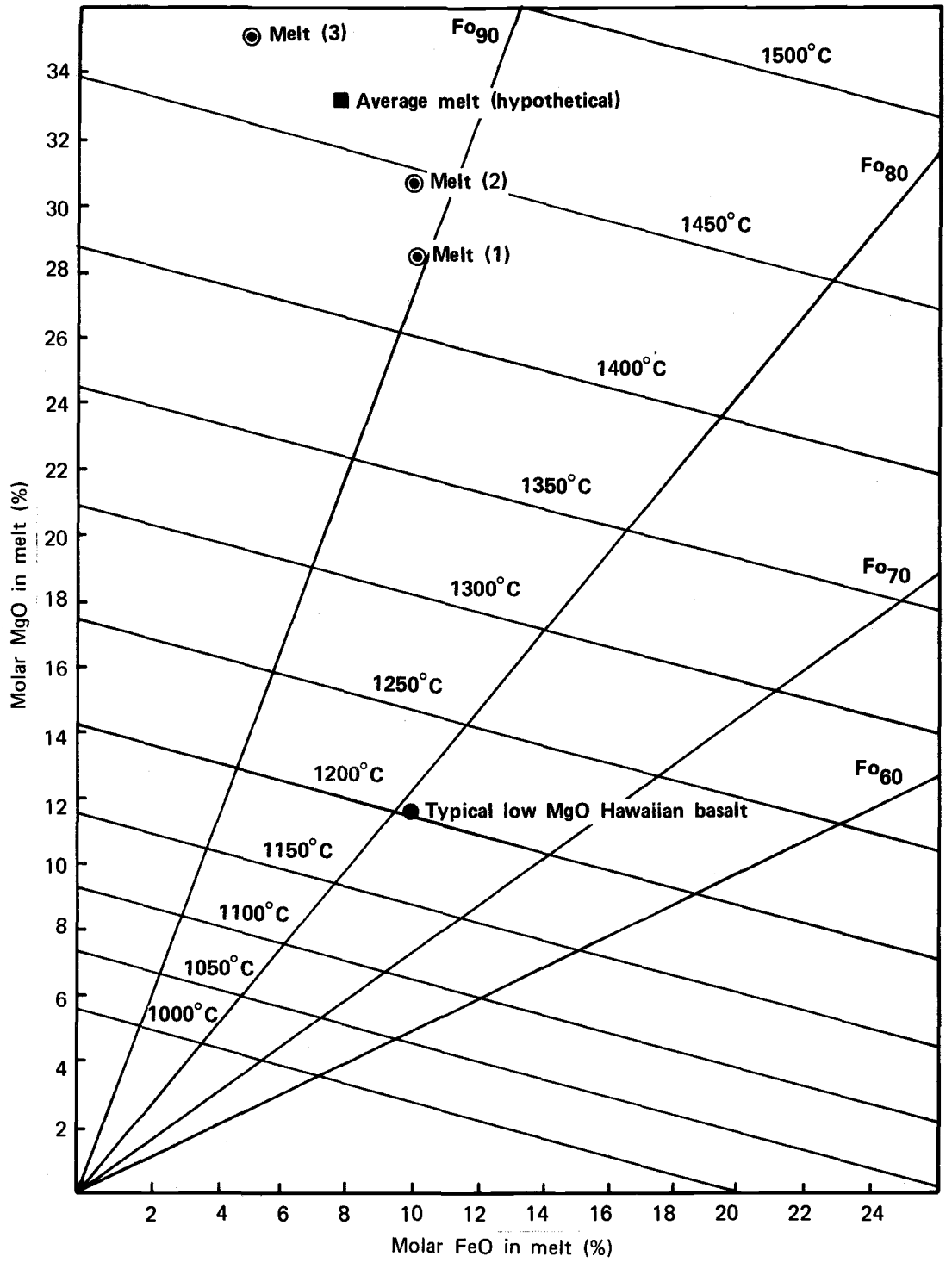

Fig. 8. Reconstructed plot presented by Roeder and Emslie (1970) illustrating compositional dependence of olivine on melt composition. See text for symbol explanation.

the composition of the initial olivine component given the bulk composition of the liquid with respect to FeO and MgO. The melt compositions represented in the figure are those presented in Tables 8 and 9 and the hypothetical melt composition proposed in the previous discussion. It can be seen from the figure that Fo_{90-93} would be the first olivine removed from the proposed melt at a corresponding temperature of ~1475°C.

The good agreement among these independent means of obtaining melt compositions and temperatures very much enhances the proposed fractionation process. It would be reasonable to assume, for instance, that olivine fractionation would occur at or nearly the same temperature of melting.

This section concerning olivine fractionation can be summarized by describing the proposed mechanisms involved in the fractionation model. Following melting of the garnet peridotite source, the primary liquid, having ~24% MgO and ~10% FeO (mg' = 0.80), fractionates olivine, Fo_{93}, at ~1475°C. As fractionation proceeds, the mg' value of the evolved melt will decrease, necessitating that subsequent olivines removed be less forsteritic (Fo_{90-85}). The FeO content of these intermediate liquids probably approaches 12%. During the final stages of olivine fractionation, FeO abundances will decrease in the resultant magma because of FeO-rich (Fo_{85-93}) olivine fractionation. The composition of the last olivine removed from a 7% MgO magma is ~Fo_{80}. Finally, it could be suggested from this discussion that 1) any observed Hawaiian basalt containing ~20% MgO and being greater than ~11.5% FeO cannot be considered as a primary melt but is probably cumulate in origin and 2) it would be very difficult to estimate olivine fractionation by way of a linear addition process since FeO initially increases and then decreases during fractionation. For this reason, an approach involving MgO partitioning only appears to be a simple, yet reasonable, procedure to evaluate this process.

VI. LIGHT RARE EARTH ELEMENT DEPLETION

The preliminary source model had attempted to generate the Hawaiian basalts from a mantle with a flat chondrite-normalized REE, Sr, Ba, and Sc pattern. As stated earlier, the observed basaltic abundance patterns cannot be produced unless the source is depleted in some of these elements, notably La, Ce, and Ba. Because of this, an estimate of light REE and Ba depletion in the source region will be made by assuming a whole-earth-crustal fractionation model. Although Sun and Nesbitt (1977) have argued that this type of fractionation cannot solely explain some of the observed trace element depletions in mid-oceanic ridge basalts (MORB), this model will nevertheless be applied as a first estimate for the Hawaiian source region(s).

The calculations are based on the mass balance relationship that must exist for selected trace elements between the whole earth and the mantle plus crust. Elemental partitioning into the core for these elements is considered to be minimal (Smith, 1977). It was further assumed that the crustal abundances of the REE are represented by those obtained by Haskin et al. (1968) in North American Shale Composite (NASC), the abundances of Ba and Sr were estimated by Mason (1970), and Sc was taken from Turekian (1968). The whole earth abundances, calculated by Ganapathy and Anders (1974), were modified using the chondrite normalization factors of this study to give a flat, chondritic pristine earth averaged from REE, Sr, Ba, and Sc data (Table 10). The data presented by Mason (1970) were used for the masses of the crust and the mantle. The expressions used in this calculation are as follows:

$$\text{whole earth content} = \text{earth mass (crust + mantle)} \times \text{earth abundance}$$

$$\text{crustal content} = \text{crust mass} \times \text{crustal abundance (NASC)}$$

$$\text{mantle abundance} = \frac{\text{whole earth content - crustal content}}{\text{mantle mass}}$$

The mantle abundances thus obtained represent the residual derived from fractionation of crustal material from the whole earth. The results of this calculation are given in Table 10. The absolute abundances of these elements in the mantle are not of interest at this point, only the depletion effect relative to the least depleted elements; namely,

TABLE 10. ESTIMATE OF LREE AND Ba DEPLETION IN THE MANTLE.

Element	Crustal Abundance (ppm) (1)	Earth Abundance (ppm) (2)	Chrondite Normalized Earth (Times Chondrite) (3)	Modified Earth Abundance (ppm) (4)	Estimated Mantle (Times Chondrite) (5)	Relative Depletion (Normalized) (6)
Sr. . .	250[a]	18.2	1.66	15.7	1.30	1.0
Ba. . .	400	5.1	1.34	5.4	0.81	0.60
La. . .	32	0.48	1.41	0.49	0.90	0.67
Ce. . .	73	1.28	1.51	1.22	0.94	0.70
Nd. . .	33	0.87	1.36	0.92	1.14	0.84
Sm. . .	5.7	0.26	1.33	0.28	1.27	0.94
Eu. . .	1.24	0.10	1.37	0.10	1.28	0.95
Tb. . .	0.85	0.067	1.43	0.067	1.33	1.0
Dy. . .	5.8	0.45	1.50	0.43	1.33	1.0
Yb. . .	3.1	0.29	1.32	0.32	1.38	1.0
Lu. . .	0.48	0.049	1.44	0.049	1.37	1.0
Sc. . .	22[b]	12.1	1.51	11.4	1.41	1.0

NOTES: (1) Crustal abundance assumed to be NASC (Haskin et al., 1968). (2) Earth abundances given by Ganapathy (1976). (3) Calculated using chondrite-normalization factors given in figure 4A. (4) Recalculated earth abundances assuming chondritic earth of 1.43 times chondrite. (5) Mantle abundances estimated from crustal fractionation model (see text). (6) Depletion of REE, Sr, Ba, and Sc relative to average of Sr, Tb, Dy, Yb, Lu, and Sc chondrite-normalized abundances.

[a]From Mason (1970).

[b]From Turekian (1970).

the LREE. Hence, the reciprocal of the relative depletion factors was multiplied to each respective trace element abundance in the Kohala-Mauna Kea-Kilauea basalts. The Koolau-Lanai and Mauna Loa basalts retained a small degree of LREE depletion and were modified further by multiplication of LREE ratios between the Mauna Loa and Kilauea basalts. The ratios used were $(La/Eu)_{Kil}/(La/Eu)_{ML}$, $(Ce/Eu)_{Kil}/(Ce/Eu)_{ML}$, and $(Nd/Eu)_{Kil}/(Nd/Eu)_{ML}$.

VII. REFINED SOURCE MODEL

General Description

Partial melting calculations were repeated using the estimated abundances of the REE and Sc in the primary melts as determined from applying the results of the previous two sections to the Rayleigh equation. Ba and Sr data were not used in these calculations because of the uncertainties in Ba depletion and Sr abundances.[10] The plots in Figures 9 and 10 depict the computer modeling results obtained for the Kilauea group and Mauna Loa group basalts, respectively. In these figures, the weight fractions of the mantle components are plotted versus the chondrite-normalized mantle abundance in order to observe more clearly the apparent single source melted in deriving the Kilauea group basalts (Fig. 9).

In contrast to the first set of calculations, real solutions were obtained for modeling the source of the southern rift basalts (Fig. 10). It will be suggested that the Lanai and Mauna Loa basalts have been derived from the same source by different degrees of partial melting, even though the source material for Lanai that would give the best fit (based on abundance residuals) actually lies to the left of the Mauna Loa source composition. That is, the Lanai source apparently has the same mineralogy as the Mauna Loa mantle, with slightly lower trace element abundances.

Source materials for the Koolau basalts are plotted in Figure 10. These results indicate a third type of material needed in generating Hawaiian basalts.

---

[10] Applying the depletion factors for Ba and Sr to these basalts results in some patterns now having Ba and Sr enrichment. Therefore, the discussion concerning these elemental abundances will be deferred.

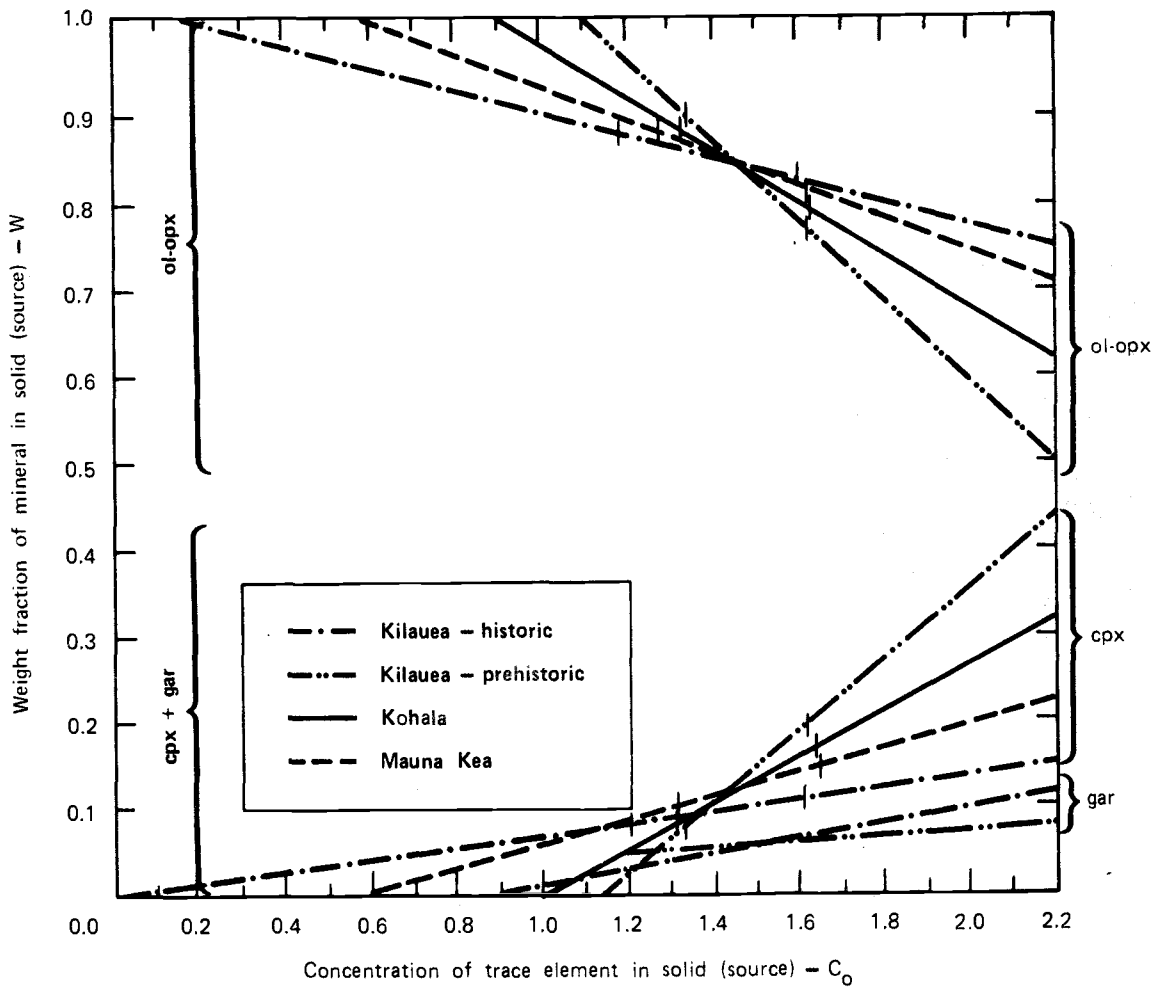

Fig. 9. Refined REE and Sc partial melting model for the Kilauea group basalts. In this figure, the weight fraction modes of a source are plotted versus the C_o value required for that particular source. Degrees of melting lie along the compositional tie lines (not shown). The perpendicular bars represent the range of compositions that yield the most optimal REE abundance patterns for each particular basalt suite (i.e., all REE abundances within 10%). Two of the garnet tie lines (Kohala and Mauna Kea) have been omitted for clarity.

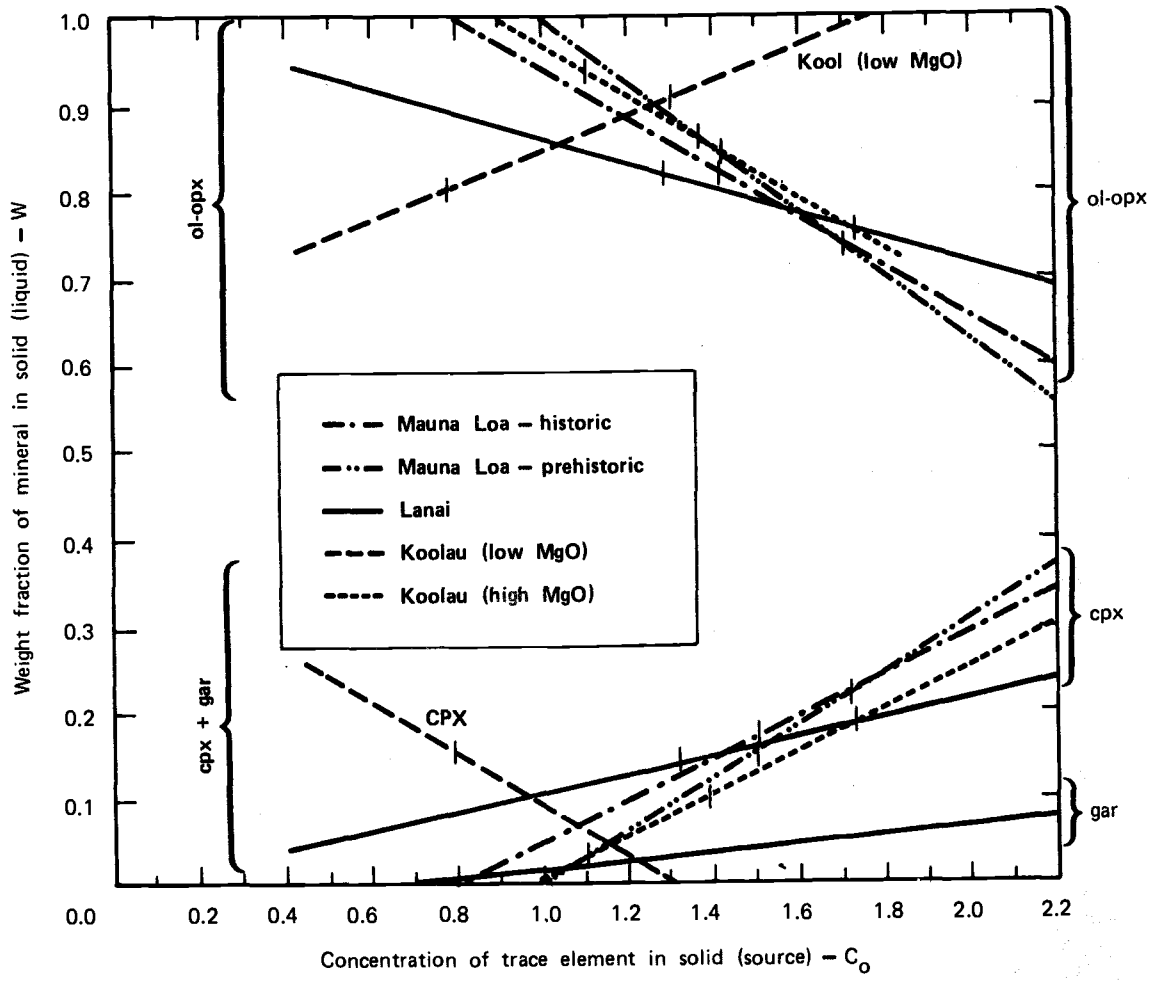

Fig. 10. Refined REE and Sc partial melting model for the Mauna Loa group basalts. Lanai refers to the average low MgO basalts. The high MgO basalt has been omitted for clarity. The perpendicular bars represent the range of compositions that yield the most optimal REE abundance pattern for each basalt suite. Garnet compositional tie lines for Mauna Loa and Koolau have also been omitted for clarity.

Elemental Description

REE and Sc Modeling - The Kohala, Mauna Kea, and Kilauea magmas appear to be generated from a compositionally identical source(s) with magmatic REE abundance patterns reflecting different degrees of partial melting — 3-6%. The mineralogy of this source(s) corresponds to ~84% ol+opx (63% ol and 21% opx), 12% cpx, and 4% gar. Such a mineralogy is, incidentally, in the range of naturally occurring garnet peridotites (Carswell and Dawson, 1970). REE and Sc abundances in this source were determined to be 1.4 to 1.5x (times chondrite).

The Lanai and Mauna Loa basalts also appear to be derived by varying degrees of partial melting (3-6%) from a single source. This source is mineralogically and compositionally different from the Kilauea group mantle; the Mauna Loa group source is significantly lower in ol-opx (75% ol+opx; 56% ol and 19% opx) but higher in cpx (20%) and gar (5%). These mineralogical differences could indicate a depth relationship of some type among mantle regions as suggested by Sun and Nesbitt (1977). On the other hand, the higher heavy REE and Sc abundances calculated for the Mauna Loa-Lanai mantle (1.6x) combined with the lower light REE abundances (recall the relative depletion observed among the basalts) imply that a simple chemical relationship does not exist. That is, they are not directly related as a result of partial melting or fractional crystallization events (although at present, it is difficult to distinguish between the heavy REE abundances in these sources).

As stated above, the Koolau mantle may represent a third type of source material melted in producing Hawaiian magmas. This source is characterized by very high ol+opx contents (90% ol+opx; 68% ol and 32% opx), low cpx (6%), and gar (4%) and has considerably lower REE and Sc abundances (~1.2x) than the other two proposed sources.

Compositional heterogeneity may be examined more closely by using the computer modeling results to calculate the REE abundance patterns required in each source to generate the observed magmatic REE patterns.

In this treatment, trace element abundances reflecting olivine fractionation only were applied to the partial melting equation presented earlier. The source mineralogies determined by the computer model were used to calculate the bulk partition coefficients of the sources. The degrees of partial melting in this case are one of the unknowns and were determined by the partitioning of Eu in each magma, dictating that the chondrite-normalized Eu abundance in each source was that given by the computer model (1.2x chondrite Koolau, 1.6x Lanai-Mauna Loa, and 1.5x Kilauea group). Other elements could have been used as the partial melting indicator, but Eu was considered most ideal for the following reasons: 1) Mineral to liquid partition coefficients for Eu are large enough in each mineral to minimize any error associated with their uncertainties. 2) Eu's analytical uncertainty is low. 3) Eu is not located on the focal point of abundance patterns resulting from melting of garnet-bearing systems; that is, P is not near unity. 4) Eu would be relatively unaffected by processes causing light REE depletion or heavy REE enrichment or depletion. 5) No Eu anomalies are observed in these magmas. The light REE's were not considered as indicators because of their actual depleted nature in the basalts and because of their very low partition coefficients. Since the heavy REE's may be anomalously enriched or depleted in the source because of high $D^{gar/\ell}$ values, Yb and Lu were not considered for this estimate.

Having obtained in this manner the degrees of partial melting required to give the Eu abundances in the magmas' suites, one can determine the remaining mantle REE and Sc abundances required in the sources. The results are given in Tables 11-12. The calculated abundances agree very well among the basalts proposed to be generated from the same source(s), considering the large analytical uncertainties in some of the elemental determinations. The average of the required chondrite-normalized REE and Sc abundances within each suite are depicted in Figure 11. The figure shows more explicitly the crossing effect of the REE patterns between the Mauna Loa and the Kilauea mantles. The light REE's exhibit much more depletion in the Mauna Loa mantle than in the Kilauea mantle, as was suspected from magmatic REE observations. On the other hand, the heavy REE abundances in the Mauna Loa source are higher

TABLE 11. CHONDRITE-NORMALIZED TRACE ELEMENT ABUNDANCES REQUIRED IN SOURCE MATERIAL COMPOSED OF 84% ol + opx, 12% cpx, AND 4% gar (FROM REE MODEL) FOR THE KILAUEA GROUP BASALTS.

Element	Kohala PM = 4.7%[b]		Mauna Kea[b] PM = 2.9%		Kilauea-PH PM = 5.7%[b]		Kilauea-H[b] PM = 3.5%		Average C_0 (a)
	C^{ℓ}/C_0	C_0 (a)	C^{ℓ}/C_0	C_0 (a)	C^{ℓ}/C_0	C_0 (a)	C^{ℓ}/C_0	C_0 (a)	
La. . .	17.10	0.96	24.29	1.06	14.61	1.24	21.24	1.15	1.10
Ce. . .	15.66	1.10	21.22	1.18	13.61	1.30	18.93	1.29	1.22
Nd. . .	14.68	1.19	19.30	1.23	12.87	1.39	17.39	1.21	1.25
Sm. . .	10.90	1.42	12.84	1.34	10.02	1.47	12.10	1.36	1.40
Eu[b] . .	9.53	1.48	10.82	1.47	8.92	1.47	10.34	1.46	1.47
Tb. . .	7.04	1.48	7.31	1.42	6.97	1.41	7.24	1.51	1.46
Dy. . .	6.02	1.50	5.99	1.49	6.03	1.56	6.00	1.61	1.49
Yb. . .	3.73	1.48	3.12	1.52	4.24	1.20	3.33	1.45	1.41
Lu. . .	3.28	1.39	2.76	1.39	3.94	1.22	2.97	1.49	1.37
Sc. . .	1.52	1.65	1.47	1.56	1.56	1.44	1.52	1.56	1.55
Sr. . .	18.52	1.07	27.47	0.99	. . .	. . .	. . .	. . .	1.03
Ba. . .	18.98	0.73	27.27	0.87	15.9	0.86	24.4	0.63	0.77
Hf. . .	8.10	1.43	9.13	1.47	7.46	1.29	8.88	1.34	1.38
Ta. . .	11.92	1.45	14.09	2.18	10.93	2.14	12.78	2.50	2.07
Th. . .	21.84	0.23	35.20	0.40	17.50	0.52	28.57	0.44	0.40
Cr. . .	1.38	3115[c]	1.38	3701[c]	1.39	3054[c]	1.38	3123[c]	3250[c]
Co. . .	0.90	82[c]	0.90	78[c]	0.90	68[c]	0.90	68[c]	74[c]
Ni. . .	0.58	2434[c]	0.58	3013[c]	0.58	2744[c]	0.58	2068[c]	2540[c]

[a]Times chondrite.

[b]Degrees of melting calculated from Eu partitioning $C_0 = 1.47$.

[c]Expressed in ppm.

TABLE 12. CHONDRITE-NORMALIZED TRACE ELEMENT ABUNDANCES REQUIRED IN THE MAUNA LOA GROUP AND KOOLAU SOURCE MATERIALS.

Element	Lanai		Mauna Loa		Avg C_0 (b)	Koolau		Avg C_0 (b)
	Low MgO PM = 2.7[a] C_0 (b)	High MgO PM = 5.3[a] C_0 (b)	PH PM = 3.7[a] C_0 (b)	H PM = 5.2[a] C_0 (b)		Low MgO PM = 2.6[a] C_0 (b)	High MgO PM = 3.5[a] C_0 (b)	
La	0.74	0.88	0.85	0.89	0.84	0.65	0.64	0.65
Ce	1.11	1.27	1.14	1.17	1.17	0.88	0.86	0.87
Nd	1.31	1.50	1.29	1.40	1.38	1.14	1.01	1.07
Sm	1.46	1.54	1.43	1.46	1.47	1.09	1.05	1.07
Eu[a]	1.53	1.54	1.53	1.54	1.53	1.23	1.23	1.23
Tb	1.81	1.73	1.48	1.38	1.60	1.31	1.24	1.27
Dy	1.57	1.52	1.72	1.51	1.58	1.31	1.26	1.28
Yb	1.97	1.69	1.86	1.62	1.79	1.23	1.31	1.27
Lu	2.19	1.85	1.74	1.57	1.84	1.23	1.24	1.24
Sc	1.67	1.66	1.73	1.67	1.68	1.38	1.25	1.32
Sr	0.60	0.92	0.80	0.81	0.78	0.57	0.94	0.75
Ba	0.54	0.76	0.57	0.56	0.61	0.57	0.61	0.59
Hf	1.09	1.08	1.15	1.19	1.13	1.06	0.90	0.98
Ta	1.37	1.62	1.79	1.64	1.60	1.01	0.99	1.00
Th	0.17	0.23	0.20	0.25	0.21	0.17	0.12	0.15
Cr	3040[c]	2618[c]	2306[c]	2982[c]	2735[c]	3037[c]	3173[c]	3100[c]
Co	64[c]	64[c]	62[c]	67[c]	64[c]	83[c]	80[c]	82[c]
Ni	1919[c]	2352[c]	1556[c]	1580[c]	1866[c]	3029[c]	2927[c]	2980[c]

[a]Degrees of melting calculated from Eu: C_0 = 1.54 (M.L.); C_0 = 1.23 (kool).

[b]Times chondrite.

[c]Expressed in ppm.

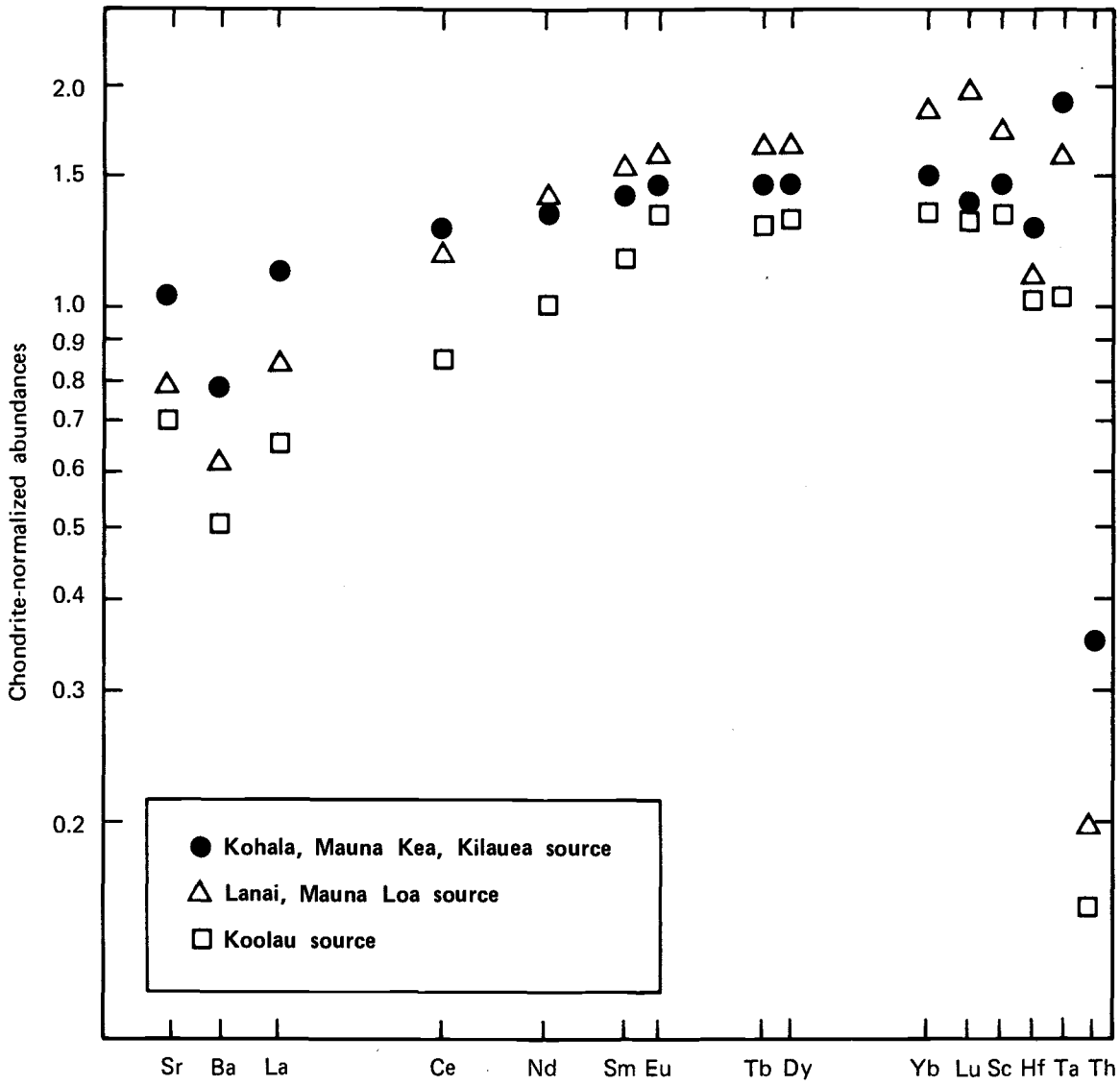

Fig. 11. Average chondrite-normalized trace element abundance patterns of the Kilauea group, Mauna Loa group, and Koolau sources. Sr, Ba, Hf, Ta, and Th abundances were estimated analogous to the REE and Sc using D values given in appendix B. Recall that these absolute abundances reflect a 45 percent olivine fractionation of the primary melt prior to eruption. Any change in the amount of fractionation would not alter the relative patterns of these sources.

than previously determined and are enriched relative to the Kilauea source by a factor of 1.2. This enrichment is large enough to be considered real. In addition, differences in heavy REE abundances between the sources are expected based on mineralogical considerations alone.

In order to produce similar heavy REE patterns between the magma groups that have resulted from nearly identical degrees of melting, the concentration of these elements must be higher in the source containing the greater amounts of cpx and gar. In other words, melting of such a source will generate liquids with lower c^{ℓ}/C_o ratios due to the strong partitioning of the heavy REE into the cpx + gar rich mantle. Thus, for identical c^{ℓ}'s between the magmas, c_o (the source abundance) must be larger in the cpx + gar rich source.

Perhaps the most significant feature of these models is the agreement between the $(Sm/Nd)_{ch}$ ratios obtained for the proposed Mauna Loa and Kilauea source materials with those calculated from mineral isotopic data. Leeman (private communication, 1977) has determined that the Sm/Nd ratio in the Kilauea mantle should be larger than that in the Mauna Loa mantle. Although magmatic elemental ratios would indicate the opposite, the source abundances obtained in this study do show this relationship: The average $(Sm/Nd)_{ch}$ ratio in the Mauna Loa group mantle is 1.07, whereas in the Kilauea group mantle, this ratio is 1.12 (Tables 11-12).

Another important aspect of these models is the close similarity between the absolute REE abundances obtained theoretically and those observed in alpine peridotites (Loubet et al., 1975; and Philpotts et al., 1972). Two types of alpine peridotite have been identified. The chondrite-normalized REE abundance patterns for each are depicted in Figure 12. Type 1 exhibits severely depleted light REE patterns, whereas type 2 has moderate to light REE depletions. The Mauna Loa and Koolau sources have REE abundance profiles that closely resemble the type 2 peridotites. In fact, these postulated sources have patterns that duplicate some of the observed peridotite patterns in both abundance and shape. The strong resemblance among these patterns tends to suggest that the fractionation and light REE depletion estimates used

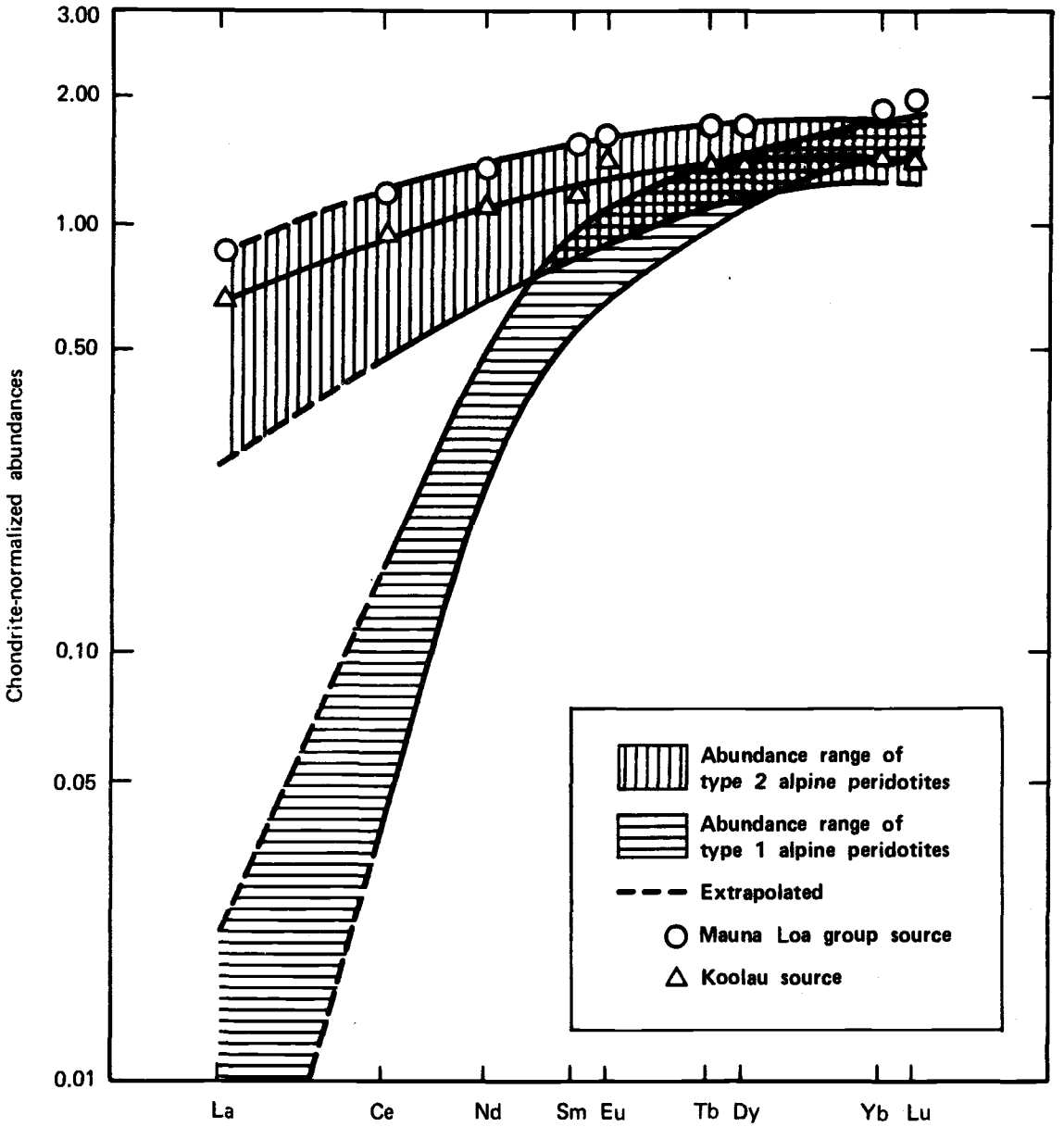

Fig. 12. Comparison of chondrite-normalized type 1 and type 2 alpine peridotite abundance patterns with those obtained from modeling the Mauna Loa group and Koolau source materials. Alpine peridotite data are from Loubet et al. (1975).

in modeling may be reasonable approximations if these peridotites represent mantle-like material. It will be noted that although the analyzed peridotites contain no garnet, they are thought to be residual material of partially melted garnet peridotites. Nevertheless, it could be argued that these abundance similarities provide considerable evidence that the proposed sources could represent the Hawaiian mantle regions.

Compositional differences among Koolau, Mauna Loa-type, and Kilauea-type basalts are thus accounted for by mineralogical and trace element heterogeneities among the mantle sources.

The factors responsible for producing the heterogeneities among the proposed sources can only be hypothesized. Olivine plus orthopyroxene crystal fractionation, for example, could explain the trace element differences between the Koolau and Mauna Loa mantles. To evolve the Mauna Loa source composition from the Koolau source would require about 30% ol-opx fractionation on the basis of REE abundances. However, the resultant lithology of the mantle would be 86% ol+opx, 9% cpx, and 6% garnet compared to 75% ol+opx, 20% cpx, and 5% gar from the model. Conversely, addition of material to the Koolau source having a flat chondrite-normalized REE pattern could also be postulated in producing the Mauna Loa mantle. A perfect fit would require the addition of 20% cpx plus gar in a 9:1 ratio with a REE abundance pattern of 4 times chondrite. This latter mechanism is not easily supported by what can be considered reasonable physical or chemical processes. The source of the cpx + gar fraction must be accounted for as well as the fact that this phase has over twice the REE abundance of any of the postulated source materials. It is interesting to note, however, that such a material is observed in the form of garnet pyroxenites on Koolau.

The unique REE pattern of the Kilauea mantle material suggests that these types of processes cannot be solely responsible for the evolution of this source. Hence, it will be proposed that the previous partial melting events between the Kilauea and Mauna Loa sources, as suggested by Loubet et al. (1975) to explain the LREE depletion anomalies of the type 1 and type 2 peridotites, may be important factors in their evolution. In addition, some type of mantle regeneration model must be

included in the process to produce the similar, heavy REE abundances observed between the sources. If it is assumed, as a first example, that the pristine mantle beneath these volcanoes had a flat chondrite-normalized REE abundance pattern of ~1.5x, the effect of varying the amounts of partial melting on such a source can be calculated. These calculations will also assume 1) that melting is eutectic-like, having an invariant point composition as indicated earlier and 2) that 50% undepleted mantle material (i.e., identical in composition to the initial material) has been mixed to the residual mantle prior to the next partial melting event. The amount and the composition of mantle material added to the residual are arbitrary choices, but selection of extreme compositions and fractions will not alter the conclusions reached. The primary difference is that the effects are either more or less noticeable. The addition of new material in this manner will represent mantle recycling due to mantle convection, equilibration with undepleted mantle material, etc. From these calculations, it can be shown that the first few degrees of melting will dictate the La/Lu ratio in the residual mantle and that thereafter any random partial melting will not affect this ratio or the REE abundances significantly. An initial sequence of events dominated by low degrees of melting (e.g., 2-4%) will result in larger La/Lu ratios in the residual mantle than an initial sequence dominated by higher degrees of melting (e.g., 6-8%). Thus, it is possible that the pristine mantle that was eventually melted to produce the Kohala-Mauna Kea and Kilauea basalts initially underwent a few rapid, small degrees of melting and that the Mauna Loa mantle was characterized by large degrees of melting. The differences in absolute abundances between the source materials could be the result of mantle recycling anomalies with the Kilauea mantle experiencing smaller amounts (that is, experiencing less "mixing" than the Mauna Loa source system).

Cr, Co, and Ni Modeling

With the data obtained from the REE partial melting model and the olivine fractionation model, the abundances of Cr, Co, and Ni can be defined in the primary melts and the mantle source regions. These

abundance estimates, if consistent with other mantle estimates, may provide an independent means of substantiating the proposed mechanisms of basalt generation of Hawaii. Primary melt abundances were calculated using the Rayleigh fractionation equation, the degree of fractionation as given in Tables 11-12, appropriate olivine to liquid partition coefficients, and magmatic elemental abundances. Mantle abundances will be determined by applying the appropriate bulk partition coefficient values to the partial melting equation presented earlier.

Chromium is one of the more difficult elements to characterize because 1) chromite has been determined to be a fractionating phase in Hawaiian basalt generation, 2) no D_{Cr} values exist for chromite partitioning, and 3) the amount of chromite fractionation is unknown. In a previous study concerning fractionation of Hawaiian basalts, Wright (1971) did not use the analytically determined composition of chromite in his estimate because he lacked Cr_2O_3 data on the end member basalts and all Cr_2O_3 was converted to Al_2O_3.

In an attempt to define this process more accurately, an arbitrary melt[11] (Appendix D) containing 1% Cr_2O_3 was used as the end member component in a computer mixing model. In the calculation, two olivines (Fo_{93} and Fo_{80}), the chromite composition quoted by Wright (1971) and the average Kilauea-historic basalt were fit to this melt (Appendix D). The results indicate that ~3% chromite and 45% olivine (Fo_{88}) have fractionated from the melt. This relative amount of olivine to chromite (15:1) will be used in determining the bulk solid distribution coefficient for Cr_2O_3.

The individual $D_{Cr_2O_3}$ value for chromite (65) was estimated by assuming that pure chromite (65% Cr_2O_3) was initially in equilibrium with the 1% Cr_2O_3 melt (this, too, is an arbitrary assumption; this value will be reevaluated shortly). The bulk D value for olivine

---

[11]The melt composition was derived from the preceding discussions concerning FeO-MgO melt abundances, CaO-Al_2O_3 requirements for 50% olivine fractionation and magma abundances, and mineral component data. This composition will thus be assumed to be most representative of the primary Hawaiian melts.

plus chromite is thus defined as 5.0 (where $D^{ol/l}_{Cr_2O_3}$ = 0.8; see Appendix B).

The abundances of Cr_2O_3 abundances in the Kilauea group primary melts were calculated using this value and estimated to be ~0.65%. Similarly, the Cr_2O_3 abundances in the Mauna Loa and Lanai primary melts were calculated with the assumption that a compositionally identical chromite has crystallized from the melt. The average Cr_2O_3 abundance in these melts is estimated to be 0.55%.

The assumed value for Cr_2O_3 partitioning into chromite can be compared to the value obtained by dividing the actual Cr_2O_3 abundance in chromite (43.5%) by the estimated melt abundance in the Kilauea primary liquid (0.65%). This value is 67 and agrees very well with the rough estimate value of 65.

The abundances of Cr_2O_3 in the Mauna Loa group mantle and the Kilauea group mantle were calculated from each individual melt abundance by using the partial melting equation presented earlier. Bulk partition coefficients for the sources were obtained by using the appropriate mineral to liquid partition coefficients under these conditions and the mantle lithologies as determined by the REE models. The degrees of partial melting also came from the REE models. The assumed modal mineralogy of the melt defined the bulk partition coefficient for the liquid. The individual mineral to liquid partition coefficients used are presented in Appendix B.

These calculations indicate that the mantle beneath the Kilauea group volcanoes would have to be richer in Cr_2O_3 (0.47%) than the mantle beneath Lanai and Mauna Loa (0.40%). This difference was suspected previously on the basis of the observed differences in abundances among the magmas. Unlike the REE, Cr_2O_3 partitioning between the mantle and the melt is almost totally independent upon the degree of partial melting because the bulk D values for the sources are fairly large (~0.7), whereas the bulk values for the liquid are relatively small (~0.3).

Nickel abundance estimates in the primary melts and in the source regions were calculated in a slightly different manner from that used

to determine Cr_2O_3. Caution must be taken before directly applying a D_{Ni} value for olivine to the Rayleigh equation since Ni partition coefficients have been shown to be highly variable as a function of temperature and composition; the compositional dependence being the most agreed upon characteristic. A few data have also indicated a possible pressure dependence of Ni partitioning into olivine. Furthermore, Ni partition coefficients greatly exceed unity throughout the fractionation process, varying from about 3.5 at the proposed onset of crystallization to about 15.7 at the end. These large values, coupled with the uncertainty involving the rate of fractionation and with the large differences observed among Ni contents in closely related basalts, can produce large variations in estimated melt abundances. In relation to Ni partitioning, a considerable amount of evidence has been presented (Hart and Davis, 1978; and Sato, 1977) arguing on the basis of 1 atm data (and large partition coefficients) that the Hawaiian basalts have been derived from a parental melt containing not more than 10-13% MgO and 400-500 ppm Ni. However, it was concluded previously that the primary melt must be rich in MgO; and it will be suggested that fractionation probably occurred at pressures greatly in excess of 1 atm and that hence lower D values must be considered.

For these reasons, a three-step model involving olivine (plus chromite) fractionation will be proposed. Each step or interval involved computing an evolved melt to primary melt ratio (C^{ℓ}/C_o) of Ni abundances under a certain set of conditions. The first interval of fractionation (~25%) will be assumed to occur from 1475-1375°C and will be suggested to represent the fractionation immediately after the partial melting event and during ascent to the intermediate storage reservoir.

The second interval (~12% olivine fractionation) occurring between 1375-1275°C will represent any low-pressure olivine fractional crystallization event. The final sequence (5-10% olivine fractionation) occurs from 1275°C to the crystallization temperature of the lava. Olivine D_{Ni} values were calculated at the initial temperature of each step (because fractionation occurs in that direction) and were assumed to remain constant throughout the event.

Although the actual fractionation process is undoubtedly a continuous equilibrium event, this type of approach has its reasons for justification: 1) It explains the limitations suggested by the observable Ni-Mg data, applying the final two sequences of olivine fractionation to the low MgO basalts produces parental magmas with 15% MgO and 400 and 770 ppm Ni for the Mauna Loa and Kilauea basalts, respectively. These types of magmas, as previously mentioned, have been suggested to represent parental magmas. 2) The calculated Ni abundances in the proposed primary melt are not so large as to be an unreasonable amount derived from a peridotite source. 3) In this fractional crystallization sequence, resultant MgO abundances are not significantly different from the abundances calculated using a constant $D_{MgO}^{Ol/l} = 2.8$ over the entire fractionation path. To verify this, $D_{MgO}^{Ol/l}$ values were calculated for each fractionation interval. At 1475°C, the olivine to liquid partition coefficient for MgO is 2.25; at 1375°C this value is 3.07; and at 1275°C, $D_{MgO}^{Ol/l} = 4.35$ (Leeman and Scheidegger, 1978). The results will be discussed shortly.

Nickel abundances in the mantles were calculated using the partial melting equation and parameters determined by the REE model. A $D_{Ni}^{Ol/l}$ of ~2 was used because this value is considered to be most appropriate to high-pressure melting on the basis of data obtained by Green et al. (1975).[12] The results further indicate the heterogeneity existing between the source regions in terms of Ni abundances; the Mauna Loa mantle containing 1870 ppm Ni and the Kilauea mantle containing 2540 ppm Ni (Tables 11-12).

The proposed evolution paths of Ni vs. MgO contents for the basalt groups are plotted in Figure 13. It is interesting to note that the komatite data of Cawthorn and McIver (1977) and the Svartenhuk and Baffin Island basalt data (Clarke, 1970) plot along, or are very near, one of the two proposed fractionation curves. Hence, it could be postulated that two sources in terms of Ni abundances can encompass the

---

[12] It is assumed that the equation presented by Hart and Davis (1978) can be extended to include mantle compositions, $D_{Ni} = 2.2$, for a mantle containing 40% MgO.

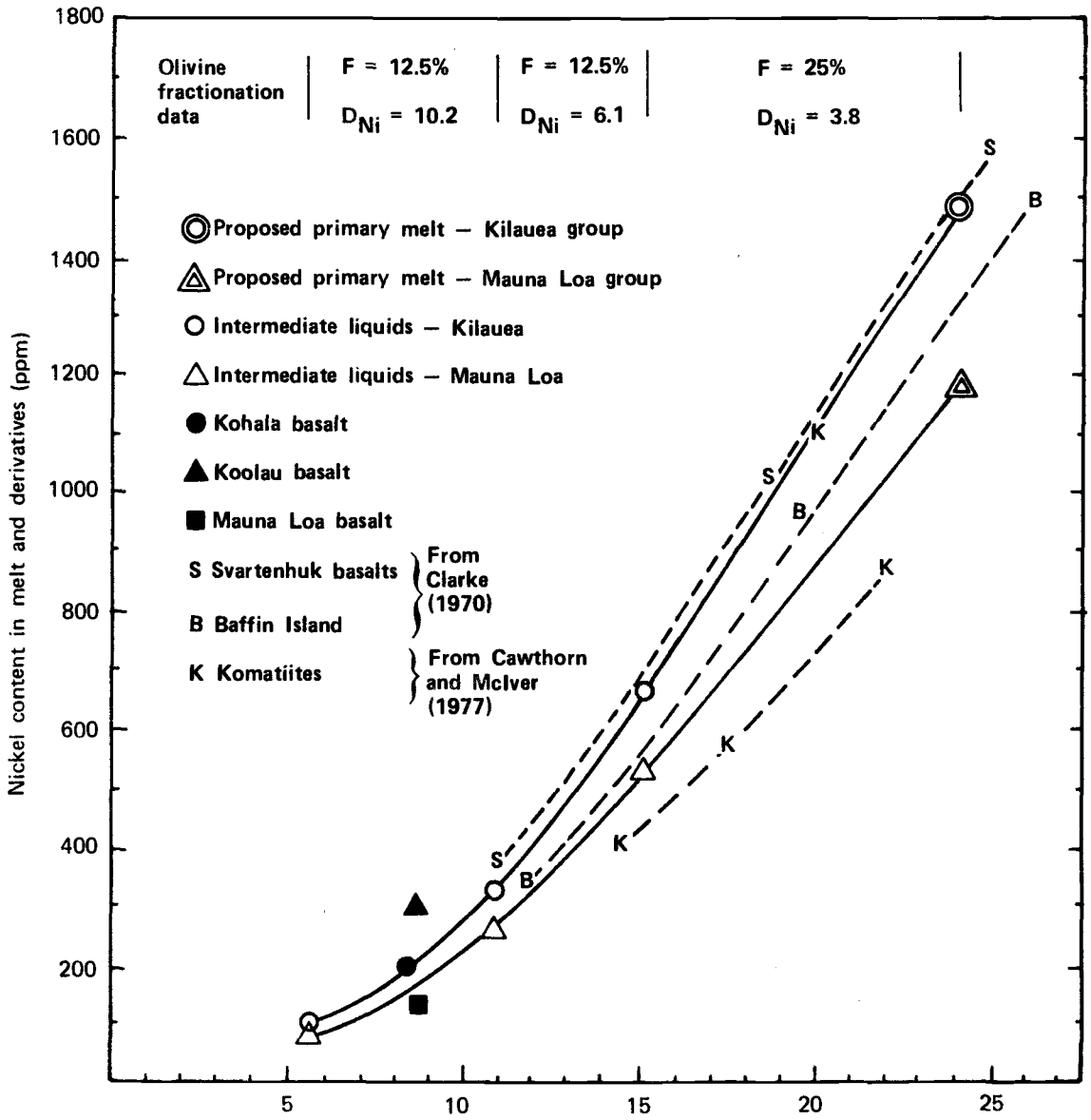

Fig. 13. Ni vs. MgO fractionation curves based on three-step fractionation models for Kilauea and Mauna Loa group basalts. For comparison, Svartenhuk, Baffin Island, and Komatiite data are plotted. Dashed lines joining these compositions are possible, but not necessarily real, fractionation relationships. See text.

generation of these basalts, which may be generated by similar processes as occurred in Hawaii. The slight deveiations observed in the high MgO (primary melt) basalts in Ni abundances can be explained by assuming that different melting conditions were at work in the generation. Partial melting at a reduced pressure or melting of an olivine-rich source material would result in lower Ni melt abundances, and the latter melting would produce melts richer in MgO.

Nevertheless, the basalt compositions plotted in the figure (other than those postulated for Hawaiian basalt generation) will not be suggested to represent primary melt compositions or even to have been derived from the primary melt by olivine fractionation; but based on these data, it would be difficult to discount this possibility. On the other hand, it can be shown that cumulate basalts could have identical compositions as those expected to be observed in primary liquids. From available olivine analyses (Leeman and Scheidegger, 1977), the entire range of compositions can be obtained by the simple addition of an olivine containing about 3300 ppm Ni and 45% MgO. Thus, it will be suggested that arguments based on Ni and MgO data alone are not strong enough evidence to determine what can or cannot be primary melts. In many cases, these models have failed to consider the effects of high pressure on Ni partitioning. As stated earlier, some authors have shown that $D_{Ni}^{Ol/l}$ is significantly lower at higher pressures. The model proposed in this study for Ni-MgO evaluation has considered these data in deriving the model. Furthermore, the hypothetical melts presented have been based on FeO-MgO considerations and thus far have been, in general, supported by analogy on REE evidence.

The low $D_{Co}^{Ol/l}$ values make possible the calculation of Co abundances in the melt and mantle regions by the use of a single-step fractionation model. In keeping with the approach taken for Ni, the same three-step model will be assumed. Olivine to liquid partition coefficients for Co were calculated at each initial temperature as given in the Ni discussion. These values were used in determining primary melt abundances. Mantle abundances were calculated in the same manner as described above. Mantle abundances for Co again reflect the heterogeneity between the two

sources; the Kilauea group mantle containing 74 ppm Co and the Mauna Loa group mantle containing about 64 ppm. These abundances are very similar to those postulated to be found in the basaltic magma source regions (Table 13).

In concluding this section, the following points will be considered: 1) As was suggested from magmatic data, the mantle source regions are heterogeneous in terms of Cr, Co, and Ni abundances. 2) Allowing for a slight decrease in $D_{Ni}^{Ol/l}$ values with increasing pressure, the proposed fractionation model will give primary melt abundances that can be obtained by melting of a typical garnet peridotite. For comparison, the Kilauea mantle is given in estimated major element composition in Table 13, along with analysis or estimations of garnet peridotite material belived to represent mantle material. (The abundances of Al_2O_3, FeO, MgO, and CaO in the Kilauea mantle estimate were calculated by using component compositions given in the table and the mantle mineralogies given by the REE model). As can be seen, the mantle estimates for Cr, Ni, and Co are in very good agreement with other estimated abundances of mantle materials. The transition element abundances are slightly lower in the Mauna Loa mantle, but they are still within the range of suggested earth mantle contents.

TiO_2 Modeling - Titanium may be regarded as a trace element in these basalts to explain its variable abundance observed among the Kilauea group basalts and between the Kilauea and Mauna Loa basalt groups.

The procedure used in Cr, Ni, and Co modeling was used to determine primary melt and mantle TiO_2 abundances. However, in this approach, only the TiO_2 abundances in the Kilauea (historic) basalt will be used for an estimate of TiO_2 in the mantle and other magma abundances predicted. Bulk D values for the mantle and the melt were calculated as described previously, and the F value was applied to the partial melting equation to obtain a mantle abundance.

Olivine and cpx mineral to liquid partition coefficients adopted for TiO_2 were determined by Lindstrom (1976). A garnet to liquid partition coefficient was estimated from relative abundances in coexisting

TABLE 13. KILAUEA GROUP MANTLE BULK COMPOSITION ESTIMATED FROM REE MODEL LITHOLOGIES AND MINERAL COMPONENT DATA.

Element	Kilauea Mantle Estimate	Sun and Nesbitt (1977) (Archean)	Range of 41 Garnet Lherzolites (b)	Carswell and Dawson (1970) (c)	Carswell (1968) Mean of 20 Garnet Peridotites
TiO_2 (%). . .	0.12[a]	0.18-0.24	<0.1-0.15	0.33-0.16	0.19
Al_2O_3 (%) . .	1.7	3.6-4.9	0.5-2.2	1.8-2.7	2.8
FeO (%)[d]. . .	6.9	8.6-9.7	7.1-9.2	6.7-7.0	7.9
MgO (%) . . .	43.8	38	38.0-45.8	42.0-41.9	41.0
CaO (%) . . .	2.1	0.3-0.4	0.35-2.8	1.5-1.9	2.6
Na_2O (%). . .	0.15	0.3-0.4	0.06-0.60	0.16-0.19	0.30
Cr_2O_3 (%) . .	0.47[a]	0.44	0.21-0.62	0.38-0.31	0.45
NiO (%) . . .	0.33[a]	0.25	0.30-0.45	0.32-0.30	0.31
Co (ppm). . .	74[a]	100	71-113	. . .	. . .

NOTES: Other estimates of the bulk composition of the upper mantle are given for comparison. Kilauea estimate calculations assumed 0.63 Fo_{92} 0.21 opx (Ca_7 Mg_{92} Fe_1) from Kushiro et al., 1972. 0.12 cpx and 0.04 gar — Clinopyroxene and garnet compositions used are from Table 9.

[a]Calculated from partial melting-fractionation models.

[b]Chen (1971).

[c]Garnet peridotites in South African kimberlite pipes.

[d]Total Fe as FeO.

garnets and clinopyroxenes [Kushiro et al. (1972); Morgan (1974); Reid et al. (1976), and Wilkinson (1976)]. These values are presented in Appendix C.

The results of this calculation indicate that the Kilauea mantle contains 0.12% TiO_2, which is in fairly good agreement with other mantle estimates (Table 13). More significantly, the predicted magma abundances (determined by applying the data to the partial melting equation for each basalt) agree very well with the observed concentrations; 2.8% was calculated for Mauna Kea (2.8% observed), 2.4% for Kohala (2.3% observed), and 2.3% for Kilauea prehistoric basalts (2.4% observed).

This same approach was applied in obtaining TiO_2 estimates in the southern rift basalts using the TiO_2 abundance of the Mauna Loa historic basalt as an indicator. The source of these basalts also contains 0.12% TiO_2. The predicted abundances for the remaining basalts are 2.3% for Mauna Loa prehistoric (2.14% observed), 1.8% for the high MgO Lanai basalt (1.76% observed), and 2.6% for the low MgO Lanai basalts (2.29% observed).

VIII. MINERALOGIES OF HAWAIIAN BASALTS — EVIDENCE FOR MELT HETEROGENEITIES

Up until now, the geochemical differences between the northern and the southern rift basalts have been suggested to be solely the result of melting heterogeneous source materials. However, mantle heterogeneity would not be a valid interpretation for explaining the differences observed in Al_2O_3 and CaO abundances if, as has been suggested, a single bulk composition is repeatedly produced in every partial melting event in Hawaii. An alternative model would be that partial melting has occurred under different conditions, therefore altering the bulk chemical composition of the melt. Evidence for melt heterogeneity, and perhaps the processes responsible for it, will come from examining basalt mineralogies.

To correlate the differences in basalt compositions, the mineralogies of selected basalts were determined by using a least-squares unconstrained mixing program described by Boynton et al. (1975). The mineral components used as end members consisted of two augites (FeO-rich and FeO-poor variety), two pigeonites[13] (FeO-rich and FeO-poor), two plagioclases (arbitrarily set at $An_{70}Ab_{30}$ and $Ab_{82}Or_{18}$), ilmenite, and magnetite. The four cpx compositions (Table 14) were chosen to allow for addition of minor olivine and to compensate for the selection of only two plagioclases. These plagioclase components, nevertheless, are those found in ~90% of the low MgO basalt ground masses. Apatite is also found in the ground mass of these basalts; but because P_2O_5 data were lacking, this component has been omitted. The computer-fitted mineralogies for some of the basalts are given in Table 14. The observed compositions are the average basalt compositions previously selected for the REE model (see Table 7), with the exception of Kohala. As can be seen, excellent agreements were obtained between the observed and the calculated compositions, the chi squares being less than 0.35

[13] In later discussions, the pigeonite components will be referred to as opx and augites as cpx (see Table 14).

TABLE 14. COMPUTER-FITTED MINERALOGIES OF SOME HAWAIIAN BASALTS.

Compositions of Minerals (From Wright, 1971)

Element	Pigeonite		Augite		Plagioclase		Ilmenite	Magnetite
	opx1	opx2	cpx1	cpx2	An_{70}	Ab_{72}		
TiO_2	0.60	0.60	0.35	1.00	0.06	0.01	48.20	23.06
Al_2O_3	0.80	0.80	2.76	2.00	30.90	19.70	0.10	1.90
FeO	15.66	24.40	3.45	13.70	0.50	0.10	48.50	73.05
MgO	19.94	17.20	16.70	14.70	0.00	0.00	1.70	1.03
CaO	4.73	4.50	20.80	16.60	13.80	0.10	0.10	0.10
Na_2O	0.00	0.00	2.01	0.20	3.29	18.94	0.00	0.00
K_2O	0.00	0.00	0.05	0.00	0.20	6.31	0.00	0.00
MnO	0.00	0.00	0.10	0.00	0.00	0.00	0.43	0.38
Cr_2O_3	0.12	0.03	2.21	0.10	0.00	0.00	0.00	0.00

Element	Observed	Calculated	Difference	Significance (%) (a)	Fit (b)	Mineralogy
Kohala (average of P71-3, P71-13, and P71-4)						
TiO_2	2.35	2.32	-0.03	10.0	0.01	opx1 = 4.4 ± 3.3
Al_2O_3	13.80	13.88	0.08	2.0	0.09	opx2 = 23.8 ± 17.6
FeO	11.30	11.30	0.00	2.0	0.00	cpx1 = 1.4 ± 0.6
MgO	8.10	8.05	-0.05	10.0	0.05	cpx2 = 18.9 ± 14.3
CaO	10.60	10.61	0.01	5.0	0.00	An = 42.6 ± 3.0
Na_2O	2.08	1.54	-0.54	10.0	6.67	Ab = 0.4 ± 1.5
K_2O	0.07	0.11	0.04	50.0	1.40	Il = 4.0 ± 8.2
MnO	0.17	0.01	-0.16	0.0	0.00	Mag = 0.0 ± 0.3
Cr_2O_3	0.06	0.06	0.00	5.0	0.00	Sum = 95.5; χ^2 = 8.17
Mauna Kea						
TiO_2	2.78	2.79	0.01	10.0	0.00	opx1 = 0.5 ± 0.1
Al_2O_3	13.60	13.60	0.00	2.0	0.00	opx2 = 8.7 ± 4.0
FeO	12.00	12.00	0.00	2.0	0.00	cpx1 = 0.3 ± 0.1
MgO	6.90	6.90	0.00	10.0	0.00	cpx2 = 35.0 ± 3.1
CaO	11.40	11.41	0.00	5.0	0.00	An = 37.1 ± 0.8
Na_2O	2.51	2.51	0.00	10.0	0.00	Ab = 6.4 ± 0.8
K_2O	0.52	0.48	0.04	50.0	0.07	Il = 2.6 ± 0.4
MnO	0.17	0.03	0.14	0.0	0.00	Mag = 4.9 ± 0.7
Cr_2O_3	0.05	0.05	0.00	5.0	0.00	Sum = 95.5; χ^2 = 0.07

[a]Percentage of significance assigned to each element (weighing factor).

[b]Fit = χ^2 fit of element.

TABLE 14. COMPUTER-FITTED MINERALOGIES OF SOME HAWAIIAN BASALTS.

Element	Observed	Calculated	Difference	Significance (%) (a)	Fit (b)	Mineralogy
Kilauea – Historic						
TiO_2	2.70	2.73	0.03	10.0	0.01	opx1 = 4.5 ± 1.1
Al_2O_3	13.70	13.70	0.00	2.0	0.00	opx2 = 11.0 ± 2.7
FeO	11.00	11.00	0.00	2.0	0.00	cpx1 = 0.8 ± 0.1
MgO	7.60	7.60	-0.00	10.0	0.00	cpx2 = 31.2 ± 2.9
CaO	11.40	11.40	0.00	5.0	0.00	An = 38.5 ± 0.7
Na_2O	2.28	2.31	0.02	10.0	0.03	Ab = 5.1 ± 0.7
K_2O	0.54	0.40	-0.14	50.0	0.27	Il = 3.9 ± 1.1
MnO	0.17	0.02	-0.15	0.0	0.00	Mag = 1.7 ± 0.4
Cr_2O_3	0.05	0.05	0.00	5.0	0.00	Sum = 96.7; χ^2 = 0.30
Koolau – High MgO Basalt [Koolau (2)]						
TiO_2	1.84	1.84	-0.00	10.0	0.00	opx1 = 41.0 ± 1.6
Al_2O_3	14.90	14.90	0.00	2.0	0.00	opx2 = 4.3 ± 0.2
FeO	9.80	9.80	0.00	2.0	0.00	cpx1 = 1.2 ± 1.0
MgO	9.20	9.20	0.00	10.0	0.00	cpx2 = 0.2 ± 0.1
CaO	8.40	8.40	0.00	5.0	0.00	An = 43.3 ± 0.3
Na_2O	2.56	2.51	-0.05	10.0	0.03	Ab = 5.6 ± 0.3
K_2O	0.40	0.44	0.04	50.0	0.02	Il = 2.7 ± 0.7
MnO	0.17	0.02	-0.15	0.0	0.00	Mag = 1.0 ± 0.6
Cr_2O_3	0.08	0.08	0.00	5.0	0.00	Sum = 99.3; χ^2 = 0.05
Koolau Low MgO Basalt [Koolau (1)]						
TiO_2	2.27	2.27	0.02	10.0	0.00	opx1 = 0.6 ± 0.0
Al_2O_3	14.60	14.60	0.00	2.0	0.00	opx2 = 26.1 ± 0.7
FeO	10.20	10.20	0.00	2.0	0.00	cpx1 = 0.9 ± 0.0
MgO	6.30	6.30	-0.00	10.0	0.00	cpx2 = 9.7 ± 0.5
CaO	8.80	8.80	0.00	5.0	0.00	An = 41.9 ± 0.2
Na_2O	2.60	2.59	0.01	10.0	0.00	Ab = 6.2 ± 0.2
K_2O	0.45	0.47	0.02	50.0	0.01	Il = 4.0 ± 0.3
MnO	0.16	0.02	-0.14	0.0	0.00	Mag = 0.3 ± 0.1
Cr_2O_3	0.04	0.04	0.00	5.0	0.00	Sum = 89.7; χ^2 = 0.01
Lanai High MgO Basalt [Lanai (2)]						
TiO_2	1.76	1.76	0.00	10.0	0.00	opx1 = 20.5 ± 1.4
Al_2O_3	14.60	14.60	0.00	2.0	0.00	opx2 = 19.2 ± 1.3
FeO	10.30	10.29	-0.01	2.0	0.00	cpx1 = 2.2 ± 0.1
MgO	8.50	8.50	-0.00	10.0	0.00	cpx2 = 4.6 ± 1.8
CaO	9.00	9.00	0.00	5.0	0.00	An = 42.8 ± 0.5
Na_2O	2.36	2.33	-0.03	10.0	0.03	Ab = 4.6 ± 0.5
K_2O	0.32	0.37	0.05	50.0	0.12	Il = 3.0 ± 1.2
MnO	0.18	0.02	0.16	0.0	0.00	Mag = 0.0 ± 0.0
Cr_2O_3	0.05	0.06	0.00	5.0	0.00	Sum = 96.9; χ^2 = 0.15

TABLE 14. COMPUTER-FITTED MINERALOGIES OF SOME HAWAIIAN BASALTS.

Element	Observed	Calculated	Difference	Significance (%) (a)	Fit (b)	Mineralogy
Lanai Low-MgO Basalt [Lanai (1)]						
TiO_2	2.29	2.29	0.00	10.0	0.00	opx1 = 1.0
Al_2O_3	14.60	14.60	0.00	2.0	0.00	opx2 = 22.5 } 54.7[c]
FeO	10.80	10.80	0.00	2.0	0.00	cpx1 = 0.6
MgO	6.60	6.60	0.00	10.0	0.00	cpx2 = 16.1
CaO	9.70	9.70	0.00	5.0	0.00	An = 42.3 } 32.1[c]
Na_2O	2.38	2.38	0.00	10.0	0.00	Ab = 5.0
K_2O	0.42	0.40	-0.02	50.0	0.01	Il = 3.4 } 10.9[c]
MnO	0.18	0.02	-0.16	0.0	0.00	Mag = 1.5
Cr_2O_3	0.04	0.04	0.00	5.0	0.00	Sum = 92.4; χ^2 = 0.01
Mauna Loa — Historic						
TiO_2	2.14	2.15	0.01	10.0	0.00	opx1 = 1.2 ± 0.1
Al_2O_3	14.00	14.00	0.00	2.0	0.00	opx2 = 20.9 ± 1.3
FeO	11.00	11.00	0.00	2.0	0.00	cpx1 = 0.3 ± 0.0
MgO	7.20	7.20	0.00	10.0	0.00	cpx2 = 22.4 ± 0.9
CaO	10.30	10.30	0.00	5.0	0.00	An = 40.0 ± 0.3
Na_2O	2.35	2.33	-0.02	10.0	0.01	Ab = 5.1 ± 0.5
K_2O	0.37	0.40	0.03	50.0	0.03	Il = 3.0 ± 0.5
MnO	0.16	0.02	-0.14	0.0	0.00	Mag = 1.3 ± 0.2
Cr_2O_3	0.04	0.04	0.00	0.0	0.00	Sum = 94.2; χ^2 = 0.03

[c]Bonhommet et al. (1977); the remaining 3.3% is olivine.

Volcano	opx + cpx/plag	opx/cpx	plag[d]
Kohala	1.13	1.40	45.0
Mauna Kea	1.02	0.26	45.6
Kilauea-Historic	1.09	0.48	45.1
Koolau (2)	0.96	37.75	49.2
Koolau (1)	0.78	2.52	53.6
Lanai (2)	0.98	5.84	48.9
Lanai (1)	0.85	1.41	51.2
Mauna Loa-Historic	0.99	0.99	47.9

[d]Normalized to 100%.

for all but one of the mixes. The percentage significance assigned to each element is based on the analytical uncertainty associated with each element.[14]

The importance of olivine in some of these basalts can be seen by comparing the ratios of pigeonite (opx) to augite (cpx) in the Koolau and Lanai basalts; these ratios are very high in the Koolau high MgO basalts (~38) and in the Lanai high MgO basalts (~6) but substantially lower (2.3 and 1.4) in the more evolved low MgO Koolau and Lanai basalts, respectively (Table 14). Since only minor differences in the amount of olivine fractionation have been postulated in producing the two compositions in these suites, caution must be taken before using these ratios in interpreting primary melt composition differences. Nevertheless, these ratios may be significant when comparing the Mauna Loa and Kilauea basalts; the ratio is lower in the Kilauea basalts even though less olivine fractionation has evolved this latter basalt composition. Pyroxene fractionation is not considered to be a viable interpretation for this effect because REE abundance patterns do not support this process between them.

Perhaps the most compelling data leading to the understanding of basalt composition variations come from the combined pyroxene/plagioclase ratios in these basalts. As can be seen by the data in Table 14, the northern rift basalts generally have higher opx + cpx/plag ratios than those in the southern rift basalts. These differences cannot be interpreted as being the result of different degrees of olivine fractionation because 1) the opx + cpx/plag ratios in the high MgO basalts of Koolau and Lanai are still less than those observed in the northern rift basalts and 2) more importantly, there is no significant difference in the amount of opx + cpx among any of the basalts. Hence, the variation in these ratios is dependent upon the plagioclase contents of the magmas (Table 14). On the basis of these observations, the following

---

[14] Na_2O, K_2O, and MnO were not weighted as heavily as their uncertainties would dictate because only two plagioclases were selected and because mineral component data for MnO are inconsistent with the basalt data.

conclusions can be made on the mineralogies of the northern rift basalts. 1) They are characterized by low opx/cpx ratios (i.e., they are low in pigeonite). 2) These basalts are lower in plagioclase than the southern rift basalts.

O'Hara and Yoder (1967) have suggested that pigeonite and anorthite normative magmas are the evolved low-pressure products of garnet-rich melts. Since a shift to garnet-rich melts occurs with reduced pressure, it can, therefore, be reasonably suggested that the Mauna Loa group basalts are the products of a lower pressure partial melting event than that involved in generating the northern group basalts. This, in turn, would imply that the Kilauea group source lies deeper in the mantle than the Mauna Loa group source.

There is some indication that a eutectic[15] composition variation also occurs among the basalts generated within the same rift; evidence relies on the opx/cpx ratios of these basalts. It would appear further that these variations are correlated to the degree of melting. Data obtained from the northern rift basalts will be examined first.

As determined from the REE partial melting model, the Kilauea historic and the Mauna Kea basalts were generated by relatively low degrees of melting: 3.5% and 2.9%, respectively. On the other hand, the Kohala and Kilauea prehistoric basalts have been postulated to be the products of larger degrees of partial melting; namely, 4.7% and 5.7%, respectively. Since the highest opx/cpx ratios are observed in the Kohala basalt (Table 14) and presumably in the Kilauea prehistoric basalt based on Al_2O_3/CaO ratios (see Table 15), it could be suggested that the eutectic composition is shifted to a more garnet-rich melt as the amount of melting increases. It would be suspected that REE data could be used to support this mechanism although this is not entirely clear.

An increase in the amount of garnet and a decrease of cpx in the melting mode would result in a relative increase in heavy REE abundances in the melt, simultaneously decreasing the light REE abundances.

---

[15]Eutectic refers to the melting relationship of clinopyroxene (opx + cpx) and garnet.

TABLE 15. BULK COMPOSITION OF THE NORTHERN RIFT BASALTS VS. PERCENT PARTIAL MELTING.

Element	Mauna Kea (a)	Kilauea (Historic Basalts) (b)	Kohala	Kilauea (Prehistoric) (b)
TiO_2.	2.78	2.70	2.28	2.41
Al_2O_3	13.6	13.7	13.8	14.0
FeO	12.0	11.0	11.1	10.9
MgO	6.9	7.6	8.0	7.3
CaO	11.4	11.4	10.8	10.7
Na_2O.	2.51	2.28	2.10	2.34
K_2O	0.57	0.54	0.15	0.43
Al_2O/CaO. . . .	1.19	1.20	1.28	1.31
Partial melting (%)	2.9	3.5	4.7	5.7
Olivine fractionation . . .	48.8	46.8	44.8	48.0

NOTES: Compositions presented are those obtained by averaging selected basalts (see Table 7).

[a]Average of 3 basalts.

[b]From Murali et al. (1977).

This observation is based on the relative REE partitioning coefficient of cpx and garnet (see Appendix B). Slight changes in the melting mode such as those postulated would undoubtedly be difficult to detect in magmatic trace element abundances. However, these variations may be more easily seen by examining the required source abundances for each basalt. These are given in Table 11. In this case, a more garnet-rich melt would give required heavy REE abundances that would be larger than those actually needed. The first indication from these data would be that the low Yb and Lu chondrite abundances calculated for the Kilauea prehistoric basalts suggest the opposite; that is, the melt should contain less garnet. Still, this apparent contradiction in partitioning behavior could be interpreted as being the result of large degrees of melting on a system containing garnet. The line of reasoning stems from the simplicity of the equation used for partial melting; namely, equilibrium partial melting. Partial melting of a garnet-bearing source may have an additional buffering process, which complicates this equation, specifically limiting the trace element abundances in derived liquids resulting from large degrees of melting. In other words, the abundances of the heavy REE reach a maximum after which no significant increase in abundances will occur regardless of the extent of melting. Mathematically, both equations do reach such a maximum, but at much higher degrees of melting than those suggested here. It will be postulated, therefore, that at some point in the melting event, the melt will become progressively richer in garnet and simultaneously reach a saturation effect in trace element abundances, probably in the cases where P for these elements is greater than unity.

This same mechanism may be observed in the southern rift basalts. Although the basalts generated by high degrees of melting do not exhibit variations in major element chemistries as significant as those in the northern rift basalts, the heavy REE abundance patterns of their respective sources may be indicative of this process (see Table 12). For example, the Mauna Loa historic basalt REE pattern requires that lower heavy REE abundances be present in its source compared to those required for generating the remaining basalts. The Mauna Loa historic basalt was postulated to be the result of 5.2% partial melting. The

Lanai high MgO basalt pattern, however, may or may not support this hypothesis. For example, the Yb abundance shows this effect, yet Lu does not. This basalt has been suggested to be the result of 5.3% partial melting.

Nevertheless, it will be concluded that some combinations of melt and mantle heterogeneities have been important factors in producing the compositional differences observed among the Hawaiian basalts. REE and trace element abundance data of the basalts almost certainly suggest that a considerable amount of mantle heterogeneity did exist among the basalt sources in terms of chemistry and mineralogy. Major element abundances (notably Al_2O_3 and CaO), on the other hand, could only be appreciably affected by a eutectic variation possibly resulting from a pressure-related phenomenon,[16] with differences in melting depths accounting for interrift variations and intrarift variations.

Finally, the combined computer-derived pyroxene compositions (opx and cpx) can be plotted on a Ca-Mg-Fe quadrilateral to deduce the relative amount of heterogeneity existing among the primary melt bulk compositions. These primary melt compositions, in terms of Ca-Mg-Fe, were calculated assuming the following: 1) The primary melts initially had an (opx + cpx)/plag ratio of 1.4. (This value allows for minor opx fractionation.) 2) The plag-component can be represented by the composition An_{70}. 3) The average olivine that has fractionated from these melts is Fo_{85}. (This olivine composition is sufficient for a first-order approximation.) These components were added in appropriate amounts to give a melt composition.

The combined pyroxene compositions (augite + pigeonite) of each magma suite used in these estimations are plotted in Figure 14 as filled squares. The open diamonds in the figure are thus the postulated melt compositions that could be parental to these suites; the

---

[16]Some well-defined models are concerned with the physical process of melting in which pressure relief mechanisms as well as compositional changes of the melting mode induce partial melting (e.g., Yoder, 1976). It would not be unreasonable to suggest that one or both of these processes could contribute to the partial melting events in Hawaii.

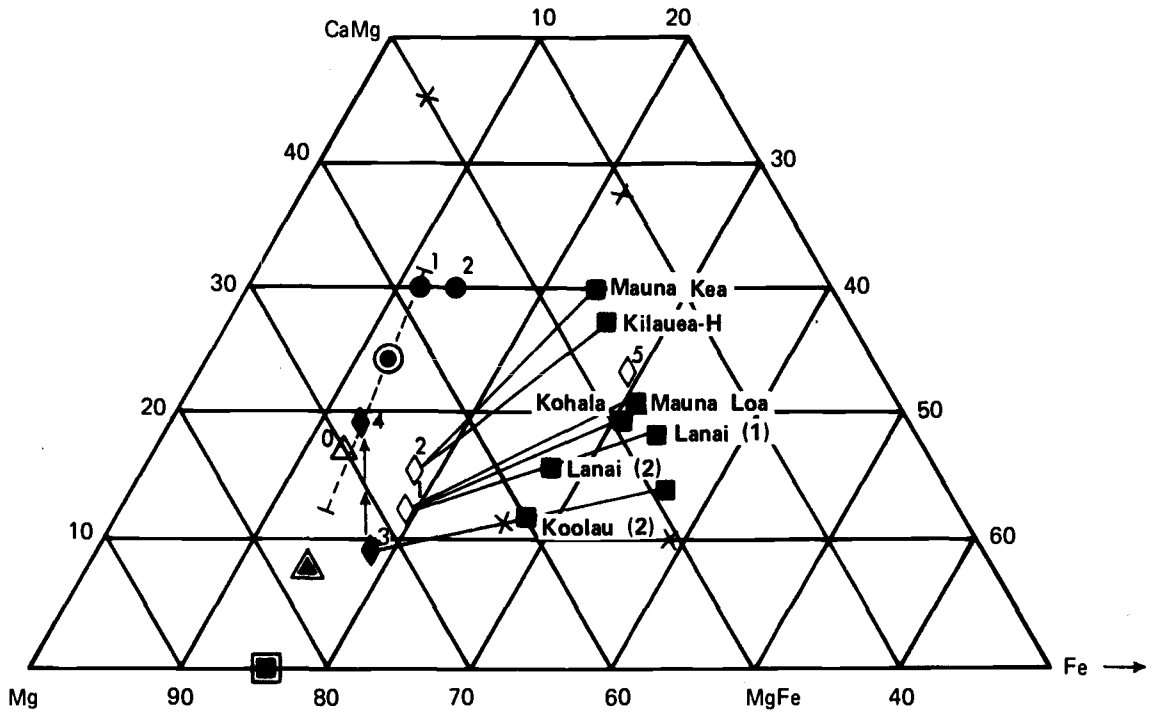

■ Basalt pyroxenes
× End member pyroxenes
◇1 Estimated primary melt composition of Mauna Loa-Kohala-Lanai
◇2 Estimated primary melt composition of Mauna Kea-Kilauea (H)
◆3 Estimated primary melt composition of Koolau
◆4 Estimated composition of 10% partial melt from Koolau
◇5 Generalized pyroxene composition in Hawaiian basalts
◉ Calculated garnet pyroxenite composition (see text)
●1 Garnet pyroxenite [(68SAL-6) Beeson and Jackson (1970)]
●2 Average garnet pyroxenite from Salt Lake Crater (Jackson, 1966)
0△ Liquid composition of garnet peridotite melt (Kushiro et al., 1969)
▣ Fo_{84}
▲ 0.66 Fo_{85} + 0.34 An_{70}
⊢----⊣ Range of garnet

Fig. 14. Ca-Mg-Fe diagram illustrating relationships of basalt mineralogies to melt compositions.

open diamond with superscript 1 identifies the melt composition parental to the Mauna Loa, Lanai, and Kohala basalts; and the open diamond, superscript 2, identifies the melt parental to the Mauna Kea and Kilauea basalt suites. (The open diamond, superscript 5, is the average pyroxene composition of the low MgO basalts (~7% MgO) having a pigeonite/augite ratio of about one). Note that both of the primary melt compositions arrived at in this manner have mg values of 0.78, very similar to those calculated in earlier estimates but that they differ in Ca contents.

For comparison, the composition of a liquid derived from melting a garnet lherzolite at 1500°C (Kushiro et al., 1972) is given by the open triangle, superscript 0. This composition, however, more closely resembles the melt proposed to be the result of large degrees of melting (filled diamond, superscript 4) relating to the generation of the garnet pyroxenites on Hawaii. These types of melts will be discussed in the section on pyroxenite formation.

IX. GARNET TRANSFORMATION – OLIVINE REACTION

The evolution of a melt containing garnet to a magma containing plagioclase implicitly suggests that some type of chemical reaction must have occurred in the melt in addition to the physical process of olivine fractionation. This reaction may involve olivine as well as garnet-plagioclase since it has been suggested that an extensive amount of olivine (40-50%) has been removed from a melt that contained only ~10% olivine. Such an interpretation is supported from the observation made by Kushiro (1968) that with decreasing pressure, the liquidus field of olivine will expand into the garnet and pyroxene fields in a garnet-pyroxene-olivine system.

An olivine reaction relation of this type, possibly occurring as part of the generation process in Hawaiian magmas, can be examined quantitatively on the basis of the results of this study. The investigation of this reaction will involve equating two apparent mineralogies of the primary melt, one containing the minerals represented in the melting mode (namely, olivine, the pyroxenes, and garnet) and the other containing the mineral components found in the final magmas, plagioclase, and the pyroxenes. The latter mineralogy will also include olivine and chromite, which represent the components that fractionate from the primary melt. The significance of this reaction in basaltic evolution processes, if any, will be determined by noting the compositional differences between the melt "mineralogies."

The apparent mineralogies of the melt were calculated by using the computer-mixing program described earlier. Mineral compositions reflecting the two conditions of interest (i.e., a high and low pressure-temperature liquid) were fit to a hypothetical primary melt composition. The melt composition used in these calculations is given in Table 16. This melt is considered to be the most general composition for the following reasons: 1) It is postulated to be parental to the "average" Hawaiian basalt given in Table 6A in terms of TiO_2, Al_2O_3, CaO, Na_2O, and K_2O. The average basalt composition will negate most of the effects that eutectic variations were suggested to have had

TABLE 16. COMPUTER-CALCULATED MINERALOGY OF HYPOTHETICAL MELT COMPOSITION.

Element	Compositions of Mineral Components (Part 1) (%)						
	Fo_{95}	Fo_{90}	opx1	opx2	cpx	gar	Il[a]
TiO_2	0.03	0.03	1.00	1.00	1.00	0.50	43.70
Al_2O_3	0.10	0.10	0.00	0.00	0.00	19.70	0.00
FeO	4.90	9.10	10.00	25.00	3.20	6.50	36.30
MgO	52.10	47.90	29.40	14.30	18.90	21.50	1.00
CaO	0.10	0.10	2.40	5.00	21.60	5.25	0.15
Na_2O	0.00	0.00	0.20	0.50	0.50	2.00	0.00
K_2O	0.00	0.00	0.00	0.10	0.10	0.31	0.00
MnO	0.17	0.17	0.14	0.14	0.14	0.20	0.44
Cr_2O_3	0.64	0.64	0.20	0.20	0.20	1.10	0.10

[a]Same ilmenite composition used in part 2 (Table 17).

Element	Observed	Calculated	Fit	Mineralogy
TiO_2	1.28	1.23	0.05	Fo_{95} = 7.1 ± 0.1
Al_2O_3	7.40	7.43	0.05	Fo_{90} = 10.4 ± 0.2
FeO	10.80	10.81	0.00	opx1 = 7.3 ± 8.5
MgO	23.50	23.69	0.01	opx2 = 22.1 ± 3.5
CaO	5.10	5.11	0.01	cpx = 8.5 ± 1.1
Na_2O	1.08	0.92	2.12	gar = 37.6 ± 0.7
K_2O	0.18	0.15	0.00	Il = 1.5 ± 0.1
MnO	0.17	0.17	0.00	Sum = 94.5
Cr_2O_3	0.60	0.60	0.00	χ^2 = 1.00

on the abundances of Al_2O_3 and CaO in the liquid. 2) MgO and FeO abundances are based on previous arguments concerning their contents in the primary melt. Recall that the addition of an olivine was not considered to be a reasonable method of deriving MgO and FeO abundances in the parental liquid. 3) The Cr_2O_3 abundance in the melt is the average of the two abundances calculated for the Kilauea group and Mauna Loa group melts.

The garnet-containing solid-solution mineralogy of the primary melt was calculated by using two olivines (Fo_{90} and Fo_{95}), three pyroxenes, garnet, and ilmenite (see Table 16, Part 1). The result is presented in Table 16. In the initial estimation of this mineralogy, a fourth pyroxene (a Ca-Fe-rich variety) was used, but the solution contained an overabundance of this component and subsequently negative abundances of the opxl and cpx components. Hence, this component was not included in obtaining the final result.

The computer-fitted mineralogy of the melt using magmatic minerals is given in Table 17. The initial fit of this melt using the magmatic components also included a fourth pyroxene and gave the same type of solution that occurred in the previous calculation; that is, negative components. The final solution, therefore, does not contain this component.

These two results can be combined, after the component sums are normalized to 100%, to give the following apparent olivine reaction (written in terms of weight fractions:

$0.185Fo_{92}$ + 0.311 opx + 0.090 cpx + 0.398 gar + 0.015 il → $0.503Fo_{84}$ + 0.014 chromite + 0.178 opx + 0.045 cpx + 0.234 plag + 0.023 il.

The net reaction $0.185Fo_{92}$ + 0.133 opx + 0.045 cpx + 0.398 gar → $0.503Fo_{84}$ + 0.014 chromite + 0.234 plag + 0.008 il suggests that the pyroxene components are partially consumed in producing a plagioclase-containing melt in accordance with Kushiro's observation. The most significant aspect of this reaction, however, is that it indicates that the pyroxenes are consumed in differing amounts; this reaction could be a controlling factor in producing the garnet-hypersthene relationships suggested to be exhibited among the Hawaiian basalts. This in turn would support the mineralogical arguments concerning melt heterogeneity.

TABLE 17. COMPUTER-CALCULATED MINERALOGY OF MELT IN TERMS OF BASALT COMPONENTS.

Element	Compositions of Mineral Components (Part 2) (%)						
	Fo_{85}	Fo_{80}	opx1	opx2	cpx	plag	chrom
TiO_2	0.04	0.04	1.00	1.00	1.00	0.06	2.10
Al_2O_3	1.10	1.10	0.00	0.00	0.00	30.90	13.40
FeO	12.60	16.75	10.00	25.00	3.20	0.50	20.90
MgO	44.40	40.25	29.40	14.30	18.90	0.00	11.60
CaO	1.20	1.20	5.00	21.60	5.25	13.80	0.00
Na_2O	0.00	0.00	0.20	0.50	0.50	3.29	0.00
K_2O	0.00	0.00	0.00	0.10	0.10	0.65	0.00
MnO	0.17	0.17	0.14	0.14	0.14	0.00	0.20
Cr_2O_3	0.10	0.10	0.20	0.20	0.20	0.00	43.50

Element	Observed	Calculated	Fit	Mineralogy
TiO_2	1.28	1.29	0.00	Fo_{85} = 43.0 ± 1.3
Al_2O_3	7.40	7.40	0.00	Fo_{80} = 2.7 ± 0.1
FeO	10.80	10.80	0.00	opx1 = 3.1 ± 15.4
MgO	23.50	23.91	0.04	opx2 = 13.1 ± 6.2
CaO	5.10	5.11	0.01	cpx = 4.1 ± 2.0
Na_2O	1.08	0.79	7.12	plag = 21.3 ± 0.6
K_2O	0.18	0.16	0.03	chrom = 1.3 ± 0.2
MnO	0.17	0.12	0.00	Il = 2.3 ± 0.1
Cr_2O_3	0.60	0.61	0.15	Sum = 90.9
				χ^2 = 2.51

This can be shown by estimating in an example the possible effects of the reaction on a more garnet-rich melt.

For the purpose of this investigation, it will be assumed that in a melting mode variation to a more garnet-rich melt, such a melt will have the same proportional increase of olivine (Fo_{92}). This assumption serves two related purposes: 1) The same olivine reaction, as determined above, can be used in obtaining the final products, and 2) the reaction will result in the total consumption of the initial olivine. This assumption seems to be valid considering the observed normative behavior of these types of melts (O'Hara and Yoder, 1967). It will be further assumed that the same pyroxene is represented in the melt and that hence no change occurs in the opx/cpx ratio.

Based on these assumptions, one possible melt could be represented by $0.209Fo_{92}$ + 0.252 opx + 0.073 cpx + 0.450 gar + 0.017 il. The composition of the liquid following the reaction with olivine will become $0.568Fo_{84}$ + 0.016 chromite + 0.102 opx + 0.022 cpx + 0.264 plag + 0.026 il. This melt will now have an opx/cpx ratio of approximately 4.6 compared to the 3.9 observed in the "average" melt. Since an increase in the opx/cpx ratio is postulated to be indicative of a garnet-rich melt, this result is consistent with that interpretation.

It will be mentioned, however, that the specific reaction as written may not be the actual reaction occurring in the melts, only that a similar reaction is possible. On the other hand, the weight fractions of the minerals calculated for both types of melts agree closely with those postulated to be in the melting mode and with the observed mineralogy of the basalts. Hence, this reaction could be a good approximation to the postulated event and will be referred to later in the discussion of garnet pyroxenite formation.

X. KOOLAU SOURCE MODEL-GARNET PYROXENITE GENERATION

The bulk of the discussion pertaining to the Koolau REE source model and trace element estimates has been deferred so as to include a possible model for the observance of garnet pyroxenite on Koolau. The Koolau volcanics are unique in the sense that Koolau is the only volcano of those studied in this work that contains the entire range of basalt compositions thus far observed on the islands. Data are available on the garnet peridotite, lherzolite, and pyroxenite xenoliths that have erupted from Koolau during the final stages of the magma generative process. If these xenoliths can be compositionally related to the proposed Koolau source by simple geochemical processes, it would provide an independent means for substantiating these findings on mantle heterogeneity, melt heterogeneity, etc.

As determined from the refined REE model, the Koolau source is characterized by 90% ol+opx (67% olivine; 23% orthopyroxene), 6% cpx, and 4% gar (Fig. 10). The required REE abundances in the source were calculated by using the same procedure as in the Kilauea-Mauna Loa determinations. As seen in Figure 11, the chondrite-normalized REE pattern of the Koolau source parallels that of the Mauna Loa mantle; however, absolute abundances in the Koolau source are lower by a factor of 1.3. This difference has been suggested to be a direct result of mantle regeneration differences.

The calculated abundances of Cr, Co, and Ni in the Koolau source, however, more closely resemble those estimated for the Kilauea mantle. These higher contents (Cr_2O_3 = 0.45%, NiO = 0.38%, and Co = 82 ppm) are easily explained by recalling that the proposed source material has a very high ol-opx content; the bulk partition coefficients for these elements is significantly larger in such a source and results in higher calculated abundances.

Major element evidence for a high ol-opx source is suggested by the low FeO content observed in these lavas (9.8 and 10.2% vs. 11.1% average in the other basalts; see Table 6B). An olivine-rich parent (Fig. 7) would shift the allowable field of partial melts to the upper left (i.e., to a more MgO-rich, FeO-poor melt). The effect is somewhat

alleviated by the fact that the bulk D_{FeO} for the solid would decrease, expanding the field in the opposite direction.

The high Al_2O_3/CaO ratios (1.7 and 1.8) in these basalts would suggest that these basalts were formed at a lower pressure than that postulated for generating the other basalts. A eutectic composition predominantly composed of garnet will increase Al_2O_3 relative to CaO in the primary melts. Mineralogies of the Koolau lavas may also reflect a low-pressure melting event (Table 14); these magmas have very high opx/cpx ratios and relatively high plagioclase contents.

The Koolau basalt pyroxenes are plotted in Figure 14 to give an estimate to primary melt composition (identified by a filled diamond with superscript 3). The heterogeneity of the Koolau melt is evident from this figure; it has a lower CaO content and is slightly more MgO-rich compared to the other melts, as was suspected from MgO-FeO source-melt partitioning. The mg' value, however, remains consistent with previous estimates (0.80).

Now that the Koolau source has been defined in terms of REE, trace, and major element abundances, the relationship of garnet pyroxenite formation can be examined. The pyroxenite chosen for this investigation is the Salt Lake Crater xenolith studied by Reid and Frey (1971) on which REE abundances are presented (Fig. 15). Although this rock was not analyzed for major elements, Reid and Frey do provide major element composition data for a similar garnet pyroxenite (Table 19) studied by Kuno (1969).

Because of the close major element similarities between the pyroxenite and the proposed primary melts (Table 18), the initial interpretation of these pyroxenites is that they represent entrapped partial melts derived from the Koolau source. This assumption is a matter for continuing debate among authors. Reid and Frey (1971) initially observed that the mineralogies of the pyroxenites may suggest this type of relationship, but later Reid and Prinz in a companion paper (1971) interpreted them as high-pressure cumulates. Green (1966) and O'Hara (1969) also support a cumulate model. A second model for garnet pyroxenite genesis involves fractional fusion of basanitic garnet clinopyroxenite (Beeson and Jackson, 1970). Finally, Wilkinson (1976) has

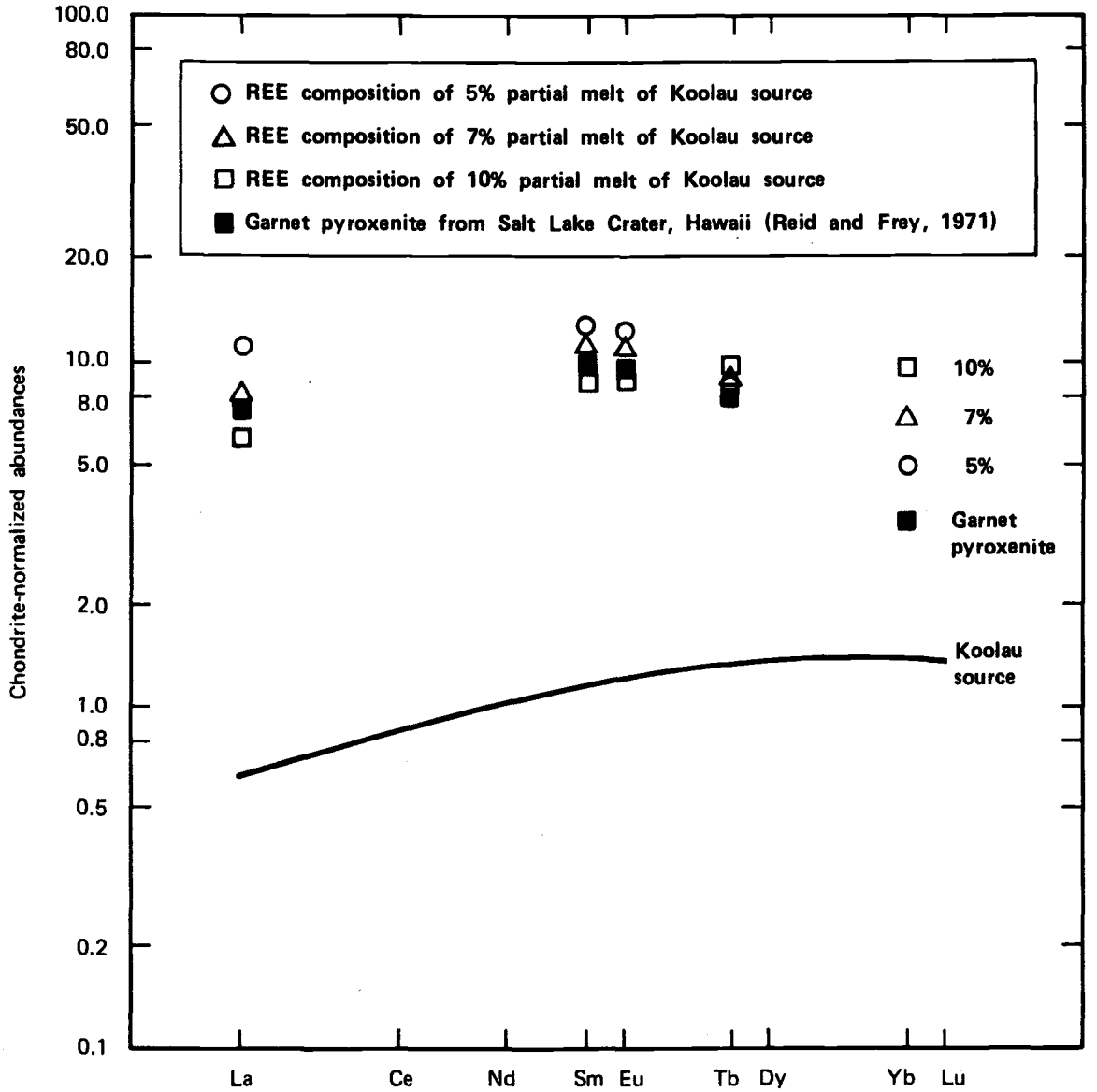

Fig. 15. Chondrite-normalized REE abundance patterns of possible partial melts generated from Koolau. The REE abundance pattern obtained by 24 percent 1:1 olivine and garnet fractionation of the 10 percent partial melt overlaps the observed garnet pyroxenite pattern. See table 19 for abundance comparison.

TABLE 18. MODEL REQUIRED FOR THE GENERATION OF GARNET PYROXENITES.

Element	6% Melt (Garnet-rich) (1)	10% Melt 0.7 Garnet-rich 0.3 cpx + ol (2)	Melt 2 Minus 24% ol + gar (3)	Garnet Pyroxenite (4)		
				A	B	C
Percentage						
TiO_2	1.28[a]	0.95[a]	1.2	0.4	0.8	. . .
Al_2O_3	9.00	7.9	7.3	8.0	10.9	. . .
FeO[b]	10.80	9.5	10.3 (9.4)	8.1	9.2	. . .
MgO	23.50	24.7	21.2 (18.8)	20.0	16.7	. . .
CaO	5.30	7.0	8.4	12.0	12.3	. . .
Na_2O	1.08	1.3	1.6	1.9	1.3	. . .
Cr_2O_3	0.61	0.6[a]	0.55	0.54	. . .	. . .
(Times Chondrite)						
La	0.65[c]	6.0	7.9	. . .	. . .	7.5
Sm	1.07[c]	8.4	10.7	. . .	. . .	9.5
Eu	1.23[c]	9.0	11.2	. . .	. . .	9.3
Yb	1.27[c]	10.3	4.3	. . .	. . .	4.0
Lu	1.24[c]	9.5	3.0	. . .	. . .	3.0

NOTES: 1) Melt composition based on postulated shift toward garnet-rich modes with higher degrees of partial melt. Calculated by assuming that the resultant melt is composed of 90% of melt parental to the Koolau basalt suite plus 10% additional garnet. Melting mode approximately 17% ol-opx, 36% cpx, 47% gar (see Table 16).

2) Major element composition of 10% partial melt estimated from mixing 70% garnet-rich melt (1) plus 30% of a melt composed at 4:1 cpx + ol-opx. Mineral compositions used in estimate given in Table 9. The REE calculated from partial melting equation (see text).

3) Composition of melt following 24% olivine + garnet fractionation. Major elements calculated by subtracting mineral compositions given in Table 9. The REE, TiO_2, and Cr_2O_3 calculated from the fractionation equation. Values for FeO and MgO in parentheses calculated using the fractionation equation, D values for garnet and olivine at 1400°C.

4) Observed garnet pyroxenite compositions for A from Kushiro (1968), B from Beeson and Jackson (1970), and C from Reid and Frey (1971).

[a]Calculated using partial melting equation.

[b]Total Fe as FeO.

[c]Koolau source (times chondrite).

suggested a third model, which is the most consistent with the proposed model of generation; that is, anatexis of upper mantle lherzolites. In this latter model, mineralogical and compositional variations among the pyroxenites are accounted for by exsolution and recrystallization processes.

In the approach taken here, the following data for REE abundances, mineralogies, and major element abundances between the hypothetical Koolau source (melt) and the garnet pyroxenite were examined to determine whether or not a possible partial melting-fractionation relationship existed. On the basis of major element data, the garnet pyroxenites appear to be evolved from the primary melt, probably as a result of olivine fractionation. Evidence relies on the lower MgO and higher Na_2O contents in the pyroxenites versus the proposed melt (Table 9). In addition, it has been widely demonstrated that olivine will be an initial phase precipitating from a partially melted liquid, provided that a liquid was derived from a parental material predominantly containing olivine. (This fractionation relationship was also true in Hawaiian tholeiitic basalt evolution). The low Al_2O_3-CaO ratio (0.8) and, consequently, the high cpx/gar ratio observed in the garnet pyroxenites suggest that one of two additional generative events may be involved in their formation; either the melting mode had a high cpx/gar ratio, or garnet has been fractionated from the melt. Considering the heavy REE depletion observed in the pyroxenites, the second mechanism is likely to be the more important process. It can be shown that a cpx-rich melting mode will not result in a liquid having such an extensive depletion in the heavy REE. Furthermore, to attain such a melting mode would require the association of very high pressures with the melting event (O'Hara and Yoder, 1967). From these observations, it will be proposed that a considerable amount of garnet plus olivine fractionation has evolved the primary melt to the final pyroxenite assemblage.

It must be determined whether or not the unevolved parent of the pyroxenite is a possible partial melt of the proposed source. Since it has been postulated that the Koolau source is melted in producing these

compositions, the chondrite-normalized REE abundance pattern of the parent must have the following features: 1) The melt must have light REE abundances that are lower than those observed in the pyroxenites. This is based on the fact that olivine plus garnet fractionation will result in raising the light REE abundances in any evolved liquid since the bulk D for the LREE in these minerals will be less than unity (see Appendix B). 2) The melt must have light Ree ratios very similar to those observed in the pyroxenites; olivine plus garnet fractionation will not significantly alter the La/Ce and La/Nd ratios in the primary liquid since the mineral to liquid partition coefficients are very similar among these elements (Appendix B). Presented in Figure 15 are three chondrite-normalized REE abundance patterns produced upon different degrees of partial melting of the Koolau source. As can be seen, the REE pattern most capable of explaining the observed pattern is the composition generated by ~10% partial melting. It will be noted at this point that this composition was derived by assuming a different melting mode than that at 5% or 7% partial melting. The reasoning behind this will be discussed shortly, but for now, it will be assumed that this melt is the most probable parent to the garnet pyroxenites. Consequently, the fractionation relationship can be defined.

The La^{ℓ}/La_0 ratio between the pyroxenite and postulated melt can be used in calculating the amount of ol + gar fractionation since any combination of olivine and garnet will give a bulk D for La $\leq$ 0.007. Hence, La fractionation will be relatively independent of the proportion of phases removed. The degree of fractionation, F, was calculated using the Rayleigh equation, $\frac{C^{\ell}}{C_0} = (1 - F)^{D-1}$, giving about 23-24% ol + gar fractionation. With F defined, the weight fractions of olivine and garnet in the cumulative solid can be calculated by solving for $\bar{D}$ (from above) for an element being substantially partitioned into the solid. Recall that $\bar{D} = x_1D_1 + x_2D_2$, where xD is equal to the weight fraction of a cumulative mineral times the mineral to liquid partition coefficient for an element and that since $x_1 + x_2$ is equal to one, x_1 or x_2 can be determined by substituting one equation into the other. The bulk partition coefficient required to fractionate Yb was

arbitrarily chosen for this estimate, and the $\bar{D}$ value was determined to be ~4.3. To obtain this value, ~50% garnet and 50% olivine are required to have been fractionated from the parental liquid. This result was used to obtain the chondrite-normalized REE abundance pattern of a hypothetical garnet pyroxenite (Fig. 15; Table 18), giving an excellent fit to the observed pattern.

The major element and mineralogical variations that will occur during this event can also be examined to see whether or not these are consistent with the observed compositional changes. Before this can be done, however, a bulk composition representative of ~10% partial melting must be estimated. The average primary melt composition presented earlier is not considered as a probable 10% melt for the following reasons: 1) It has been postulated that at higher degrees of partial melting (>5%), the melting mode will become more garnet-rich. This will result in a melt having a higher Al_2O_3 abundance but a similar CaO abundance. 2) After ~7% partial melting of the Koolau source, the postulated source material will be depleted in garnet. Further melting will produce a cpx + ol-opx normative liquid and again alter the bulk composition of the partial melt. These observations were also considered in calculating the REE abundance pattern.

The bulk composition given in Table 18, column 2, will be suggested to represent the melt produced from this type of melting. Most of the abundances are based on simply adding 70% of a garnet-rich melt (Table 18, column 1), which represents a slight shift toward a garnet-normative melt and 30% of a melt composed of ~80% cpx and 20% ol-opx, the melting proportion of a garnet-free system (Yoder, 1976). The abundances of TiO_2 and Cr_2O_3 were calculated from the partial melting equation by assuming a melting mode estimate of ~18% ol-opx, 45% cpx, and 37% garnet. The REE abundance pattern presented earlier for the 10% partial melt were also calculated by using this melting mode. Since the actual effect that excessive melting has on trace element abundances in derived liquids has not been adequately studied, this type of approach has been pursued.

To simplify the major element variations predicted for the fractionation of garnet and olivine, an arbitrary but plausible composition of the cumulate solid representing a 1:1 ratio of olivine (Fo_{93}) and garnet (see Table 8) was subtracted from the melt in the amount given above (24%) and the residual composition calculated. Estimates for TiO_2 and Cr_2O_3 concentrations in the liquid, nevertheless, were obtained from the fractionation equation by using appropriate D values. The residual (garnet pyroxenite) composition is also given in Table 18. The close agreement obtained between the calculated and the observed major element compositions of the pyroxenite indicates that this may be an acceptable generative process. Furthermore, neither the partial melting nor the fractional crystallization events proposed are beyond the scope of reasonable explanation. For instance, the anomalously high melting episode suggested for garnet pyroxenite formation compared to the low degree of melting for the tholeiitic basalts may be representative of the final stages involved in Hawaiian magma generation. Some authors [for example, Shaw (1969, 1970) in his shear melting hypothesis; see Introduction] have proposed a "runaway" mechanism associated with the cyclic nature of basalt generation. In this type of event, the initial melting episodes (e.g., tholeiitic basalts) are characterized by low (<10%) melting with large increases in partial melting occurring with time (e.g., the late-stage pyroxenites). Melting ceases and the cycle starts anew when the energy source is depleted. Finally, garnet on the liquidus (resulting in its fractionation) would be expected since garnet was consumed in the source region.

Mineralogically, the garnet pyroxenite analyzed by Reid and Frey (1971) is composed of 65% cpx, 18% gar, and 17% ol+opx; this composition is comparable to the average composition of the garnet pyroxenites from Koolau: 65% cpx, 15% gar, and 20% ol+opx (Jackson and Wright, 1970). Fractionation of garnet plus olivine from the proposed melt (45% cpx, 37% gar, and 18% ol+opx) described above would produce a solid with a mineralogy of 59% cpx and 33% gar and 8% ol+opx. The discrepancy observed between the observed and the postulated mineralogies could suggest that a garnet transformation (olivine reaction) relationship may be a characteristic of any Hawaiian melt. Analyses

of olivine in garnet pyroxenites (Wilkinson, 1976) can be used to support this observation. Olivines found in association with garnet pyroxenites have a forsterite content of ~83 — very similar to the olivine produced in the transformation reaction (Fo_{84}). Furthermore, the exsolution features found in gar-cpx pairs can be used to suggest that some type of reaction has occurred between these minerals. The contribution of a garnet transformation reaction to the evolution of garnet pyroxenite will be examined.

From the previous discussion of the reaction, it was suggested that such a reaction proceeded to its end point, presumably when garnet was consumed. It is interesting to note that in the net reaction involving the 10% partial melt (written in terms of weight percentage), both olivine and garnet will be completely consumed:

$$18.0\ Fo_{92} + 12.9\ opx + 4.4\ cpx + 37.0\ gar_{prim}$$

$$38.9\ Fo_{84} + 22.7\ gar_{sec}$$

An allowance has been made for the pressure effect associated with garnet pyroxenite formation (Wilkinson, 1976); that is, one of the products will remain garnet and not transform to plagioclase (plus chromite) as before. Fractionation of olivine (Fo_{84}) and garnet from this resultant liquid (corresponding to ~28% cpx, ~23% gar, and 49% ol+opx) will produce a mineralogy of 37% cpx, 15% gar, and 48% ol+opx. In the actual event, olivine fractionation and the olivine reaction probably occur simultaneously. Assuming that these occur at equal rates, the mineralogy 48% cpx, 24% gar, and 28% ol+opx is one possible composition.

The relationship of other observed garnet pyroxenite compositions to this hypothetical melt can be shown by plotting whole rock analyses on a Ca-Mg-Fe diagram (Fig. 14). The estimated melt composition resulting from 10% partial melting of the Koolau source is represented by the filled diamond with superscript 3. The garnet pyroxenite composition derived from this melt by gar + ol fractionation as described above is given by the open circle. Other garnet pyroxenite compositions (given by the broken line) include the garnet pyroxenites of Beeson and Jackson (1970) and Jackson (1966), identified by the filled circles, superscripts 1 and 2, respectively. These exhibit almost perfect

ol + gar fractionation relationship to that proposed. Variations in temperature and pressure, rates of fractionation, and exsolution, nevertheless, could be additional factors in producing the wide range of garnet pyroxenite compositions observed.

In summarizing the proposed model of garnet pyroxenite formation in Koolau, the following scenario will be presented:

The final stages of magmatic activity were dominated by anomalously high (10-15%) partial melting events. The melts produced were cpx-rich and characterized by REE abundance patterns resembling the source.[17] Upon cooling, olivine and garnet simultaneously reacted and crystallized from the liquid. The resultant magmas have low Al_2O_3/CaO ratios and evolved REE patterns exhibiting heavy REE depletion. Prior to complete crystallization, reactions involving gar and cpx resulted in textural and compositional variations among these minerals.

[17] Although it was not pointed out in this discussion, there is indirect evidence suggesting that the olivine fractionation estimate is fairly accurate. If the garnet pyroxenites are evolved partial melts of the Koolau mantle, as postulated, the REE correlation can only be attained by assuming that the absolute Koolau chondrite-normalized REE abundance pattern is a representative mantle composition. If a smaller degree of olivine fractionation was used earlier in calculating the REE abundances in the Koolau mantle, these abundances would have been higher. Such a source could not have been melted to produce a liquid having REE abundances as low as those observed in the garnet pyroxenites.

XI. SUMMARY OF THOLEIITIC BASALT GENERATION

Three types of mantle material have been identified by REE modeling as possible sources of the Hawaiian tholeiitic basalts. Three sources are characterized by mineralogical and compositional differences and account for the major variations observed among the basalts trace element compositions.

A garnet peridotite composed of 84% ol+opx, 12% cpx, and 4% gar having REE abundances gradually increasing from 1.1x (times chondrite) for La to 1.4x for Lu is capable of producing the observed chondrite-normalized REE abundance patterns in the Kohala, Mauna Kea, and Kilauea basalts by simply varying the degree of partial melting. Transition element abundances for Cr_2O_3, Ni, and Co in the mantle estimated from the REE modeling data and olivine fractionation calculations are 0.4% Cr_2O_3, 2540 ppm Ni, and 74 ppm Co.

A single source material, identical in terms of mineralogy, REE, and trace element abundances has been postulated to be parental to the Mauna Loa and Lanai basalts. Different degrees of partial melting of a source composed of 75% ol+opx, 20% cpx, and 5% gar is attributed to producing the observed trace element composition differences in these basalts. The chondrite-normalized REE abundance pattern of this mantle exhibits more light REE depletion (0.84x La) and heavy REE enrichment (1.8x Lu) relative to the Kilauea group source. The Mauna Loa and Lanai basalts have Cr_2O_3, Ni, and Co abundances that indicate derivation from a source containing 0.40% Cr_2O_3, 1870 ppm Ni, and 64 ppm Co.

The proposed source of the Koolau basalts has the lithology 90% ol+opx, 6% cpx, and 4% gar. The chondrite-normalized REE abundance pattern of the Koolau mantle has a shape identical to the Mauna Loa source, but the absolute abundances are lower by a factor of 1.3. The estimated mantle abundances for Cr_2O_3, Ni, and Co, however, closely resemble those estimated for the Kilauea group source; namely, 0.46% Cr_2O_3, 2900 ppm Ni, and 82 ppm Co.

It has been postulated that these source regions may have evolved from a common primordial mantle composition as a result of a different initial partial melting events combined with varying amounts of mantle regeneration or equilibration rates.

Some of the compositional differences observed among interrift and intrarift basalts have been suggested to be the result of heterogeneities in primary melt compositions due to changes in the pressure of partial melting. This type of melting variation would produce garnet-rich or garnet-poor melts, thereby evolving magmas with a range of Al_2O_3/CaO ratios. Among the basalts generated from the northern rift, those having higher Al_2O_3/CaO ratios were also the result of higher degrees of melting and led to the postulation of a pressure-relief model. Among all of the Hawaiian basalts, the Koolau basalts have the largest Al_2O_3/CaO ratios (~1.7). This fact indicates that melting occurred at a lower pressure than the Lanai and Mauna Loa episodes. These latter basalts have Al_2O_3/CaO ratios of 1.5 and 1.4, respectively. The Kilauea group source has been suggested to be located at the greatest depth on the basis of their low (1.25) Al_2O_3/CaO ratios.

Most of the available means for estimating the amount of olivine fractionation evolving these basalts are consistent with the interpretation that 40-50% olivine has been removed from the primary melt. Calculations using available FeO-MgO partitioning data, mineral component data, and mg' value considerations indicate that the primary liquids evolving to the Hawaiian basalts must be MgO-rich, between 20 and 30% MgO. Subsequently, large amounts of olivine fractionation are required to produce the low-MgO basalts. Additional evidence for high amounts of olivine fractionation comes from the close similarities observed between the postulated sources' REE abundances patterns and those found in naturally occurring alpine peridotites believed to represent mantle material.

Finally, the proposed Koolau mantle has a composition in terms of REE abundances that can produce melts capable of being evolved to the garnet pyroxenites of Koolau. The large degrees of melting needed are equivalent to those postulated to occur in the final stages of a "runaway" melting model (Shaw, 1969). Garnet is depleted in the source material during these episodes and results in melts having very low Al_2O_3/CaO ratios. Garnet and olivine fractionation, combined with the reaction of the excess garnet with the liquid, evolves the melts to the final pyroxene composition.

XII. MAUNA ULU VARIANTS

Introduction

The five samples studied from Mauna Ulu represent temporally distinct magma batches that erupted from the flank of Kilauea between 1969 and 1971. These magma batches have been termed variants, and the first three variants have been identified as being compositionally similar to the magmas that erupted from Halemaumau during the 1967-68 eruption. The last two variants have compositions that are distinctly different from the previous magmas (Wright et al., 1975).

These lavas also represent magmas that have been erupted by varying types of activity during the volcanic sequence. The initial volcanic activity was characterized by short periods of high fountaining, followed by long intervals of weak spattering and overflow of the caldera (Variants 1-3). The eruptions producing Variant 4 were dominated by continuous weak fountaining with periodic overflows as was the activity producing Variant 5, the final composition observed.[18]

Results

The major, minor, and trace element data (including nine REE abundances) are presented in Table 5E for these basalts. The samples analyzed represent different splits of the same basalts previously analyzed by Wright et al. (1975) for major elements (see Appendix A). For comparison, their data for Variant #5 are given to show the typical precision of neutron activation analysis. As can be seen, the agreement is quite good for the major elements considering the analytical uncertainties reported.

The chondrite-normalized REE and trace element abundance patterns are presented in Figure 16. These abundances are similar to those observed in the other Hawaiian basalts; La abundances among the variants range from 35 to 40x (times chondrite), and Yb abundances vary from

[18]Volcanic activity from the east flank of Kilauea was resumed in early 1972. These basalts are currently being investigated by Wright et al. (1975).

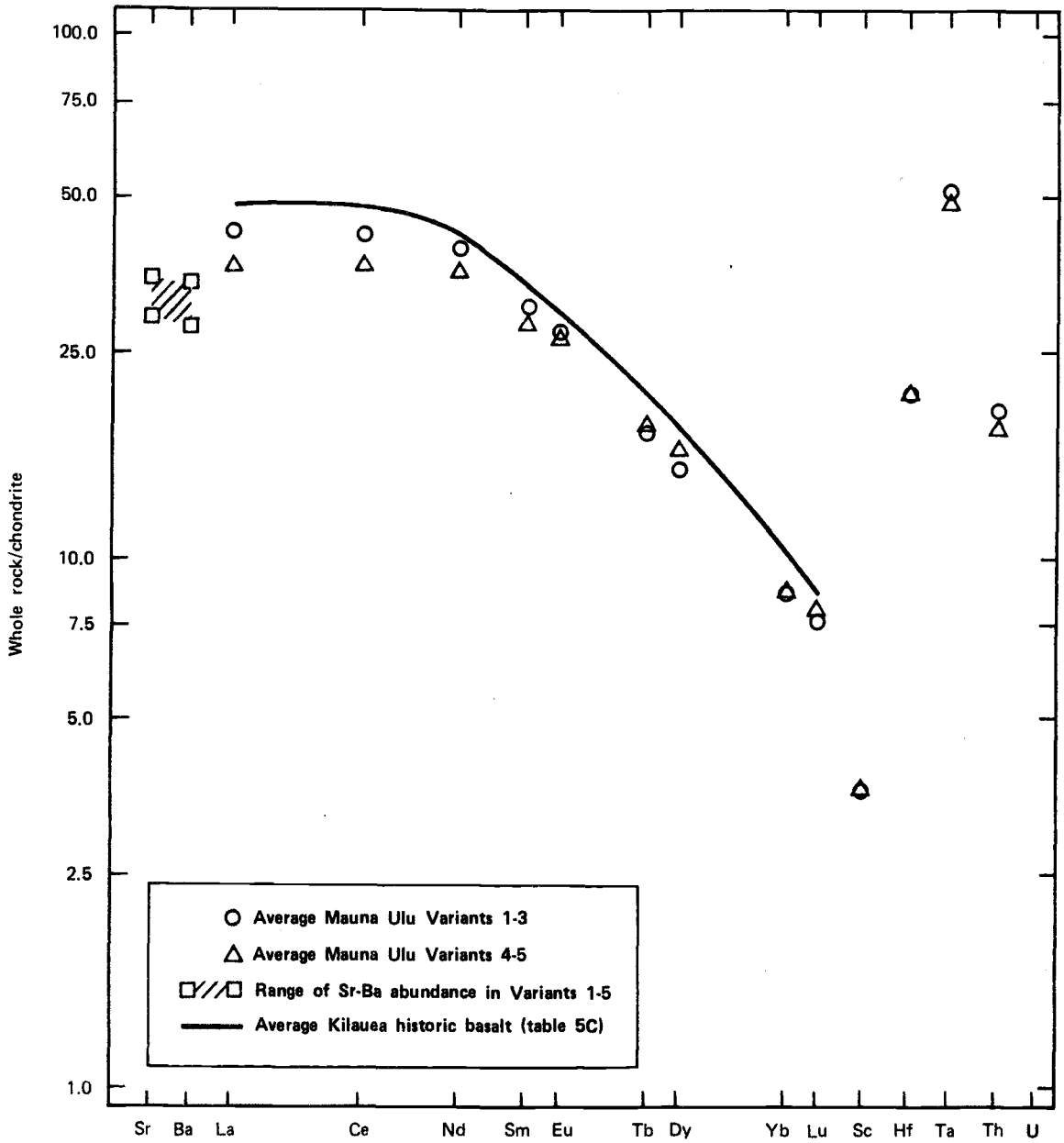

Fig. 16. Chondrite-normalized trace element abundance patterns of the Mauna Ulu variants analyzed in this work.

8 to 9x. The $(La/Nd)_{c.n.}$ ratios in these basalts are slightly greater than unity (1.03) and are similar to those found in the northern rift basalts.

Discussion

Since Wright et al. (1975) have noted most of the compositional relationships among the variants and also between the other Kilauea basalts, most of the following discussion will be focused on verifying their observations based on REE and trace element data and on determining the possible relationship of the variants to the proposed primary melt and mantle of Kilauea. This assumes, of course, that the Mauna Ulu source is similar to the Kilauea source, if not the same.

A few points will be considered, however, concerning some major element data: First, the Al_2O_3/CaO ratios among the variants are very similar (1.23) to those observed in the average Kilauea basalts (1.20), suggesting that these magmas were generated at or near the same depth as the Kilauea basalts. These low ratios, relatively speaking, have been identified as being characteristic of the Kilauea group basalts. Second, the high TiO_2 abundances (average 2.5%) have also been suggested to be representative of basalts generated from the northern rift volcanic center. Hence, it will be concluded that these variants have compositions that indicate that they are products of melting the Kilauea group source.

It was stated earlier that Wright et al. (1975) believe that Variants 1-3 are compositionally similar to the 1967-68 Halemaumau basalts. (It will be mentioned that this latter basalt composition was used in obtaining the average Kilauea historic basalt composition; see Table 7C). The REE data of the variant basalts support this observation. The average chondrite-normalized REE pattern of the three variants nearly parallels that of the average Kilauea historic basalt pattern, the former being lower by a factor of about 1.13. Assuming that differences in the amount of olivine fractional crystallization have evolved the two REE compositions, other elemental abundance variations must also show an olivine fractionation relationship. For example, applying the REE factor to other incompatible elements, such as TiO_2, Al_2O_3, CaO, K_2O, Hf, Ta, and Th, in the average variant gives a composition that is very similar to

that of the average Kilauea historic basalt (Table 19). Thus, Mauna Ulu Variants 1-3 could quite easily be described as less evolved (olivine-fractionated) Kilauea basalts generated during the same or similar melting process that produced the historic basalts on Kilauea. If the basalts can be related to the same magma batch, estimates of olivine to liquid partition coefficients for FeO, MgO, Ni, and Co can be made. These values can then be evaluated in terms of the average temperature of olivine fractionation. Using the Rayleigh fractionation equation and the degree of fractionation of ~11% [for La, $c^{\ell}/c_o = 1.12 = (1 - F)^{D-1}$ and since $D_{La} = 0.007$, then F = 11%], $D^{ol/l}$ values for these elements were calculated giving D = 1.16 for FeO, 3.21 for MgO, 4.7 for Ni, and 2.5 for Co. The corresponding temperatures of fractionation are 1334°C, 1369°C, 1429°C and 1301°C (Leeman and Scheidegger, 1977).

The high temperature of crystallization indicated by Ni partitioning can probably be attributed to a pressure-dependent effect unaccounted for in the Ni partitioning values used. The temperature and compositional equations arrived at by various workers were based upon experimental data at 1 atm pressure. Based upon limited amount of data that do exist at 15-20 kb and assuming these data can be extrapolated (that is, if $\ell n\ D_{Ni}^{ol/l}$ at constant T is a linear function with respect to pressure), then a $D_{Ni}^{ol/l}$ value of 4.7 at 1331°C (the geometric mean of 1334°C, 1360°C, and 1301°C from above) is expected at ~7 kb. It may or may not be coincidental that this pressure corresponds to that expected at ~20 km, the location of the intermediate magma storage reservoir (see Introduction). If it is not accidental, then the Ni-MgO fractionation path proposed earlier and shown in Figure 13 should be adjusted to account for these lower D values. However, because highly reliable values at these pressures are lacking, this will not be done; it will only be noted that Ni melt abundances may be lower and in turn would imply lower Ni abundances in the mantle regions.

The basalt compositions represented by Variants 4-5 have been previously suggested (Wright et al., 1975) to be unrelated to the previous variant lavas. This is also supported by the REE data. The lower light REE abundances found in these basalts (Fig. 14), coupled with the lower MgO contents, rule out any olivine fractionation relationship that may

TABLE 19. POSSIBLE CHEMICAL RELATIONSHIP BETWEEN MAUNA ULU VARIANTS #1, #2, AND #3 AND KILAUEA HISTORIC BASALTS BY OLIVINE REMOVAL.

Element	Average Mauna Ulu Variants #1, #2, #3	Average Mauna Ulu Variant Minus 11% Olivine Fo_{81}	Average Kilauea Historic
TiO_2	2.45	2.75	2.70
Al_2O_3	12.9	14.5	13.7
FeO[a]	11.2	[$D_{FeO}^{Ol/l} = 1.16$]	11.0
MgO	9.7	[$D_{MgO}^{Ol/l} = 3.21$]	7.5
CaO	10.4	11.7	11.4
K_2O	0.48	0.54	0.54
Cr	424	[$D_{Cr}^{Ol/l} = 2.34$]	363
Co	51	[$D_{Co}^{Ol/l} = 2.5$]	43
Ni	230	[$D_{Ni}^{Ol/l} = 4.7$]	150
La	13.9	15.6	15.6
Ce	34.3	38.5	38.8
Nd	24	27	[25]
Sm	5.87	6.6	6.0
Eu	1.95	2.19	2.06
Tb	0.82	0.92	0.96
Dy	4.4	4.9	5.0
Yb	1.85	2.08	1.98
Lu	0.26	0.29	0.28
Sc	29	31.5	30
Hf	4.0	4.5	4.3
Ta	1.0	1.1	1.2
Th	0.75	0.84	0.95

NOTES: Values in brackets are D values required for the proposed relationship by olivine fractional crystallization. See text.

[a]Total Fe as FeO.

exist among these variant basalts (Wright et al. arrived at this conclusion from K_2O and TiO_2 abundance considerations). Thus, these variants could be termed the "Mauna Ulu magma batch" as suggested by these authors.

There is some indication that the latter variants could be generated by a degree of melting slightly higher than that producing the Kilauea historic basalts. Evidence comes from application of the chondrite-normalized Eu abundances to the partial melting model for Kilauea group basalts. After normalization for olivine fractionation, the same calculations were performed to estimate the degree of partial melting and to derive a REE pattern for the Mauna Ulu source as performed for the Kilauea basalts. The degree of partial melting required to produce the Eu abundance observed in the Mauna Ulu magma batch is ~4%. These calculations assume that the Kilauea group source material is being melted. The calculated abundances for the REE, Sc, Hf, Ta, and Th in the Mauna Ulu source material are presented in Table 20. As can be seen, these calculated abundances agree rather well with the average mantle composition postulated for the northern rift volcanics.

The calculated Cr, Co, and Ni abundances in the Mauna Ulu melt and mantle system (Table 20) indicate that the Mauna Ulu source has a composition in terms of these elements that are also characteristic of the Kilauea mantle. The estimated abundances for Cr_2O_3, Co, and NiO in this source are 0.45%, 80 ppm, and 0.28%, respectively.

TABLE 20. AVERAGE TRACE ELEMENT COMPOSITION OF MAUNA ULU VARIANTS #4 AND #5.

Element	Average Composition (ppm)	Source Abundance For 4% PM (Times Chondrite)	Kilauea Source (Times Chondrite)
La	12.6	1.06	1.10
Ce	31.1	1.14	1.22
Nd	23	1.37	1.25
Sm	5.49	1.38	1.40
Eu	1.95	1.47	1.47
Tb	0.84	1.51	1.46
Dy	4.7	1.50	1.49
Yb	1.91	1.58	1.41
Lu	0.27	1.54	1.37
Sc	30	1.61	1.55
Hf	4.0	1.32	1.38
Ta	1.0	2.23	2.07
Th	0.7	0.36	0.40
Cr	392	3083[a]	3250[a]
Co	48	80[a]	74[a]
Ni	143	2220[a]	2540[a]

NOTES: Source trace element abundances required to generate the average variant by 4% partial melting. Trace element abundances of Kilauea-group source given for comparison.

[a]Expressed in ppm.

XIII. ALKALI OLIVINE BASALTS

No quantitative computer modeling of alkali olivine basalt generation was performed in this study. However, a semiquantitative model based upon available data and the postulated nature of basaltic magma generation will be suggested in order to complete the discussion on Hawaiian basalt formation.

It has been clearly shown that each volcano within Hawaii goes through a cycle in basalt generation. Initially erupting tholeiitic magmas during the primary mountain-building episode, the sequence of basalt generation continues with the less voluminous alkali olivine basalts and finally erupts the high alkaline basalts (e.g., nephelenite) to conclude its activity. The model proposed herein to account for these variable chemistries suggests that each successive sequence is dominated by higher degrees of partial melting; tholeiites being the result of 3-6% partial melting and the garnet pyroxenites, presumably the end products, the results of ~10% partial melting.

Hence, the alkali olivine basalts must be the results of 6-9% partial melting in order for their generation to be consistent with the cyclic nature of magma generation. Such a model is possible if the following assumptions are made on the description of the source material and evolution process. 1) The source material is undepleted in the light REE (and Ba). 2) The source material lies deeper in the mantle relative to the tholeiitic source. 3) As a result of the greater depth and the higher degree of partial melting, more extensive crystal fractionation involving olivine and garnet has occurred.

A model involving these parameters has its reasons for justification; it explains many of the compositional characteristics of the alkali olivine basalts from Hawaii. (When necessary, the discussion will be focused on basalts from Koolau since the most complete description of magma generation thus far proposed involves basalt from this volcano.)

The alkali olivine basalts do not exhibit the depletion effect of La (and Ba) relative to Nd that was a distinguishing feature of many of

the tholeiitic magmas (Fig. 4A). A high degree of melting (6-9%) of an undepleted source is one possible mechanism that can produce magmas with REE abundance patterns capable of being evolved to the final alkali basalt composition; it has been proposed on the basis of Nd isotopic data (Richard et al., 1976) that alkali basalt sources are less depleted in light REE than tholeiitic basalt sources. It is not unreasonable to assume that this undepleted mantle material would lie below the mantle melted into producing the tholeiitic magmas, where it would be unaffected by either partial melting or fractionation events. In general, Sr^{87}/Sr^{86} ratios are lower in alkali olivine basalts (0.7023-0.7040; mean 0.7031) than those in tholeiitic magmas (0.7016-0.7076; mean 0.7046), indicating a more primitive origin. The greater depth at which melting occurs may also be supported by the lower Al_2O_3/CaO ratios found in the alkali basalts (Kay and Gast, 1973). Partial melting at pressures in excess of 40 kb will produce a cpx normative melt and would account for these ratios.

Finally, the excess depth and the high degree of melting could explain why the alkali elements are enriched in these basalts and simultaneously poor in SiO_2 while maintaining a high (8%) MgO content. The high degree of equilibrium partial melting would probably produce a melt high (>25%) in MgO (see Fig. 7) and low in SiO_2, K_2O, and Na_2O. However, by fractionating more olivine relative to the tholeiitic primary melt, higher abundances of the alkalis would be obtained while keeping the SiO_2 and MgO compositional characteristics intact. The greater depth and hence the additional time required for the magma to reach the surface could be important factors in the amount of fractionation that occurs during the ascent.

By analogy, one additional mechanism could be involved in alkali basalt generation, that being minor garnet fractionation. In the model postulated for garnet pyroxenite, a substantial amount of garnet fractionation occurred as a result of garnet depletion in the mantle; hence, garnet would be on the liquidus of the melted phase. This may also be true at 6-9% partial melting.

Two possible REE models for alkali basalt generation in Koolau are outlined in Table 21. In the first model, it was assumed that the source material being melted was 1) lithologically identical to the tholeiitic source and 2) undepleted or only slightly depleted in the light REE and Ba, having chondrite-normalized abundances of ~1.7. The final composition given is that evolved by ~60% crystal fractionation (12% garnet + 48% olivine). As can be seen from the fit, additional fractionation of cpx may also be occurring. The second model is based on the same initial assumptions as the first, the difference being in the proportion of minerals in the melting mode; namely, ~30% ol+opx, 50% cpx, and 20% gar. This mode may in fact be the better estimate of the melt produced at high pressure (Yoder, 1976). Fractionation of garnet would not be expected to occur in this melt, nor is it required in producing the alkali basalt REE abundance pattern.

TABLE 21. POSSIBLE PARTIAL MELTING-FRACTIONATION MODELS FOR ALKALI BASALT GENERATION.

Element	Model I		Model II		Alkali Basalts	
	Melt 8%	Magma 60%	Melt 80%	Magma 60%	Hawaii	
					(a)	(b)
Times Chondrite						
La	19.3	47.9	19.3	48.0	65.6	55.9
Ce	19.3	47.8	19.3	47.9	52.1	41.1
Nd	17.5	43.3	17.6	43.7	36.7	31.3
Sm	15.8	37.7	15.3	37.9	29.1	25.7
Eu	14.8	34.1	14.2	35.1	26.6	22.6
Dy	11.4	20.7	9.8	24.3	16.0	18.3
Yb	11.3	8.5	4.9	12.1	8.6	8.7
Lu	12.1	6.1	4.6	11.5	7.9	8.2
Sc	2.9	3.5	2.3	4.5	. . .	3.1
Ba	21.5	53.4	21.5	53.5	86.3	96.1

NOTES: Model I: REE source abundance = 1.7x (times chondrite). Degree of partial melting — 8%. Melting mode — 20% ol+opx, 40% cpx, 40% gar. Degree of fractionation — 60% (12% gar, 48% ol).

Model II: REE source abundance = 1.7x. Degree of partial melting — 8%. Melting mode — 30% ol+opx; 50% cpx, 20% gar. Degree of fractionation — 60% olivine.

Alkali Basalts: (a) 04-Oahu (from Kay and Gast, 1973); (b) Kan FL-Hualalai (this work).

XIV. CONCLUSION

The models postulated for Hawaiian basalt generation appear plausible in the general sense that

1. They are consistent with processes thought to be involved in basalt formation (that is, partial melting of mantle material produces a magma that is subsequently evolved by olivine crystal fractionation).
2. They indicate sources that are mineralogically and compositionally consistent with material proposed to represent the mantle. It is widely accepted that the mantle is some form of garnet peridotite (or lherzolite), and more recently, it is believed that the mantle is depleted to some extent in the light REE.
3. They indicate the heterogeneities that may exist within the mantle. Hawaiian source region heterogeneities have been previously emphasized by Leeman et al. (1977).

Specific results of these models provide indirect evidence that the source materials postulated may be realistic representations of these regions. For example,

1. Absolute REE abundances that closely resemble those observed in the alpine peridotites are postulated to represent mantle material.
2. A reasonable partial melting fractionation model was obtained for garnet pyroxenite formation. The proposed REE abundance pattern of the Koolau source is exactly that which is required for the interpretation that garnet pyroxenites are entrapped partial melts.
3. The models provide for reasonable estimates to bulk composition of the mantle in terms of transition element abundances (Cr, Co, and Ni).
4. The models are capable of explaining the systematic variations in some of the major and trace element chemistries among tholeiitic basalts from the same source and between the basalts from the different sources without introducing radical changes to the source compositions.

5. The models will conform to the hypothesis on the geophysical nature of the melting process. The generation of initially tholeiitic basalts at low degrees of partial melting and ending with garnet pyroxenites at high degrees of melting supports the hypothesis that basalt generation is cyclic (Shaw, 1969).

Direct evidence must ultimately come from detailed analysis of the actual source material(s) or of a magma that can undeniably be described as primary melt material. A direct consequence of this model, however, is that a "true" primary melt will never be sampled since such a material will simultaneously undergo some fractionation as melting ceases. Furthermore, it is the author's opinion that it is highly improbable that a sample of the mantle will ever be obtained that is not altered to some degree by the host basalt, particularly in trace elements. Of course, it has been shown that unaltered xenoliths do occur in the basalts, but such xenoliths are probably not parental to those basalts as suggested by this work but are accidental xenoliths.

Confirmation or denial of the proposed models must then come from detailed studies especially concerned with the trace element geochemistry (notably the REE) of associated rock types in Hawaii. Additional data are needed on the garnet pyroxenites on Koolau as well as on the other modules found in the late stage magmas to determine their role in basalt formation. Further sampling and analysis of tholeiitic basalts on all the islands could also prove to be beneficial in this description.

Finally, it must be emphasized that these models are only applicable to Hawaiian-type volcanism. Much further work, on the part of petrologists and geochemists, is needed to define more fully the processes involved in worldwide basaltic magma generation. The results of these studies will be very beneficial in the understanding of the dynamic world around us.

BIBLIOGRAPHY

Anderson, D. L., and Spetzler, H. 1970. Partial melting and the low velocity zone. Phys. Earth Planet. Inter. 4: 62-64.

Arakami, S., and Moore, J. G. 1969. Chemical composition of prehistoric lavas at Makaopuhi Crater, Kilauea volcano and periodic change in alkali content of Hawaiian tholeiitic lavas. Tokyo Univ. Earthquake Research Inst. Bull. 47 (Pt. 2): 257-270.

Arth, J. G., and Hanson, G. N. 1975. Geochemistry and origin of the early precambrian crust of northeastern Minnesota. Geochim. Cosmochim. Acta. 39: 325-362.

Beeson, M. H., and Jackson, E. D. 1970. Origin of the garnet pyroxenite xenoliths at Salt Lake Crater, Oahu. Mineral Soc. Am. Spec. Papers. 3: 95-112.

Bonhommet, N., Beeson, M. H., and Dalrymple, G. B. 1977. A contribution to the geochronology and petrology to the island of Lanai, Hawaii. Geol. Soc. Amer. Bull. 88: 432-444.

Borchardt, G. A., Hoagland, G. W., and Schmitt, R. A. 1970. Spectra: a computer program for gamma-ray analysis. J. Radioanal. Chem. 6: 241-271.

Boyd, F. R., and Nixon, P. H. 1975. Ultramafic nodules from the Kimberly Pipes, South Africa. Carnegie Inst. Washington Yearbook. 544-546.

Boynton, W. V., Baedecker, P. A., Chou, C.-L., Robinson, K. L., and Wasoon, J. T. 1975. Mixing and transport of lunar surface materials: evidence obtained by determination of lithophile, siderophile and volatile elements. Proc. Lunar Sci. Conf. 6th. 2: 2241-2259.

Carmichael, I. S. E., Turner, F. J., and Verhoogen, J. 1974. Igneous petrology. New York: McGraw-Hill.

Carswell, D. A., and Dawson, J. B. 1970. Garnet pyroxenite xenoliths in South African pipes and their petrogenesis. Contrib. Mineral. Petrol. 25: 163-184.

Cawthorn, R. G., and McIver, J. R. 1977. Nickel in komatiites. Nature. 266: 716-718.

Chen, J. 1971. Mineralogy and chemistry of the earth's upper mantle based on the partial fusion-partial crystallization mode. Bull. Ecol. Soc. Am. 81: 2021-2034.

Clarke, D. B. 1970. Tertiary basalts of Baffin Bay: Possible primary magma from the mantle. Contrib. Mineral. Petrol. 25: 203-224.

Dalrymple, G. B., Silver, E. A., and Jackson, E. D. 1973. Origin of the Hawaiian Islands. Am. Scientist. 61: 296-308.

Dana, J. D. 1849a. The United States exploring expedition during the years 1838-1839, 1840, 1841, 1842. Vol. 10: Geology. Philadelphia: C. Sherman.

_____. 1849b. Characteristics of volcanoes. New York: Dodd, Mead and Company.

Danchin, T. V., and Boyd, F. R. 1975. Ultramafic nodules from the Premier Kimberlite Pipe, South Africa. Carnegie Inst. Washington Yearbook. 531-538.

Davis, B. T. C. 1964. The system diopside-forsterite-pyrope at 40 kilobars. Carnegie Inst. Washington Yearbook. 63: 165-171.

Davis, B. T. C., and Shairer, J. F. 1965. Melting relations in the join diopside-forsterite-pyrope at 40 kilobars and at one atmosphere. Carnegie Inst. Washington Yearbook. 64: 123-126.

Duke, J. M. 1976. Distribution of period four transition elements among olivine, calcic pyroxene and mafic silicate liquid: experimental results. J. Petrol. 17: 499-521.

Eaton, J. P. 1962. Crustal structure and volcanism in Hawaii. Mongr. Am. Geophys. Union. 6: 13-29.

_____. 1967. Evidence on the source of magma in Hawaii from earthquakes, volcanic tremor and ground deformation. Abst. Trans. Am. Geophys. Union. 48: 254.

Eaton, J. P., and Murata, K. J. 1960. How volcanoes grow. Science. 132: 925-938.

Finnerty, T. A. 1976. Exchange of Mn, Ca, Mg and Al between synthetic garnet, orthopyroxene, clinopyroxene and olivine. Carnegie Inst. Washington Yearbook. 76: 572-579.

Fiske, R. S., and Jackson, E. D. 1972. Orientation and growth of Hawaiian volcanic rifts; the effects of regional structure and gravitational stress. Phil. Trans. Royal Soc. London. A329: 299-326.

Fiske, R. S., and Kinoshita, W. T. 1969. Inflation of Kilauea volcano prior to its 1967-1968 eruption. Science. 165: 341-350.

Frey, F. A., and Green, D. H. 1974. The mineralogy, geochemistry and origin of lherzolite inclusions in Victorian basanites. Geochim. Cosmochim. Acta. 38: 1023-1059.

Ganapathy, R., and Anders, E. 1974. Bulk composition of the moon and earth, estimated from meteorites. Proc. Fifth Lunar Science Conf. 2: 1181-1206.

Gast, P. W. 1968. Trace element fractionation and the origin of tholeiitic and alkaline magma types. Geochim. Cosmochim. Acta. 32: 1057-1086.

Green, D. H. 1966. The origin of the "eclogites" from Salt Lake Crater, Hawaii. Earth Planet. Sci. Letters. 1: 414-420.

_____. 1971. Compositions of basaltic magmas as indicators of conditions of origin: applications to oceanic volcanism. Phil. Trans. Roy. Soc. London. 268: 707-725.

_____. 1975. Genesis of Archean peridotite magmas and constraints on Archean geothermal gradients and tectonics. Geology. 3: 15-18.

Green, D. H., and Ringwood, A. E. 1967. The genesis of basaltic magmas. Contrib. Mineral. Petrol. 15: 103-190.

Grove, T. L., and Bence, A. E. 1977. Experimental study pyroxene-liquid interaction in quartz-normative basalt 15597. Proc. Lunar Sci. Conf. 8th. 2: 1549-1579.

Grutzeck, M. W., Kridelbaugh, S. G., and Weill, D. F. 1974. Distribution of Sr and REE between dioxide and silicate liquid. Geophys. Res. Letters. 1: 273-275.

Hanson, G. H., and Langmuir, C. H. 1977. Use of distribution coefficients for major elements in mantle-melt systems. Abstr. Presented to the Internat. Conf. of Experimental Trace Element Geochemistry, 38-40.

Harrison, W. J. 1977. On experimental study of the partitioning of samarium between garnet and liquid at high pressures. Abstr. Presented to the Internat. Conf. of Experimental Trace Element Geochemistry, 41-42.

Hart, S. R., and Brooks, C. 1974. The geochemistry and evolution of early precambrian mantle. Carnegie Inst. Washington Yearbook. 73: 967-970.

Hart, S. R., and Davis, K. E. 1978. Nickel partitioning between olivine and silicate meH. Earth Planet. Sci. Letters. 40: 203-219.

Haskin, L. A., Haskin, M. A., Frey, F. A., and Wildeman, T. R. 1968. Relative and absolute terrestrial abundances of the rare earths. In Origin and Distribution of the Elements. Edited by L. H. Ahrens. New York: Pergamon Press, pp. 889-912.

Irving, A. J. 1978. A review of experimental studies of crystal/liquid trace element partitioning. Geochim. Cosmochim. Acta. 42: 743-770.

Irving, A. J., and Frey, F. A. 1978. Distribution of trace elements between garnet and megacrysts in volcanic liquids of kimberlitic to rhyolitic compositions. Geochimica Acta Physica. 42: 771-787.

Ito, K., and Kennedy, G. C. 1967. Melting and phase relations in a natural garnet peridotite to 40 kilobars. Am. J. Sci. 265: 519-538.

Jackson, E. D. 1966. "Eclogite" in Hawaiian basalts. USGS Professional Papers. 550-D: 151-157.

Jackson, E. D., and Wright, T. L. 1970. Xenoliths in the Honolulu volcanic series, Hawaii. J. Petrol. 11: 405-430.

Kay, R. W., and Gast, P. W. 1973. The rare-earth content and origin of alkali-rich basalts. J. Geol. 6: 653-682.

Kuno, H. 1969. Mafic and ultramafic nodules in the basaltic rocks of Hawaii. Geol. Soc. Am. Mem. 115: 189-233.

Kushiro, I. 1968. Composition of magma formed by partial zone melting of the earth's upper mantle. J. Geophys. Res. 73: 619-634.

Kushiro, I., Shimizu, N., Nakamura, Y., and Akomoto, S. 1972. Composition of coexisting liquid and solid phases formed upon melting of natural garnet and spinel lherzolites at high pressures: a preliminary report. Earth Planet. Sci. Letters. 14: 19-25.

Langmuir, C. H., and Hanson, G. H. 1977. Dynamic melting of mantle. Abstr. Presented to the Internat. Conf. of Experimental Trace Element Geochemistry, 68-70.

Laul, J. C., and Schmitt, R. A. 1973. Chemical composition of Luna 20 rocks and soil and Apollo 16 soils. Geochim. Cosmochim. Acta. 37: 927-942.

Leeman, W. P., Murali, A. V., Ma, M.-S., and Schmitt, R. A. 1977. Mineral constitution of mantle source regions for Hawaiian basalts — rare earth evidence for mantle heterogeneity. Proc. Chapman Conf.

Leeman, W. P., and Scheidegger, K. F. 1977. Olivine/liquid distribution coefficients and a test for crystal-liquid equilibrium. Earth Planet. Sci. Letters. 35: 247-257.

Lindstrom, D. J. 1976. "Experimental study of the partitioning of the transition metals between clinopyroxene and coexisting silicate liquids." Ph.D. dissertation, University of Oregon.

Lindstrom, D. J., and Weill, D. F. 1978. Partitioning of transition metals between dioxide and coexisting silicate liquids. I. Nickel, cobalt, and manganese, pp. 817-832.

Loubet, M., Shimizu, N., and Allegre, C. J. 1975. Rare earth elements in alpine peridotites. Contrib. Mineral. Petrol. 53: 1-12.

Maaloe, S., and Aoki, K.-I. 1977. The major element composition of the upper mantle estimated from the composition of lherzolites. Contrib. Mineral. Petrol. 63: 161-173.

McBirney, A. R., and Williams, H. 1969. Geology and petrology of the Galapagos Islands. Geol. Soc. Am. Mem. 118: 197.

Macdonald, G. A. 1949. Hawaiian petrographic province. Geol. Soc. Am. Bull. 60: 1541-1596.

Macdonald, G. A. 1969. Composition and origin of Hawaiian lavas. Geol. Soc. Am. Mem. 116: 477-522.

Macdonald, G. A., and Katsura, T. 1964. Chemical composition of Hawaiian lavas. J. Petrol. 5: 82-133.

McDougall, I. 1964. Potassium-argon ages from lavas of the Hawaiian Islands. Geol. Soc. Am. Bull. 75: 107-128.

_____. 1971. Volcanic island chains and sea-floor spreading. Nature. 231: 141-144.

McDougall, I., and Swanson, D. A. 1972. Potassium-argon ages of lavas from the Hawaii and Pololu volcanic series, Kohala volcano, Hawaii. Geol. Soc. Am. Bull. 83: 3731-3738.

Machado, F. 1974. The search for magmatic reservoirs. In Physical Volcanology. Edited by L. Civetta, P. Gasparini, G. Luongo, and A. Rapolla. New York: American Elsevier Scientific Publishing, Inc., pp. 255-275.

McKay, G. A., and Weill, D. F. 1976. Petrogenesis of KREEP. Proc. 7th Lunar Science Conf., pp. 2427-2447.

Mason, B. 1970. Principles of geochemistry. 4th Ed. New York: Wiley.

May, R. J. 1975. "Thermoluminescence dating of Hawaiian basalts." Ph.D. dissertation, Stanford University.

Morgan, B. A. 1974. Chemistry and mineralogy of garnet pyroxenites from Sabah, Malaysia. Contrib. Mineral. Petrol. 4: 301-314.

Morgan, W. J. 1971. Convection plumes in the lower mantle. Nature. 230: 42-43.

_____. 1972. Deep mantle convection and plate motion. Am. Assoc. Petrol. Geol. Bull. 56: 203-213.

Mori, T., and Green, D. H. 1975. Pyroxenes in the system $Mg_2Si_2O_6$ - Ca Mg Si_2O_5 at high pressure. Earth Planet. Sci. Letters. 3: 277-286.

Murali, A. V., Leeman, W. P., Ma, M.-S., and Schmitt, R. A. 1977. Evaluation of fractionation and hybridization models for Kilauea eruptions and probable mantle source of Kilauea and Mauna Loa tholeiitic basalts, Hawaii — a trace element study. J. Petrol.

Murati, K. J., and Richter, D. H. 1966. The settling of olivine in Kilauean magma as shown by lavas of 1959 eruption. Am. J. Sci. 264: 194-203.

Mysen, B. O. 1973. Melting in a hydrous mantle: phase relations of mantle peridotite with controlled water and oxygen fugacities. Carnegie Inst. Washington Yearbook. 72: 467-478.

Mysen, B. O., and Kushiro, I. 1975. Compositional variation of coexisting phases with degree of partial melting of peridotite under upper mantle conditions. Carnegie Inst. Washington Yearbook. 75: 546-555.

Nisbet, E. G., and Pearce, J. A. 1977. Clinopyroxene composition in mafic lavas from different tectonic settings. Contrib. Mineral. Petrol. 63: 149-160.

O'Hara, M. J. 1969. The origin of eclogite and ariegite nodules in basalt. Geol. Mag. 106: 322-330.

O'Hara, M. J., and Yoder, H. S. 1967. Formation and fractionation of basic magmas at high pressures. Scot. J. Geol. 3: 67-113.

Philpotts, J. A., and Schnetzler, C. C. 1970. Speculations on the genesis of alkaline and sub-alkaline basalts following exodus of the continental crust. Can. Mineralogist. 10: 374-379.

Philpotts, J. A., Schnetzler, C. C., and Thomas, H. H. 1972. Petrogenetic implications of some new geochemical data on eclogite and ultrabasic inclusions. Geochim. Cosmochim. Acta. 36: 1131-1166.

Porter, S. C., Stuiver, M., and Yang, I. C. 1977. Chronology of Hawaiian glaciations. Science. 195: 61-63.

Powers, H. A. 1955. Composition and origin of basaltic magma of the Hawaiian Islands. Geochim. Cosmochim. Acta. 7: 77-107.

Raheim, A., and Green, D. H. 1974. Experimental determination of the temperature and pressure dependence of the Fe-Mg partition coefficient for coexisting garnet and clinopyroxene. Contrib. Mineral. Petrol. 48: 179-203.

Reid, A. M., Brown, R. W., Dawson, J. B., Woodwille, G. G., and Siebert, J. C. 1976. Garnet and pyroxene compositions in some diamondiferous eclogites. Contrib. Mineral. Petrol. 58: 203-220.

Reid, J. B., and Frey, F. A. 1971. Rare earth distributions in lherzolite and garnet pyroxenite xenoliths and the constitution of the upper mantle. J. Geophys. Res. 76: 1184-1196.

Reid, J. B., and Prinz, M. 1971. High pressure pyroxenite dikes in xenoliths from San Carlos, Arizona and Salt Lake Crater, Hawaii. Geol. Soc. Am. Ann. Mtg. 1971: 679-680.

Richard, P., Shimizu, N., and Allegre, C. J. 1976. $^{143}Nd/^{146}Nd$, a natural tracer: an application to oceanic basalts. Earth Planet. Sci. Letters. 31: 269-278.

Roeder, P. L., and Emslie, R. F. 1970. Olivine-liquid equilibrium. Contrib. Mineral. Petrol. 29: 275-289.

Schreiber, H. D. 1976. "Experimental determination of redox states, properties, and distribution of chromium in synthetic silicate thases and application to basalt petrogenesis." Ph.D. dissertation, University of Wisconsin.

Sato, H. 1977. Nickel content of basaltic magmas. Identification of primary magmas and a measure of the degree of fractionation. Lithos. 10: 113-120.

Shaw, D. M. 1970. Trace element fractionation during anatexis. Geochim. Cosmochim. Acta. 34: 237-242.

Shaw, H. R. 1969. Rheology of basalt in the melting range. J. Petrol. 10: 510-535.

_____. 1973. Mantle convection and volcanic periodicity in the Pacific; evidence for Hawaii. Geol. Soc. Am. Bull. 84: 1505-1526.

Smith, J. V. 1977. Possible controls on the bulk composition of the earth: implications for the origin of the earth and moon. Proc. Lunar Sci. Conf. 2: 333-369.

Spetzler, H., and Anderson, D. L. 1968. The effect of temperature and partial melting on velocity and attenuation in a simply binary system. J. Geophys. Res. 73: 6051-6060.

Sun, S.-S., and Nesbitt, R. W. 1977. Chemical heterogeneity of the Archean mantle, composition of the earth and mantle evolution. Earth Planet. Sci. Letters. 35: 429-448.

_____. 1978. Petrogenesis of Archean ultrabasic and basic volcanics: evidence from rare earth elements. Contrib. Mineral. Petrol. 65: 301-326.

Tatsumoto, M. 1966. Isotopic composition of lead in volcanic rocks from Hawaii, Iwo Jima, and Japan. J. Geophys. Res. 71: 1721-1733.

Tilley, C. E. 1960. Differentiation of Hawaiian basalts — some variants in lava suites of dated Kilauea eruptions. J. Petrol. 1: 47-55.

Turekian, K. K. 1968. Composition of the crust. In Vol. XXX: Origin and distribution of the elements, pp. 549-557. Edited by L. H. Ahrens. Internat. Series of Monographs in Earth Science. New York: Pergamon Press.

Whittaker, E. J. W., and Muntus, R. 1970. Ionic radius for use in geochemistry. Geochim. Cosmochim. Acta. 34: 945-956.

Wilkinson, J. F. G. 1976. Some subcalcic clinopyroxenites from Salt Lake Crater, Oahu and their petrogenetic significance. Contrib. Mineral. Petrol. 58: 181-202.

Wilson, J. T. 1963. A possible origin of the Hawaiian Islands. Canadian J. Physics. 41: 863-870.

Wright, T. L. 1971. Chemistry of Kilauea and Mauna Loa in space and time. U.S. Geol. Survey Prof. Papers, 735.

Wright, T. L., and Fiske, R. S. 1971. Origin of the differentiated and hybrid lavas of Kilauea volcano, Hawaii. J. Petrol. 12: 1-65.

Wright, T. L., Swanson, D. A., and Duffield, W. A. 1975. Chemical compositions of Kilauea east-rift lava, 1968-1971. J. Petrol. 16: 110-133.

Yoder, H. S., Jr. 1976. Generation of basaltic magma. Washington, D.C.: National Academy of Sciences.

Yoder, H. S., Jr., and Tilley, C. E. 1962. Origin of basalt magma: an experimental study of natural and synthetic rock systems. J. Petrol. 3: 342-532.

APPENDICES

APPENDIX A

Description of Samples Analyzed in This Work

Volcano	USGS No.	Description	Location-age
Kohala	P71-5	Olivine basalt	90 m below top of Pololu series; ~0.45 m.y.
	P71-13	Olivine basalt	East wall of Waipio Valley, 18 flows from top of Pololu series; ~0.33 m.y.
	C66	See Macdonald and Katsura (1964)	
	C53	See Macdonald and Katsura (1964)	
	C62	See Macdonald and Katsura (1964)	
	P71-4	Olivine basalt	110 m below top of Pololu series (second or third flow); ~0.5 m.y.
	C70	See Macdonald and Katsura (1964)	
	P71-3	Olivine basalt	40 m below top of Pololu series; ~0.4 m.y.
	72M-36	See Macdonald and Katsura (1964)	
	H71-3	Mugearite	Flow filling Pololu Valley of Hawi series; ~0.16 m.y.
	72M-42	See Macdonald and Katsura (1964)	
	H71-10	Mugearite	Top flow of Hawi series; ~0.06 m.y.
	72M-33	See Macdonald and Katsura (1964)	
	72M-35	See Macdonald and Katsura (1964)	

SOURCES: Samples with prefixes P71, H71, and 72M received from R. J. May; C prefix from M. Tatsumoto. Major element analyses of these basalts reported by Macdonald and Katsura (1964), McDougall and Swanson (1972), May (1975).

Volcano	USGS No.
Mauna Kea	C74, 710826-1, 741011-11, 720803-9, 720819-1, 720817-1, 720821-2, 710818-1, 720900-1, 710805-2, 710810-5, 710827-1, 720803-5, and 710826-2

SOURCES: Sample C74 received from M. Tatsumoto; 700000 series samples received from S. C. Porter et al. (1977); major element analyses of these basalts reported by Porter et al. (1977).

Volcano	USGS No.	Description	Location-age
Koolau	D101471	Tholeiite	Flow beneath Sugar Loaf ash, west of Makiki Stream, Oahu
	D101473	Tholeiite	Flow beneath Salt Lake tuff, south side of Moanalua road, Oahu
	D101474	Tholeitte	Kailua basalt dike, margin of 0.75 m thick dike on west side of Kapaa Valley, Oahu
	D101472	Tholeiite	Flow beneath Punchbowl tuff, Tantalus drive overcrossing Oahu
Lanai	OX069	Tholeiite	See Bonhommet et al. (1977)
	OX068	Tholeiite	See Bonhommet et al. (1977)
	OX067	Tholeiite	See Bonhommet et al. (1977)
	OX078	Tholeiite	See Bonhommet et al. (1977)

SOURCES: Samples for Koolau received from Jackson and Wright (1970). Sample for Lanai received from Bonhommet et al. (1977).

Volcano	USGS No.	Description	Location-age
Mauna Loa	TLW67-56	Tholeiite	Spatter, SW rift flow, Puu o Keokeo, 1907 A.D.
	TLW67-62	Tholeiite	Spatter, NE rift flow, Puo Ulaula, 1942 A.D.
	TLW67-65	Tholeiite	Spatter, NE summit flow, Kokoolau, 1899 A.D.
	TLW67-67	Tholeiite	Spatter, NE rift flow, Kokoolau, 1935 A.D.
	TLW67-68	Tholeiite	Pumice, NE summit flow, Mauna Loa, 1942 A.D.
	TLW67-73	Tholeiite	Sulfur cone spatter, SW rift flow, 1950 A.D.
	TLW67-77	Tholeiite	Spatter, SW rift flow, Alika cone, 1919 A.D.
	ML775-26	Tholeiite	Mauna Loa summit flow, 1975 A.D.
	TLW67-59	Tholeiite	Spatter, SW rift, Puu o Keokeo, 1887 A.D.
	TLW67-29	Tholeiite	Mauna Loa NE rift flow, Wood Valley, prehistoric
	TLW67-70B	Tholeiite	Mauna Loa summit flow, prehistoric
	TLW67-119	Tholeiite	Spatter, NW slope, Puu o Uo, prehistoric
	TLW67-123	Tholeiite	Spatter, NW slope, Kokoolau, prehistoric
Mauna Ulu	DAS69-1-3	Tholeiite	Spatter, 0.4 km W Aloi, 1969 A.D.
	DAS69-78-9	Tholeiite	Spatter, main vent, 1969 A.D.
	DAS69-8-1	Tholeiite	Pumice, Aloi crater, 1969 A.D.
	DAS70-1213-25	Tholeiite	Lava crust, main vent, 1970 A.D.
	DAS71-1213-134	Tholeiite	Lava crust, 9 km SSE Alae, 1971 A.D.

SOURCES: Samples for Mauna Loa received from T. L. Wright. Major element analyses of these samples in Wright (1971).

APPENDIX B

Partition Coefficients Used in Modeling (Trace Elements)

Element	ol/l	opx/l	cpx/l	gar/l
Sr	0.003	0.009	0.03	0.04
Ba	0.005	0.009	0.01	0.01
La	0.007	0.005	0.069	0.01
Ce	0.007	0.006	0.098	0.02
Nd	0.008	0.010	0.175	0.026
Sm	0.009	0.013	0.26	0.21
Eu	0.010	0.014	0.26	0.42
Tb	0.0105	0.021	0.30	1.26
Dy	0.011	0.035	0.33	2.03
Yb	0.014	0.056	0.29	8.37
Lu	0.016	0.068	0.28	10.36
Sc	0.15[a]	1.4	1.6	3.4
	0.27[c]			
Hf	0.06	0.06	0.13	0.57
Ta	0.0	0.0	0.3	0.3
Th	0.0	0.0	0.0	0.0
U	0.0	0.0	0.0	0.0
Ni	2.0[a]	3.1	0.3	0.4
	3.85[b]	. . .	. . .	. . .
	6.08[c]	. . .	. . .	. . .
	10.1[d]	. . .	. . .	. . .
Co	1.36[a,b]	1.35	0.17	0.2
	2.23[c]	. . .	. . .	. . .
	2.77[d]	. . .	. . .	. . .
Cr	0.8	1.6	1.5	2.0
	(5.0)[e]			

SOURCES: Sr, Ba, and REE (La, Ce, Nd, Sm, Eu, Tb, Dy, Yb, and Lu) — ol, Arth and Hanson (1975); opx, McKay and Weill (1976); cpx, Grutzeck et al. (1974); gar, Arth and Hanson (1975) and Philpotts et al. (1972).

Sc — ol, Leeman and Scheidegger (1977) and McKay and Weill (1976); opx and cpx, estimated from data of McKay and Weill (1976) and Lindstrom (1976) (average); gar, Irving and Frey (1978).

Hf, Ta, Th, and U — all estimated from partial melting model assuming common parental material.

Ni, Co, and Cr — ol for Ni and Co, Leeman and Scheidegger (1977) and ol for Cr, Schreiber (1976); opx for Ni and Co, Lindstrom (1976) and Schreiber (1976) for Co; cpx for Ni and Co, Lindstrom and Weill (1978) and Schreiber (1976) for Cr; gar for Co and Cr, Irving and Frey (1978) and gar for Ni, estimated.

[a]Values used in the partial melting model.

[b]Value used in olivine fractionation model: 1475°C.

[c]Value used in olivine fractionation model: 1375°C.

[d]Value used in olivine fractionation model: 1275°C [calculated from Leeman and Scheidegger (1978)].

[e]Includes ~7% chromite (see text).

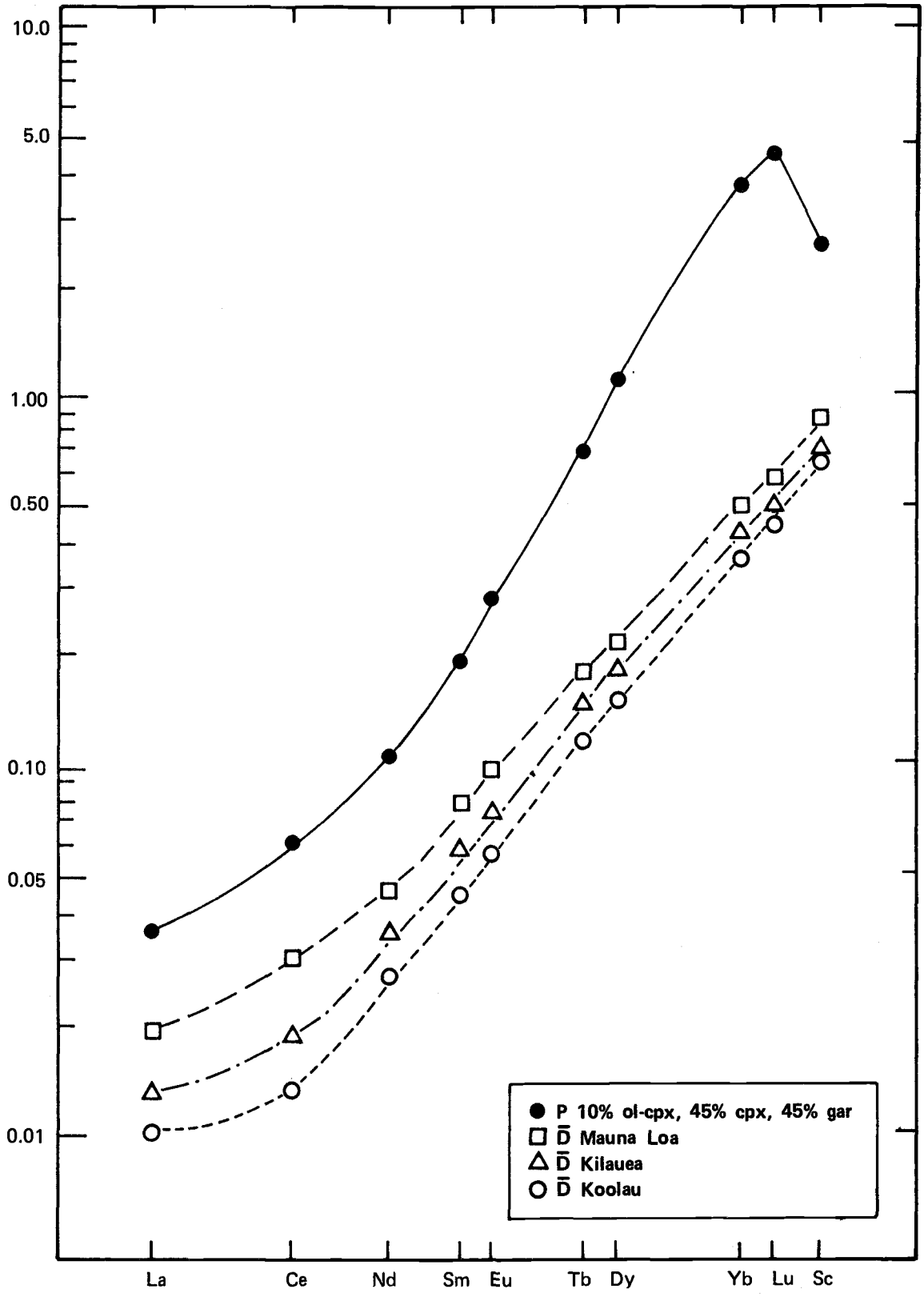

Fig. B-1. Bulk partition coefficients for REE, Sc.

APPENDIX C

Partition Coefficients Used in Modeling (Major Elements)

MgO						
Temperature	ol/l	opx/l	cpx/l	gar/l	$\overline{D}_{MgO}$	P_{MgO}
1600°C	1.6	1.0	0.9	0.9	1.3	1.1
1400°C	2.8	1.4	1.2	1.2	2.1	1.3
1200°C	5.8	2.5	1.5	1.5	4.1	2.1
FeO						
Temperature	ol/l	opx/l	cpx/l	gar/l	$\overline{D}_{FeO}$	P_{FeO}
1600°C	0.5	0.7	0.6	0.8	0.58	0.68
1400°C	0.9	0.8	0.7	1.2	0.86	0.93
1200°C	1.8	0.9	0.8	2.3	1.44	1.53

SOURCES: ol-MgO, Leeman and Scheidegger (1978) and FeO-$K_{D(Fe-Mg)}^{ol}$, 0.32; opx-MgO and FeO, Grove and Bence (1977); cpx-MgO (1200°C), Grove and Bence (1600 and 1400°C), estimated FeO set equal to 0.9 $D_{FeO}^{opx/l}$; gar-MgO set equal to $D_{MgO}^{cpx/l}$ and FeO from Raheim and Green (1974).

Other data considered in estimates from Duke (1976): e.g., $K_{Fe-Mg}^{ol/cpx}$ = 0.65 @ 1200°C and shown to decrease with increasing T. From above K_D = 0.58 @ 1200°C; 0.47 @ 1600°C.

Element	ol/l	opx/l	cpx/l	gar/l
TiO_2	0.025	0.11	0.25	0.16

SOURCES: ol, opx, and cpx — Lindstrom (1976); gar, estimated from coexisting gar/cpx pairs (see text).

APPENDIX D

Estimate of Chromite Fractionation

Mineral Compositions			
Element	Olivine (Fo_{80})	Olivine (Fo_{93})	Chromite
TiO_2	0.04	0.03	2.10
Al_2O_3	1.10	0.40	13.40
FeO	14.90	7.70	20.90
MgO	40.50	49.30	11.60
CaO	1.20	0.06	0.00
Na_2O	0.00	0.00	0.00
K_2O	0.00	0.00	0.00
MnO	0.17	0.17	0.20
Cr_2O_3	0.05	0.05	43.50

NOTES: Composition of Kilauea basalt given in Table 7C.

Element	Hypothetical Melt	Calculated	Difference	Mineralogy
TiO_2	1.28	1.23	-0.05	Fo_{80} = 19.7 ± 14.0
Al_2O_3	6.40	6.56	0.16	Fo_{93} = 25.3 ± 11.5
FeO	10.50	10.15	-0.35	Chromite = 2.3 ± 0.1
MgO	24.00	24.02	0.02	Kilauea = 43.1 ± 2.1
CaO	4.70	5.17	0.47	Sum = 90.6
Na_2O	1.08	0.98	-0.10	$\chi^2 = 1.39$[a]
K_2O	0.18	0.23	+0.05	
MnO	0.17	0.15	-0.02	
Cr_2O_3	1.00	1.05	0.05	

[a]Weighting factors used: TiO_2, 10.0; Al_2O_3, 5.0; FeO, 5.0; MgO, 10.0; CaO, 10.0; Na_2O, 10.0; K_2O, 50.0; MnO, 0.0; Cr_2O_3, 10.0.